TRANSCRIPTIONAL AND TRANSLATIONAL REGULATION OF CARDIAC DEVELOPMENT IN MAMMALS

Approved by the Supervisory Committee

_____
Chairperson: Thomas Kodadek, PhD

_____
Michelle Tallquist, PhD

_____
Keith Wharton, MD, PhD

_____
Mentor: Deepak Srivastava, MD

To my parents,
Colleen and Randy Ransom

For their never ending support

ACKNOWLEDGEMENTS

I've been very lucky to be a member of Deepak Srivastava's lab. Thanks to both past and present member's camaraderie, which created such a wonderful working environment in which to do research, the long nights always seemed short. I would like to make a special thank you though to Kim and Morgan for their help and friendship on so many different occasions. Special thanks also go to Kathy, Isabelle, and Vidu for their thoughtful insights and constructive criticism - their mentoring was second only to Deepak's.

I'm so thankful for the trust, mentoring and patience that Deepak provided in the five years I've been in his lab. He helped to make me a better scientist and provided so many great opportunities and guidance to prepare me for the transition onto the next stage. His leadership of the lab has provided an example that I hope I can mimic for the rest of my life.

More than anything though, I would like to thank my parents for everything they have done throughout my life; instilling a sense of curiosity and drive at a young age, and providing so much support throughout graduate school while I was so far from home. They never let me settle for delivering less than the best I could do. I'd also like to thank my brother, Grahm, and sister, Ellie, for their encouragement, love, and conversations that reminded me of why I love what I do. Words cannot convey how blessed I feel to have you as my family.

TRANSCRIPTIONAL AND TRANSLATIONAL REGULATION OF CARDIAC DEVELOPMENT IN MAMMALS

by

JOSHUA FULLER RANSOM

DISSERTATION

Presented to the faculty of the Graduate School of Biomedical Sciences

The University of Texas Southwestern Medical Center at Dallas

In Partial Fulfillment of the Requirements

For the Degree of

DOCTOR OF PHILOSOPHY

The University of Texas Southwestern Medical Center at Dallas

Dallas, Texas

April, 2008

TRANSCRIPTIONAL AND TRANSLATIONAL REGULATION OF CARDIAC DEVELOPMENT IN MAMMALS

JOSHUA FULLER RANSOM, Ph.D.

The University of Texas Southwestern Medical Center at Dallas, 2008

DEEPAK SRIVASTAVA, M.D.

The heart is the first organ to form in the embryo to support the growing need for oxygen and nutrients. To form correctly, this vital organ requires a high degree of regulation. Thus far, almost every known form of regulation that the mammalian cell has evolved is utilized in the proper development of the heart. Because the heart is so highly regulated, there are many steps at which a wrong turn can be made, leading to congenital cardiovascular malformations, which occur in one percent of all births and are the leading non-infectious cause of death in the first year of life.

The majority of genes known to be involved in cardiogenesis in mammals are grouped at nodes which control many simultaneous aspects of differentiation,

morphology, and heart size. This thesis work will discuss three separate lines of inquiry into cardiogenic nodes in mammalian heart development. The first deals with post-translational regulation of the Myocardin-dependent transcriptional node. The second story delves into the role of the Notch signaling pathway in human disease and how Notch regulates Myocardin and its downstream target gene, microRNA-1. The final account looks into regulation of protein translation through microRNAs in the heart with emphasis on microRNA-1-2.

TABLE OF CONTENTS:

Title *i*
Dedication *ii*
Acknowledgements *iii*
Abstract *vi*
Table of Contents *viii*
List of Publications *xi*
List of Figures *xii*
List of Tables *xiii*
List of Abbreviations *xiv*

CHAPTER 1: INTRODUCTION TO HEART DEVELOPMENT 1
A. Critical Events in Cardiogenesis as Relates to Disease 2
a. Heart Tube Formation 2
b. Septal Morphogenesis 3
c. Outflow and Inflow Tract Morphogenesis 4
d. Cardiac Conduction Development 5
B. Congenital Cardiovascular Disease Gene Discovery 5
a. Haplotype Mapping of CCVM 8
b. Copy Number Variation in Chromosomal Sub-centrimorgan Duplications/Deletions 8
c. Candidate Gene Screen 9
C. Regulatory Nodes in Cardiogenesis 9
a. Transcriptional Nodes 9
i. Tbx5 and Holt-Oram Syndrome 9
ii. Nkx2.5 10
iii. Gata4 10
b. Translational Nodes 11
c. Post-translational Nodes 11
i. Notch Signal Transduction in Alagille Syndrome and Outflow Tract Defects 12
ii. RAS/RAF/MAPK Signal Transduction in the Noonan Syndrome Family (Cardio-Facio-Cutaneous, Costello, and Noonan) 13
D. Conclusions 14

CHAPTER 2: HUMAN SEQUENCE VARIANTS ARE ASSOCIATED . . . . 15 WITH OUTFLOW TRACT DEFECTS AND REVEAL MYOCARDIN AUTOINHIBITION
A. Abstract 15
B. Introduction 16
C. Materials and Methods 19
D. Results 23
a. Sequence Variants in the MYOCD Gene in Patients with Congenital Cardiac Malformations 23

b. MYOCD Sequence Variations K259R and Q647H are Hypomorphic and K259R Has Reduced SRF Affinity 26
c. MYOCD Q647H is Located Near And Dysregulates Predicted Kinase Phosphorylation Motifs 27
d. Cardiac But Not Smooth Muscle Myocardin K259R Is Hypomorphic and Has Reduced SRF Affinity 29
e. The MYOCD MHD Inhibits MYOCD-Dependent Transcription in Vitro by Binding to MYOCD and Blocking Its Interaction with SRF 30
f. The MYOCD MHD Inhibits MYOCD-Dependent Smooth Muscle Production and Cardiomyocyte Hypertrophy and Disrupts Normal Cardiac Morphogenesis 31
g. The Histone Acetyltransferase, p300, Acetylates MYOCD Directly To Directly Regulate MHD Autoinihibtion 33
E. Discussion 35

CHAPTER 3: MUTATIONS IN NOTCH1 CAUSE AORTIC VALVE DISEASE 54
A. Abstract 54
B. Introduction 55
C. Materials and Methods 55
D. Results 58
a. NOTCH Inhibits MYOCD-Dependent miR-1 Expressionxx 63
E. Discussion 64

CHAPTER 4: DYSREGULATION OF CARDIOGENESIS, CARDIAC CONDUCTION, AND CELL CYCLE IN MICE LACKING MICRORNA-1-2 75
A. Abstract 75
B. Introduction 76
C. Materials and Methods 79
D. Results 81
a. Disruption of the Dicer Allele in Cardiac Progenitors 81
b. Targeted Deletion of miR-1-2 in Mice 82
c. Cardiac Morphogenetic Defects in miR-1-2 Mutants 83
d. Cardiac Electrophysiologic Defects in miR-1-2 Mutants and miR-1-2 Regulation of Irx5 84
e. miR-1-2 Regulates Cardiac Cell Cycle and Karyokinesis 85
f. Enrichment of miR-1 Seed Matches Among mRNAs Upregulated in miR-1-2 Mutants 86
g. Accessibility of miRNA Binding Sites Defined by Local Free Energy 88
E. Discussion 90
a. miR-1-2 Regulates Cardiac Morphogenesis 91
b. miR-1-2 Regulation of Cardiac Conduction 92
c. Cell-Cycle Dysregulation in miR-1-2 Mutants 93

d. Sequence Matching and Target Site Accessibility During miRNA:mRNA Interactions *94*

CHAPTER 5: DISCUSSION OF FUTURE DIRECTIONS 108
A. *Valve Disease and Human Mutations* *109*
B. *Notch Regulation of miR-1 cluster* *113*
C. *microRNAs in Heart Development* *114*

CHAPTER 6: BIBLIOGRAPHY 118

CHAPTER "THE END." - VITAE 137

LIST OF PUBLICATIONS

Mason, JM, **Ransom, J**, and Konev, AY. (*2004*) A Deficiency Screen for Dominant Suppressors of Telomeric Silencing in Drosophila. *Genetics*, 168(3):1353-70.

Garg, V, Muth, AN, **Ransom, JF**, Schluterman, MK, Barnes, R, King, IN, Grossfeld, PD, and Srivastava, D. (*2005*) Mutations in NOTCH1 Cause Aortic Valve Disease. *Nature*, 437(7056): 270-4. Epub 2005 July 17.

Ransom, J and Srivastava, D. (*2007*) The Genetics of Cardiac Birth Defects. *Seminars in Cell and Developmental Biology*, 18(1):132-9. Epub 2006 Dec 20.

Zhao, Y*, **Ransom, JF***, Li, A, Vedantham, V, von Drehle, M, Muth, AN, Tsuchihashi, T, McManus, M, Schwartz, R, and Srivastava, D. (*2007*) Dysregulation of Cardiogenesis, Cardiac Conduction, and Cell Cycle in Mice Lacking miRNA-1-2. *Cell*, 129 (3): 303-17. Epub 2007 March 28. (* Contributed Equally)

Ransom, JF, King, IN, Garg, V, and Srivastava, D. A Rare Human Sequence Variant Reveals Myocardin Autoinhibition. In preparation

LIST OF FIGURES

1.1 Mammalian Heart Development 3

2.1 Discovery of Evolutionarily Conserved Myocardin Sequence Variations Associated With Outflow Tract Valve Disease 40
2.2 Generation of Mice with Targeted Knock-In of MYOCD K259R 42
2.3 Cardiac MYOCD K259R and Q647H are Hypomorphic *In vitro* and K259R has Reduced SRF Binding Affinity 43
2.4 MYOCD Q647H is Located Near Putative Phosphorylation Sites and Dysregulates GSK3β-Dependent Signals 44
2.5 Loss of MYOCD MHD rescues K259R 45
2.6 The MYOCD MHD acts as an autoinhibitory domain by binding to and repressing MYOCD-dependent *in vitro* activity 46
2.7 The MHD of MYOCD inhibits MYOCD-dependent conversion of fibroblasts into smooth muscle cells 48
2.8 The MYOCD MHD inhibits PE-dependent cardiomyocyte hypertrophy 49
2.9 p300 Acetylates MYOCD Directly to Inhibit MHD-Dependent Autoinhibition and Binding 51

3.1 NOTCH1 mutations segregate with familial aortic valve disease 67
3.2 Cardiac expression of mouse Notch1 mRNA by radioactive-section in situ hybridization 68
3.3 Notch1, Hrt1 and Hrt2 repress Runx2 transcriptional activity 69
3.4S Clinical phenotype of Family A and Family B 70
3.5S Pedigree of Family A with haplotype data 72
3.6S Ethnicity data for *NOTCH1* polymorphisms 73
3.7 NOTCH1 can activate or repress MYOCD targets including miRNA-1 74

4.1 miRNA Biogenesis is Necessary for Cardiogenesis 97
4.2 Generation of Mice With Targeted Deletion of miR-1-2 98
4.3 Partial Penetrance of Cardiac Morphogenesis Defects in miR-1-2 Mutants 100
4.4 Cardiac Electrophysiologic Defects in miR-1-2 Mutants and miR-1-2 Regulation of Irx5 101
4.5 Cardiomyocyte Hyperplasia and Proliferation in miR-1-2 Mutants 103
4.6 Dysregulated Genes in miR-1-2 -/- Hearts 104
4.7 Enrichment of miR-1 5' Seed Matches Among Genes Upregulated in miR-1-2 -/- Hearts 105
4.8 Bias of miRNA Target Sites to "Accessible" Regions Defined by High Free Energy 106

LIST OF TABLES

Table 1.1: The Genetic Etiologies of Syndromic CCVM 7
Table 1.2: The Genetic Etiologies of Non-Syndromic CCVM 7

Table 2.1: List of Taqman Assays Used 53

Supplementary Table 3.1 107
Supplementary Table 3.2 107

LIST OF ABBREVIATIONS

CCVM = Congenital Cardiovascular Malformation
BAV = Bicuspid Aortic Valve
FHF = First Heart Field
SHF = Second Heart Field
OFT = Outflow Tract
IFT = Inflow Tract
CNC = Cardiac Neural Crest
ASD = Atrial Septal Defect
VSD = Ventricular Septal Defect
AVSD = Atrio-ventricular septal defect
HLHS = Hypoplastic Left Heart Syndrome
SNP = Single Nucleotide Polymorphism
BAC = Bacterial Artificial Chromosome
HOS = Holt-Oram Syndrome
miR = Micro-RNA
PS = Pulmonic Valve Stenosis
AS = Aortic Valve Stenosis
JAG1 = JAGGED1
TOF = Tetrology of Fallot
HRT = Hairy Related Transcription Factor
MYOCD = Myocardin
$MYOCD^{935}$ = Cardiac Muscle Myocardin (1-935)
$MYOCD^{\Delta MHD}$ = Smooth Muscle Myocardin (128-935)
MHD = Myocardin-Family Homology Domain
K259R = Lysine 259 Missense Mutation to Arginine 259
Q647H = Glutamine 647 Missense Mutation to Histadine 647
SRF = Serum Response Factor
MEF2 = Myocyte Enhancing Factor 2
MRTF = Myocardin Related Transcription Factor
SM22 = Smooth muscle 22 kD protein
ANF = Atrial natriuretic factor
HAT = Histone acetyltransferase
HDAC = Histone deacetylase
miR-1 = microRNA-1
MAPK = Mitogen Activated Protein Kinase
ERK = Extracellular signal regulated kinase

CHAPTER 1. INTRODUCTION TO HEART DEVELOPMENT:

The heart is the first organ to form in the embryo, pumping blood by three weeks of gestation when adequate nutrients and oxygen can no longer be provided to the developing fetus by simple diffusion. Cardiogenesis is a complex process involving multiple cell types and appears to be highly susceptible to perturbations, which result in malformations of the heart. In humans, the resulting congenital cardiovascular malformations (CCVM) have been reported to occur in approximately 8 out of every 1,000 live births (1), but this is likely an underestimate. The most common form of CCVM, bicuspid aortic valve (BAV) is present in about 1-2% of all neonates, but is generally excluded from estimates of CCVM since it is asymptomatic in childhood. However, BAV often causes significant heart disease later in life (2). Overall, CCVM remains the leading non-infectious cause of mortality in the first year of life (3).

Despite these statistics, advances in neonatal diagnosis and surgery in the past few decades have reduced the morbidity and mortality for many CCVM (4). As a result, an increasing number of survivors are reaching childbearing age and may be at risk for transmitting disease at a higher frequency than the general population. A better understanding of the molecular and genetic mechanisms involved in cardiogenesis and CCVM could lead to future diagnostics aimed at identifying populations at greater risk for having offspring with CCVM and ultimately towards therapies to prevent the occurrence of CCVM.

CRITICAL EVENTS IN CARDIOGENESIS AS RELATES TO DISEASE:

Due to the complexity of development, this discussion will briefly review of cardiac morphogenesis focusing on its relationship to diseases discussed herein. A more complete review of heart development can be found in recent reviews (5-7). Clinical reference books provide a more thorough description and visualization of the CCVM described (8).

Heart Tube Formation

The heart begins forming by the second week of human gestation when a crescent of mesoderm tissue commits to the cardiac lineage and differentiates into two distinct pools of progenitors known as the first heart field (FHF) and second heart field (SHF). By human embryonic day 21-23, this cardiac crescent tissue fuses at the embryonic primitive streak to form a beating heart tube. Positioned at either end of the heart tube are the outflow tract (OFT) and inflow tract (IFT). The OFT will eventually differentiate into the aorta and pulmonary arteries while the IFT will become the atrioventricular canal. As the heart tube begins to beat, SHF cells migrate from the pharyngeal mesoderm into the anterior part of the tube (reviewed in (9)). As the SHF migrates in, the future atria at the posterior end of the tube begin to kink and twist towards the left side of the embryo in the first display of left-right chirality. At about the 6^{th} week of human development, after heart looping, cardiac neural crest cells (CNC) migrate from the neural tube into the OFT and pharyngeal arches and are involved in patterning the aortic arch and in septation of the OFT. While the cardiac cell lineages are well understood, the mechanisms underlying subsequent morphogenetic events are complicated and remain to be elucidated.

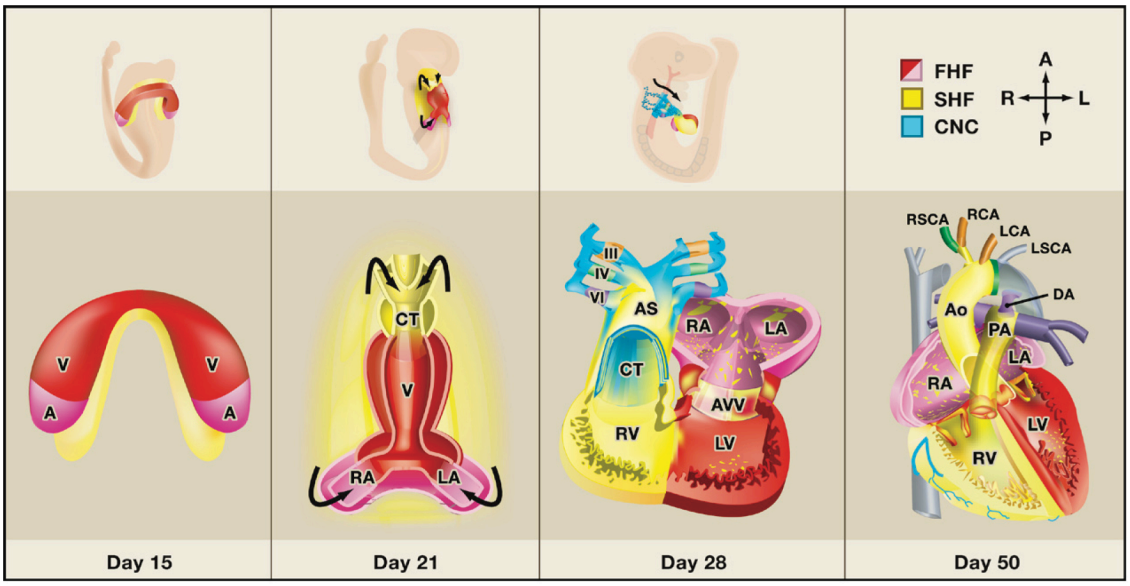

Figure 1: Mammalian Heart Development. Oblique views of whole embryos and frontal views of cardiac precursors during human cardiac development are shown. (First panel) First heart field (FHF) cells form a crescent shape in the anterior embryo with second heart field (SHF) cells medial and anterior to the FHF. (Second panel) SHF cells lie dorsal to the straight heart tube and begin to migrate (arrows) into the anterior and posterior ends of the tube to form the right ventricle (RV), conotruncus (CT) and part of the atria (A). (Third panel) Following rightward looping of the heart tube, cardiac neural crest (CNC) cells also migrate (arrow) into the outflow tract from the neural folds to septate the outflow tract and pattern the bilaterally symmetric aortic arch arteries (III, IV, and VI). (Fourth panel) Septation of the ventricles, atria, and atrioventricular valves (AVV) results in the four-chambered heart. V, ventricle; LV, left ventricle; LA, left atrium; RA, right atrium; AS, aortic sac; Ao, aorta; PA, pulmonary artery; RSCA, right subclavian artery; LSCA, left subclavian artery; RCA, right carotid artery; LCA, left carotid artery; DA, ductus arteriosus. (Borrowed with permission from Srivastava, Cell 2006 (REF), image by K.R. Cordes)

Septal Morphogenesis

In the final stages of cardiac morphogenesis, a complex parallel series of remodeling events occur to align the IFT and OFT of the heart with their corresponding chambers. During this time the cardiac septae also develop to divide the heart into four distinct chambers. Atrial septal defects (ASD) occur when either the primum or secundum septum does not fully form, creating a shunt for deoxygenated and oxygenated blood to mix inappropriately between the atria. The interventricular septum, on the other

hand, is made up of muscular, membranous, and conotruncal components. Like ASD, ventricular septal defects (VSD) can result from incomplete proliferation of cardiomyocytes in the muscular septum and it is interesting that a subset of muscular VSD and some ASD close spontaneously after birth. The membranous portion of the interventricular septum is responsible for separating the chambers at the crest of the septum, just below the aorta and pulmonary arteries. Similarly, the conotruncal septum is derived from a muscle bundle separating the aorta and pulmonary arteries that normally aligns with the muscular septum. Conotruncal septal defects typically arise from misalignment of the conotruncal septum with the muscular septum and therefore do not have the potential to close spontaneously. Finally, the atrioventricular canal cushions can be malformed, resulting in an atrio-ventricular septal defect (AVSD) that allows communication between both atria and both ventricles.

Outflow and Inflow Tract Morphogenesis

After the common OFT divides in a neural crest-dependent fashion into the two great arteries, the vessels rotate to connect to their respective ventricles, with the aorta connecting to the left ventricle and the pulmonary artery to the right ventricle.

The OFT and part of the IFT are also the precursors for all four cardiac valves, which are necessary for unidirectional blood flow. The valves are thin fibrous tissue that can open and close in a precise and flexible manner. The valves first develop at the border between either the OFT and ventricle or the IFT/atria and the ventricle (10). Extracellular matrix invades into these border zones between the endocardium and the myocardium, creating “cushions” that are the first visible structure that will give rise to the valve tissue. The myocardium then releases signaling factors that trigger the

endocardium to transdifferentiate into mesenchymal tissue (EMT) and then invade the cardiac cushion extracellular matrix. In a poorly understood process, the valve tissue then undergoes remodeling to form the mature valve. The mesenchymal cells proliferate and presumably differentiate into the fibroblasts that will compose the valves. Finally, the hypercellular valve tissue is remodeled, partially by apoptosis, into the mature, thin, valve leaflet (10).

Thickened valve leaflets cannot properly open and close and are one of the most common forms of childhood valvular disease. Thickening in any one of the four valves can result in a narrowing of the valve opening (stenosis) or allow blood to regurgitate across the valve. Severe thickening can result in complete obstruction across a valve as seen in hypoplastic left heart syndrome (HLHS) and pulmonary atresia. These conditions may result from excessive proliferation of valve cells or incomplete apoptotic loss during leaflet remodeling.

Cardiac Conduction Development

While vital for correct heart function, relatively little is known about the differentiation of the cardiac conduction system (reviewed in (11)). Work from model organisms is beginning to elucidate the conduction system lineages and genes necessary for their formation, but the cardiac conduction cells are specialized cardiomyocytes that are electrically coupled and have quicker rates of spontaneous contraction (12-14).

CONGENITAL CARDIOVASCULAR DISEASE GENE DISCOVERY

Due to the multifactorial nature of the disease, the etiologies of CCVM in humans are largely unknown. There are known environmental components, which have been

revealed from the increased risk of CCVM when a fetus is exposed to teratogens such as alcohol or anti-epileptic drugs early in pregnancy (15,16). Over the past decade of a number of single gene mutations that cause many forms of CCVM have revealed a significant genetic contribution as well. Many of these highly informative mutations were identified through the study of syndromes where multiple organs are affected. These syndromes are reviewed below (Table 1).

While these syndromes have helped elucidate some of the mechanisms of CCVM, the majority of CCVM occurs in isolation of any other organ malformation. Since 1998, a small number of genes have been linked to CCVM by performing linkage analysis on large families that have a clinical history consistent with autosomal dominant inheritance. There are also a number of other genes that may be risk factors for isolated CCVM from smaller preliminary studies that are not discussed here (Table 2).

Even though these families have provided clear evidence that single genes can cause isolated CCVM, most cases of CCVM are sporadic, in that there is no immediate family history. Recent work suggests that most of these sporadic CCVM are multifactoral with no single gene being totally responsible (47). As work with NKX2.5 suggests, some of these sporadic cases will be due in part to mutations in NOTCH1, JAGGED1, GATA4, MHC6, or TBX5, but each will probably account for less than 5% of CCVM (40-42,63-66). Due to the scarcity of pedigrees that lend themselves to forward genetic screens, new approaches will probably have to be taken to discover the other genes involved in human CCVM. A good example was the recent evidence that three copies of the mouse DSCR1 and DYRK1a genes, which are located on human chromosome 21, result in dysregulation of NFATc activity, which could then be

responsible for the CCVM seen in Down syndrome; while compelling, direct causality in humans still needs to be shown (67). Because of this, more work will need to be done to discover the common genetic polymorphisms that confer risk for sporadic CCVM. In the post-genomic era, the discovery of such risk factors may now be possible.

Table 1
Genetic etiologies of syndromic CCVM

Gene	Syndrome	Cardiac malformation	Reference
Fibrillin1/2	Marfan	Aortic aneurysm	[75,76]
TGFBR2	Marfan	Aortic aneurysm	[77]
NF1	Neurofibromatosis	PS	[78,79]
NF1	Neurofibromatosis–Noonan syndrome	PS	[33,34]
Elastin	William	SVAS	[80]
TBX5	Holt-Oram	ASD, VSD, conduction	[25,26]
JAG1	Alagille	PS, TOF	[42,43]
NOTCH2	Alagille	PS, TOF	[45]
ZIC3	Heterotaxy syndrome	d-TGA with heterotaxy	[81]
CFC1	Heterotaxy syndrome	d-TGA with heterotaxy	[82]
EVC/EVC2	Ellis-van Creveld	ASD	[83–85]
TFAP2β	Char	PDA	[28,29]
TBX1	DiGeorge/22q11.2 deletion syndrome	VSD, PTA, IAA, TOF	[20–22]
VEGF promoter (− 2578A/− 1154A/− 634G)	DiGeorge modifier	VSD, PTA, IAA, TOF	[61]
PTPN11/Shp2	Noonan	PS	[30]
MEK1 and MEK2	Cardio-Facio-Cutaneous	PS	[38]
B-Raf	Cardio-Facio-Cutaneous	PS	[39]
H-Ras	Costello	PDA, PS	[40]
K-Ras	Cardio-Facio-Cutaneous	PS	[39]
K-Ras	Noonan	PS	[41]
CHD7	CHARGE association	ASD, VSD, mitral valve defects	[86]
Sema3E	CHARGE association	ASD, VSD, mitral valve defects	[87]

ASD, atrial septal defect; d-TGA, dextrous-transposition of the great arteries; IAA, interrupted aortic arch; PDA, patent ductus arteriosus; PS, pulmonic valve stenosis; PTA, persistent truncus arteriosus; SVAS, supravalvular aortic stenosis; TOF, tetralogy of Fallot; VSD, ventricular septal defect.

Table 2
Genetic etiologies of non-syndromic CCVM

GENE	Inheritance	Cardiac malformation	Reference
NKX2.5	Autosomal dominant	ASD, conduction	[50,51–55]
JAG1	Partial penetrance	TOF	[46]
GATA4	Autosomal dominant	VSD, ASD	[57]
PROSIT240	Chromosomal translocation	d-TGA	[88]
MYH6	Autosomal dominant, partial penetrance	ASD	[58]
VEGF promoter (− 2578A/− 1154A/− 634G)	Modifier gene	TOF	[62]
NOTCH1	Autosomal dominant	BAV, calcification	[47]

ASD, atrial septal defect; BAV, bicuspid aortic valve; d-TGA, dextrous-transposition of the great arteries; TOF, tetralogy of Fallot; VSD, ventricular septal defect.

Table 1 and 2: **Genetic Etiologies of CCVM. (17-62)**

Haplotype Mapping of CCVM

The HapMap project (68) has identified 10,000,000 single nucleotide polymorphisms (SNPs) that occur in at least 5% of the general population and can be used to identify common variants associated with complex traits. Because genetic recombination is relatively rare and not uniform across the entire genome, there are SNPs that are in close proximity that will be inherited as blocks or haplotypes. The HapMap project identified a core group of 500,000 common SNPs that describe the haplotypes of most of the genome in four different ethnic groups. Using this core list, one could investigate cohorts of CCVM patients and controls to determine which haplotypes occur more often in the disease state. However, hundreds, maybe even thousands, of patients will be necessary to determine which haplotypes are subtle risk modifiers and could ultimately overlook the most deleterious risk factors that occurs in less than 5% of the general population (69).

Copy Number Variation in Chromosomal Sub-centimorgan Duplications/Deletions

The incorporation of gene copy number as a potential genetic risk factor may also be important as it is becoming clear that relatively small genetic duplications or deletions may segregate with disease (70). Improved genome-wide bacterial artificial chromosome (BAC) and oligonucleotide arrays will allow broader and more detailed screening for such events. A combination of copy number evaluation with genome-wide SNP associations may ultimately begin to reveal the genetic basis for common forms of CCVM.

Candidate Gene Screen

Knowledge from model organisms could help elucidate the molecular mechanisms underlying CCVM by allowing a shift from forward genetic positional cloning of human pedigrees to reverse genetic screens of candidate genes. Over 150 genes have been implicated in the cardiogenesis of model organisms so far, and the number continues to grow. From these candidates there is a clear bias for genes that act as nodal points that can affect the expression or activity of many genes simultaneously.

REGULATORY NODES IN CARDIOGENESIS

Transcriptional Nodes

The classical central dogma of molecular biology places "DNA transcription into mRNA" as the primary point where cellular components are produced. Transcription factors, proteins that bind to DNA and activate the transcription of nearby mRNAs, can be responsible for transcribing dozens if not hundreds of genes as parts of gene networks or programs in temporal or spatial patterns. If either the DNA or the DNA binding protein is mutated then part or all of a gene program may be disrupted or brought to a complete halt. Not surprisingly, many of the genes that have been linked to CCVM in humans and in model organisms regulate transcription either directly or indirectly.

TBX5 and Holt-Oram Syndrome

Holt-Oram Syndrome (HOS) leads to limb anomalies and cardiac defects that include ASD, TOF, and atrioventricular conduction defects. Haploinsufficiency of *TBX5* causes HOS and was the first single gene mutation described to cause human septation defects (71,72). Individuals with HOS can display broad phenotypic variability,

sometimes having severe CCVM with subtle hand abnormalities, or *vice versa*. TBX5 missense mutations can lead to defects of either the limbs or the heart depending on the domains affected (63). This has also provided an avenue for delineating the targets of TBX5 that give rise to the CCVM versus the hand abnormalities, such as Connexin 40, which may underlie the conduction defects in HOS (13).

NKX2.5

Linkage of four families with histories of ASD and atrioventricular conduction block to mutations in NKX2.5 was the first example of single gene mutations causing non-syndromic CCVM (73). NKX2.5 sequence variants have also been found in sporadic CCVM, although the contributions of these variants to the disease phenotype remains uncertain (40-42,65,66). Subsequent studies of Nkx2.5 in mouse models suggests that the conduction defect may be due to progressive loss of specialized conduction cells at the atrioventricular node and therefore familial ASD populations may benefit from periodic electrophysiologic monitoring (74).

GATA4

Another cause of septal defects (ASD, VSD, and AVSD), without conduction abnormalities, was identified in two families that had mutations in the GATA4 transcription factor (75). One of the families harbored a frameshift mutation with a premature stop codon that probably resulted in non-sense mediated decay of the mRNA. The second family had a missense point mutation, Gly295Ser, that affects a residue evolutionarily conserved from humans to yeast. Investigation of potential protein-protein interactions based on the common phenotype observed in humans with GATA4, TBX5 or NKX2.5 mutations revealed that GATA4 not only binds to TBX5, but that GATA4

Gly295Ser specifically disrupted this interaction. Strikingly, human mutations in TBX5 also disrupted interactions with GATA4 and NKX2.5. This provided evidence that a transcriptional complex including all three proteins may be necessary for proper septation of the human heart.

Translational Nodes

Most of the last two decades in human disease research has focused on transcriptional regulation. The recent discovery of a novel mechanism for translational regulation that utilizes small non-coding RNAs, microRNA (miR), has opened a whole new avenue for study. Thus far, only a handful of microRNAs have been shown to affect heart development (75) (mir133 DZ Wang 2005) and in humans no genes that regulate translation have yet been linked to CCVM. On the other hand, changes in microRNA expression has been characterized in multiple human disease states, including cardiac hypertrophy (76), which makes them tantalizing candidates for CCVM as well. Furthermore, multiple microRNAs have been characterized that target many of the same nodes that are disrupted in human disease (75,77). To determine which microRNAs should be treated as candidates for sequencing, it will be necessary to analyze their expression pattern and function in vitro and in model organisms (78). Many tools that were developed for the study of transcriptional node regulation are easily modified to the study of microRNAs and the validation of their targets (75) (79) although the prediction of which microRNA targets to focus on remains a difficulty for the field (75,80-82).

Post-Translational Nodes

Organogenesis requires finely regulated coordination of many cellular and extracellular cues. The signaling pathways that recognize and transduce the appropriate

response to these cues will many times carry out their program by post-translationally regulating various transcription factors. Signaling pathways for cardiogenesis have been shown to utilize post-translational modifications, such as adding phosphate, lipid, or even protein adducts. Other times the signaling effectors will translocate to different cellular compartments (i.e. the nucleus, etc.) to form larger order complexes, such as the mediator for activating transcription.

Notch Pathway Signaling in Alagille Syndrome and Outflow Tract Defects

Alagille Syndrome is a complex disease characterized by liver disease, pulmonic artery stenosis (PS), and occasionally tetralogy of Fallot (TOF) (83,84). Mutations in JAGGED1 (JAG1), a transmembrane ligand for the Notch family of receptors, are found in most cases of Alagille syndrome (33). Not surprisingly, mutations in the NOTCH2 receptor were also recently found to cause Alagille Syndrome in patients that lacked Jagged1 mutations (34). Together, mutations in Jagged1 and Notch2 account for nearly 75-95% of all cases of Alagille Syndrome.

The most recent gene linked to isolated CCVM also belongs to the Notch signal transduction pathway. A family with a history of OFT defects, predominately BAV and/or early-onset aortic valve calcification was linked to chromosome 9q34-35. Premature stop codons in the NOTCH1 gene were found to segregate with the CCVM in this family and a second unrelated family with a similar phenotype (85).

Given that three genes involved in Notch signal transduction have been implicated in the proper development of the mammalian outflow tract, it seems likely that other members of the Notch pathway may also be responsible for OFT and valvular CCVM. Since HRT1 and HRT2 mediate the Notch signal [50], they may function as

genetic modifiers for OFT defects such as BAV, pulmonic stenosis (PS), aortic stenosis (AS), or even sporadic TOF.

RAS/RAF/MAPK Signal Transduction in the Noonan Syndrome Family (Cardio-Facio-Cutaneous, Costello, and Noonan)

Three syndromes with many overlapping clinical symptoms have revealed a signal transduction pathway controlling formation of the pulmonary valve. Mutations in the *PTPN11* gene, encoding the protein phosphatase Shp2, were linked to Noonan syndrome, characterized by a thickening of the pulmonary valve leading to stenosis (23). Patients with Noonan Syndrome may also have characteristic facial features and chest deformities. Two other syndromes, Cardio-Facio-Cutaneous syndrome and Costello syndrome, have similar clinical features but no mutations in *PTPN11* could be linked to them (24,86). One of the known roles of Shp2 involves the RAS/MAPK pathway, and mutations in the RAS inhibitor, NF1, have been associated with patients with clinical symptoms of Noonan and neurofibromatosis (25,26). *In vitro* studies of Noonan syndrome mutations also found an increase in the MAPK/RAS signal transduction pathway (87,88). Additionally, mice with *PTPN11* mutations exacerbated the valve defects induced by hypomorphic epithelial growth factor alleles, which also affect RAS/MAPK signaling (89).

Consistent with this, mutations in MEK1/2 (27), K-RAS (28), and B-RAF (28), have recently been associated with CFCS, and mutations in H-RAS were observed in Costello syndrome (29). However, K-RAS mutations were also recently discovered in patients with Noonan syndrome (30), suggesting that there may be genetic overlap between Noonan syndrome and CFCS. Given that valve stenosis can require multiple

surgical interventions throughout life, and that the MAPK/RAS pathway has already being studied as therapeutic targets for certain cancers, there could be a potential for non-surgical therapies for patients suffering from cardiac valve stenosis by targeting these oncogenes.

CONCLUSIONS

Using the genes discovered in the syndromes and large families, a few, small scale, candidate-gene-screen trials have already searched for mutations in patients with no family history of CCVM. These screens, focusing on 4-10 genes, have thus far found that mutations are relatively rare in individual genes, suggesting that the number of candidates needs to be increased (90,91). On the other hand, the number of genes known to play a role in cardiogenesis continues to grow, so any sequencing effort will need to update their lists often. Traditional Sanger-reaction derived sequencing will probably have to focus only on exonal coding sequence and nearby extend to intragenic introns and intergenic enhancers/promoters. Newer methods of sequencing, such as the platforms offered by Illumina and 454 will allow high throughput sequencing to search more and more genes with less starting material. As the cost of sequencing continues to follow Moore's Law and gets below the $1,000/genome range, this type of candidate screen will become increasingly tractable for the evaluation of complex traits like CCVM (92).

CHAPTER 2. HUMAN SEQUENCE VARIANTS ARE ASSOCIATED WITH OUTFLOW TRACT DEFECTS AND REVEAL MYOCARDIN AUTOINHIBITION.

Joshua F. Ransom[1,3,4], Sebastian Schroeder[2], Isabelle N. King[1,4], Melanie Ott[2], Vidu Garg[5], and Deepak Srivastava[1,3,4]

Gladstone Institute of Cardiovascular Disease[1] and Neurological Disease[2] and Departments of Biochemistry & Biophysics[3] and Pediatrics,[4] University of California, San Francisco, California, and Departments of Pediatrics and Molecular Biology[5], University of Texas Southwestern Medical Center, Dallas, Texas

ABSTRACT

Congenital cardiovascular malformations (CCVM) occur in nearly 1% of births worldwide, but to date only a handful of genes have been linked to human CCVM. In a search for novel CCVM mutations in candidate heart development genes we identified two human sequence variations in Myocardin (MYOCD). These variations resulted in a missense mutation at 1) codon 259 (K259R) or 2) codon 647 (Q647H). Genotyping of multiple patient cohorts revealed that the Q647H variation was enriched in patients with thickened/stenotic outflow tract valves, but that the K259R variation was too rare to determine association.

Myocardin (MYOCD) is a transcriptional coactivator that promotes cardiac or smooth muscle gene programs through its interaction with myocyte-enhancing factor (MEF2) or serum-response factor (SRF).

Both the K259R and Q647H variations created hypomorphic cardiac isoforms in *in vitro* reporter assays. Q647H resulted in attenuated transcriptional coactivation, but had no effect on interactions between MYOCD and SRF. *In silico* sequence analysis suggests that Q647H is near two potential phosphorylation sites for the mitogen activated protein kinase (MAPK) and/or glycogen synthase kinase 3 beta (GSK3β). Mutations in

the three serines nearest to Q647 revealed a potentially phospho-dependent activating signal at the two predicted kinase recognition sites. Preliminary results suggest that Q647H disrupts a GSK3β–dependent activation signal that may be dependent on priming by a MAPK.

The K259R variation created a hypomorphic cardiac isoform with impaired SRF binding but did not impair the smooth muscle isoform of MYOCD, which lacks the amino terminus. The cardiac-specific amino terminus (MHD) acted in an autoinhibitory fashion to bind and repress SRF-dependent MYOCD activity *in vitro*. Consistent with these results, MYOCD-K259R had a greater response to amino terminus–dependent inhibition. The amino terminus was also sufficient to impair MYOCD-dependent fibroblast conversion into smooth muscle cells as well as cardiomyocyte hypertrophy. Furthermore, the K259R mutation resulted in hyperacetylation of the MYOCD protein by the p300 histone acetyltransferase. Overexpression of p300 was found to relieve MHD-dependent autoinhibition of MYOCD through a disruption of the intramolecular interactions between the MHD and MYOCD.

These findings identify novel mechanisms that regulate levels of MYOCD-dependent activation of the SRF gene program and may have implications for human congenital cardiovascular malformations.

INTRODUCTION

The majority of patients with CCVM have sporadic disease, with no immediate family history of CCVM. Furthermore, CCVM is a multifactorial disease with many contributing genetic factors (93,94). As such, classic genetic linkage analysis is highly

unlikely to reveal genetic etiologies that have only minor contributions to the resultant phenotype. Over 100 candidate genes are known to play a role in heart development based upon expression analysis and genetic manipulation in model organisms.

Myocardin (MYOCD) was the first recognized member of a family of transcriptional coactivators that bind to serum response factor (SRF) to activate cardiac or smooth muscle gene programs (95). SRF-dependent activation of MYOCD is dependent upon the ratio of SRF to MYOCD, and disproportionately high levels of SRF lead to reduced MYOCD activity reminiscent of inhibitory feedback (95). The two other MYOCD-related transcription factors (MRTF), MRTF-A (also known as MAL, MKL1, or BSAC) and MRTF-B (MKL2), also co-activate SRF but to different extents (96) (rev. in (97-99). All three members of the MYOCD family are coexpressed in the developing myocardium and in distinct populations of smooth muscle cells (100-102). In mice, targeted deletion of the SRF interaction domain in MYOCD or MRTF-B led to early embryonic lethality from cardiovascular defects, apparently due to insufficient smooth muscle specification in the distal aorta or outflow tract (100,101). Conditional deletion of MYOCD from smooth muscle derived from the cardiac neural crest lineage resulted in neonatal lethality due to outflow tract defects, including patent ductus arteriosus (103).

Cardiac and smooth muscle both express MYOCD, but the smooth muscle isoform ($MYOCD^{\Delta MHD}$) lacks part of the MYOCD homology domain (MHD) (104). The MHD, found in the amino terminus of cardiac MYOCD, contains three RPEL motifs that regulate actin-dependent nuclear localization in MRTF-A/B but not in MYOCD (105). While MYOCD is constitutively nuclear, its MHD contains a binding site for myocyte-enhancing factor 2 (MEF2), which activates portions of the cardiac gene program that are

distinct from the SRF-dependent program (104). MYOCD's SRF binding motif is similar to that in ELK1. In cardiac muscle, ELK1 and MYOCD compete for binding to SRF (106), but the mechanisms that regulate MYOCD-SRF interactions or the SRF dose-dependent decrease in MYOCD activity are unknown.

MYOCD is a potent inducer of cardiomyocyte hypertrophy and dominant negative MYOCD, lacking the transactivation domain, can inhibit a variety of hypertrophic stimuli (107). Furthermore, these hypertrophic stimuli are able to activate the MYOCD protein post-translationally, but through an unknown mechanism (107). The hypertrophic response in cardiomyocytes can be inhibited by activation of the GSK3b kinase, which directly phosphorylates MYOCD (108). It is unknown whether hypertrophic stimuli activate MYOCD solely by inhibiting GSK3β or through other unknown post-translational modifications (109). Multiple members of the MAPK family of kinases also are involved in the hypertrophic response. Phenylephrine is able to induce hypertrophy through the extracellular response kinase (ERK) 1/2 but the stress activated kinase, p38a, is able to inhibit hypertrophy both in vitro and in vivo (110).

Here, we describe one uncommon and one rare missense mutation that we discovered in the gene encoding MYOCD of three patients with pulmonary or aortic valve stenosis. Both mutations resulted in hypomorphic cardiac MYOCD. One mutation, Q647H, was statistically associated with cardiac outflow tract defects, predominately aortic and pulmonic valve stenosis. Q647H disrupts a kinase-dependent activation motif between amino acids K644 to P653. The other mutation, K259R, despite creating a hypomorphic cardiac isoform, did not affect activity of $MYOCD^{\Delta MHD}$. In exploring the mechanism, we found that the amino terminus regulated MYOCD activity in an

autoinhibitory fashion by binding to MYOCD and disrupting SRF-dependent activation. This autoinhibition was more pronounced in the MYOCD K259R mutant and was regulated by p300-dependent MYOCD acetylation. These findings suggest a novel mechanism for regulation of MYOCD activity *in vivo*.

MATERIALS AND METHODS

Plasmid Construction—FLAG-MYOCD truncations, atrial natriuretic factor–luciferase (ANF-Luc), and smooth muscle 22_–luciferase (SM22_-Luc), were kindly provided by Eric Olson, University of Texas Southwestern Medical School, Dallas, TX and have been described (95). MHD truncations were created by PCR amplification of MYOCD cDNA with added 5′ end *Not*I and 3′ end *Xba*I restriction enzyme sites. K259R, R71R115>AA, and D130E135>AA were mutated with the Quickchange II kit (Stratagene), according to the manufacturer's instructions. All mutations were confirmed by sequencing. Primer sequences are available upon request.

Cell Culture and Transfections—Cos-1 cells (American Type Culture Collection) were maintained and passaged as described (111). Transfections were carried out in 12-well dishes, unless otherwise indicated. Cells were transfected with 50 ng of each reporter plasmid and 100 ng of each cDNA for 40-44 h and harvested in Passive Lysis Buffer (Promega). Total amounts of DNA were kept constant with corresponding expression vector without a cDNA insert. A CMV-LacZ plasmid was cotransfected for internal transfection efficiency control (95). Western analysis was performed for all transfected proteins to ensure equal expression. Luciferase assays were performed with a PerkinElmer Victor3 plate reader as described (111).

CH310T1/2 cells (American Type Culture Collection) were maintained and passaged as described, except that the plates were coated with 1% gelatin for 30 min before passaging (112). Transfections were performed with FuGene6 (Roche), according to the manufacturer's instructions. Twenty-four hours after transfection, the cells were switched to Dulbecco's modified Eagle's medium containing 2% horse serum. Seven days later, immunocytochemistry and quantitative real-time (RT) PCR (Taqman, Applied Biosystems) were performed. For each experiment, 500 ng of each cDNA was used for each well of a six-well plate. A CMV-eGFP plasmid (100 ng, Amaxa) was cotransfected as an internal control for transfection efficiency. Cells were transfected and counted double-blind. Conversion efficiency was calculated as the number of SM-_-actin-positive cells divided by the number of GFP-positive cells.

Primary cardiomyocytes were harvested from 0–2-day-old Sprague-Dawley rats as described (107) with minor modifications. The cardiomyocytes were enzymatically separated with 1 mg/ml pancreatin, plated on 0.1% gelatin-coated dishes, and infected 1 day later with lentivirus (pLenti6 Gateway System, Invitrogen) overexpressing protein under control of the EF1 promoter. Twenty-four hours later, phenylephrine (PE) was added to the medium (final concentration, 20 μM.) Forty-eight hours after infection, immunofluorescence and quantitative RT-PCR were performed. Area calculations of the alpha-actinin-positive cells were made using Image-Pro 5.0 software; control cells without PE were set at an arbitrary value of 100 then each condition were set proportionate to the control cells. Cardiomyocyte infection and area calculations were performed double-blind.

Quantitative RT-PCR—Whole RNA was purified with TRIreagent (Applied Biosystems), treated with DNAfree DNAse (Ambion), and synthesized into cDNA with poly-dT primers (Superscriptase III kit, Invitrogen), according to the manufacturer's instructions. RT-PCR was performed with Applied Biosystems 2X master mix and Taqman primers (see Supplemental Table S1) as described (111). Analyses were performed using the $2^{(-\Delta\Delta Ct)}$ method.

Protein Interaction Assays—Coimmunoprecipitation (Co-IP) and electromobility shift assays (EMSA) were performed as described (95). For Co-IP, 1 μg of FLAG-MYOCD and 100 ng of hemagglutinin-tagged SRF were transfected, and harvested 40 hours later. For EMSA, protein was translated from 1 μg of each plasmid with the Promega TnT kit. An oligonucleotide containing the c-*fos* CArG box (95) was ^{32}P-labeled with the Roche high-prime labeling kit.

Immunocytochemistry and Western Blot—Immunocytochemistry and Western analysis were performed as described (111). Antibodies were diluted as follows: mouse anti-SM-_-actin (Sigma), 1:1000; mouse anti-alpha-actinin (Sigma), 1:200; mouse anti-FLAG (M2, Sigma) 1:5000 (Western) or 1:500 (immunocytochemistry); and mouse anti-Myc (9a7, Santa Cruz Biotechnology), 1:1000. FITC- or TRITC-conjugated goat anti-mouse secondary antibodies were used for immunocytochemistry, and alkaline phosphatase-conjugated goat anti-mouse or goat anti-rabbit antibodies were used for Western analysis (Jackson Immunologicals).

Knock In Strategy—Children's Hospital Oakland Research Institute BACs (BPRC, Library RPCI-22 #382-17B and #416-6H, derived from 129/Sv6 mice (100,101)) were obtained for chromosome eleven that contain the mouse Myocardin

gene. A 10 kilobasepair portion of *Myocardin* that spans exons 7-10, was obtained by enzymatic digestion of the BACs with EcoRI, which was subsequently ligated with an EcoRI digested pBluescript2 KS+ vector. The ligated plasmids were transformed into chemically competent E.Coli (One Shot TOP10, Invitrogen). Colonies were screened for exon 8 of Myocardin and then sequenced to confirm correct DNA sequence for the entire 10 Kb genomic region. K259R and an AvrII restriction enzyme site were introduced into exon 8 by PCR sewing mutagenesis followed by ligation to insert the mutated exon 8 into the targeting vector. A LoxP-Neomycin-LoxP resistance cassette (from the pDelboy 3 plasmid, kind gift of Olson lab) was inserted 1.5 Kb downstream of exon 8 into a PacI site in the midst of an evolutionarily non-conserved intronic region. Vector linearization was performed using either SspI or the NheI and ApaLI restriction enzymes, followed by agarose gel purification of the approximately 8 Kb digested band. Electroporation of the DNA into E14 ES cells (derived from 129/Ola mice), growth and picking of ES colonies in selection media, and DNA purification from ES colonies has all been described previously (113). Southern blot analysis was performed as previously described (100,101) on DNA from ES colonies digested with EcoRI and BglI. Probes for southern analysis were a kind gift from DaZhi Wang (UNC Chapel Hill, (100,101)). Wildtype bands were 10 Kb, while targeted ES cells are 7 Kb 5' bands and 5 Kb 3' bands.

RESULTS

Sequence Variants in the MYOCD Gene in Patients with Congenital Cardiac Malformations

To bypass the limitations of using reverse genetics for genetic linkage in our cohort of CCVM patients with no family history of disease, we decided to use a forward genetic candidate gene screen. At the time of our study's inception, approximately 100 genes were known to play a role in heart development based upon expression analysis and genetic manipulation in mammals (Mus musculus), avians (Gallus gallus), amphibians (Xenopus laevis), fish (Danio rerio), and invertebrates (Drosphila melanogaster). An initial sequencing screen was performed of every known exon for these 100 candidate genes in 60 patients (Garg et al., in preparation). From this sequencing, 3 patients were found to harbor sequence variations in the MYOCD gene's coding sequence (GenBank Accession No. AF532596). Two of the patients (one Asian, and one Caucasian) had G>C mutations at coding sequence residue 1943. This resulted in a change at the wobble position of codon 647 (G1941C, Fig. 2.1C) of Glutamine to Histadine (Q647H). The other patient (Hispanic) had an adenonsine-to-guanosine mutation at residue 776 that resulted in an arginine substitution for a highly conserved lysine at codon 259 (A776G, Fig. 2.1B). Each patient had thickened aortic or pulmonic valve leaflets that resulted in valve stenosis (narrowing of outflow across the valve). Neither of these mutations were present in 300 control chromosomes that were sequenced along with the patients. Sequence alignments show that both K259 and Q647H are evolutionarily conserved from all known mammals and in avians (Fig. 2.1*D,E*), suggesting that both residues are under selective pressure and may be important for

MYOCD function. K259R is also conserved in MRTF-A, but MRTF-B contains an arginine at the corresponding codon (R288, Fig. 2.1*D*). In *in vitro* assays, MRTF-B is less active than MYOCD or MRTF-A on most promoters (96). This appeared to be a statistically rare confluence based upon the many varieties of CCVM present in the cohort of 60 patients and the number of genes that were sequenced.

We next determined if either of the two sequence variations were present in other patient cohorts. Taqman SNP assays (Applied Biosystems) were designed for K259R and Q647H. Four separate patient cohorts were tested including, (1) 207 patients with various CCVM from UT Southwestern, Dallas, Tx, (2) 1152 members of the Reynolds Population from UT Southwestern, Dallas, Tx (which includes patients with adult onset valve calcification), (3) 47 patients with Aortic valve stenosis from Dr. Paul Grossfeld (UC San Diego), San Diego, Ca, (4) 267 patients with adult onset valve calcification from Dr. Salah Mohammed, Lübeck, Germany, and (5) a family from Quebec, Canada that has a history of bicuspid aortic valve, which is a risk factor for developing aortic valve stenosis later in life. From this analysis the prevalence of the Q647H variation was higher in the general population than our initial sequencing of 150 control patients suggested; approximately 1.3% of all controls had one allele that was Q647H. During analysis of racial genotypes, we observed that in Caucasian populations the prevalence of Q647H was even higher, approximately 3.2% (11 QH vs 328 QQ), while only about 1% of Hispanic controls had a Q647H allele (2 QH vs 212 QQ). We never observed a case of homozygous Q647H, but the predicted incidence is very low, even in Caucasians only about 1 in every 4400 people would be predicted to be homozygous. Strikingly, we observed that even though there was broad variety in the types of CCVM that were

present in the Dallas cohort, seven out of the eight patients that had MYOCD mutations also had some form of outflow tract valve disease (Fig. 2.1*F*). When we analyzed the cohorts for the prevalence of Q647H we found that patients who were specifically diagnosed with childhood outflow tract defects (Dallas and San Diego) had a statistically enriched prevalence of Q647H. Just over 7% of Caucasians in Dallas (5 QH vs 62 QQ, $p<0.05$ versus controls, χ^2 df=1, Fig. 2.1*G*) and 5% of Hispanics in San Diego (2 QH vs 35 QQ, $p<0.01$ versus controls, χ^2 df=1, Fig. 2.1*G*) had Q647H. Taken together this was about two to three fold more prevalent than the race matched controls, but because no Q647H alleles were found in Dallas Hispanics (n=26) or San Diego Caucasians (n=9) we did not achieve statistical significance when we merged the two geographical data sets ($p<0.11$ versus controls, χ^2 df=3). On the other hand, the patient populations for the adult valve disease (Germany or Reynold's population in Dallas) and non-outflow tract CCVM (Philadelphia) did not show any signs of statistical enrichment for Q647H ($p<0.20$ for either cohort versus controls, χ^2 df=1). Based on these results, Q647H is probably associated with CCVM of the aortic and pulmonary valves, but not adult onset valve disease, although a larger cohort will be needed to provide statistical significance.

K259R was found one time in a Hispanic control and not in any other patient population (control n=1152, patients n=598, Fig. 2.1*F*). Due to the rarity of K259R, there was statistical enrichment between the 212 Hispanic controls and 26 patients in Dallas (1 KR vs 25 KK, $p<0.01$, χ^2 df=1) but a low frequency raises the issue of true significance. When our calculations included the San Diego Hispanics we lost statistical significance (1 KR vs 50 KK, $p<0.19$, χ^2 df=1). To determine if K259R can reduce MYOCD activity enough to disrupt cardiogenesis, we are attempting to create a mouse line that has had an

arginine knocked-in to lysine 255 (which is homologous to human lysine 259) via homologous recombination (Fig 2.1B).

The targeting vector was first digested with SspI, generating a 5' long arm of 4 KB and a 3' short arm 1.1 KB (Fig 2.2A). After electroporation and Neomyocin selection, 500 colonies were collected and screened via southern blotting for targeting at the MYOCD locus. Only one colony showed targeting at the 5' arm (long arm) but the 3' end was not targeted. I hypothesized that the ineffective targeting was due to the length of the 3' arm and so the targeting vector was prepared for reelectroporation using a different linearization protocol. The plasmid DNA was digested using ApaLI and NheI to generate a long arm of 4.6 KB and a short arm of 2.1 KB. This construct was then electroporated and selection was repeated as before. Southern screening of 250 colonies revealed 1 colony with 5' and 3' arm targeting (Fig 2.2*B*). This colony, with targeting at both arms, was sent to UC Davis for revival and expansion. Unfortunately, the colony would not expand. At this time, since we were able to target the MYOCD locus, the linearized targeting vector is being repurified and sent to the UCSF knockout core for a third round of electroporation using the new linearization protocol.

MYOCD Sequence Variations K259R and Q647H are Hypomorphic and K259R Has Reduced SRF Affinity

Both MYOCD sequence variations occurred in evolutionarily conserved regions. Since the Q647H sequence variant was associated with CCVM we hypothesized that the variations would affect MYOCD-dependent promoter activation of SRF-dependent targets (95). Transient cotransfection of the 935–amino acid, cardiac-specific isoform of MYOCD ($MYOCD^{935}$) with luciferase reporters driven by the SM22α–Luc or ANF–Luc

promoter showed that K259R and Q647H MYOCD^{935} were hypomorphic compared to wildtype (WT) MYOCD^{935} (Fig. 2.3*A,B*). The reduced activity was not due to changes in cellular localization, as WT, K259R, and Q647H MYOCD^{935} all localized to the nucleus (Fig 2.3*C*).

K259 is not contained in the SRF-binding B-box, but does lie within the lysine-rich basic domain that is necessary for SRF binding (95). We hypothesized that the reduction in MYOCD K259R and Q647H activity was due to a corresponding reduction in binding between MYOCD and SRF. In co-IP assays we were unable to detect an interaction between MYOCD^{935} K259R and SRF, but WT MYOCD^{935} showed normal SRF binding (Fig 2.3*D*). In the more sensitive EMSA, MYOCD^{935} K259R bound to SRF but with less affinity than WT MYOCD^{935} (Fig 2.3*E*). Q647H MYOCD^{935} bound to SRF normally though (Fig 2.3*E*).

MRTF-B is a weaker activator than MYOCD or MRTF-A, and we hypothesized this may be due, in part, to the evolutionarily divergent arginine at codon 288. Mutation of arginine 288 to lysine (R288K) increased MRTF-B-dependent activation of SM22α-Luc nearly 5-fold (Fig 2.3*F*). While this was still well below the levels achieved with MYOCD or MRTF-A *in vitro,* it demonstrates that the two basic amino acids are not functionally equivalent in this domain and that an arginine at this residue of the MYOCD family of proteins is sufficient to limit their transactivation potential of MYOCD proteins.

MYOCD Q647H is Located Near And Dysregulates Predicted Kinase Phosphorylation Motifs

Q647H is located in an evolutionarily conserved region that has no known function. This region is highly enriched for serines, from amino acids 615 to 712 there are 27 serines out of the 98 residues (MotifScan, http://myhits.isb-sib.ch/cgi-bin/motif_scan). Multiple of these serines near to Q647 (including S650 and 654) are predicted to be phosphorylated, especially serine 654 (NetPhos, http://www.cbs.dtu.dk/services/NetPhos), but no program used predicted phosphorylation of Serine 645.

We hypothesized that Q647H was hypomorphic due to the dysregulation of the predicted phosphorylation sites at S650 or S654. The serines closest to Q647 (Fig. 2.1*E*, S645, 650 and 654) were mutated to either glutamates (S>E) to mimic the negative charge of phosphorylation or to alanines (S>A) to mimic constant dephosphorylation. Mutation of S645 to either E or A had no appreciable effect on MYOCD activity, but mimicking phosphorylation with either S650E or S654E increased MYOCD-dependent activation of the SM22-Luc reporter (Fig. 2.4*A*). Conversely, S650A and S654A reduced MYOCD-dependent activation of the SM22-Luc reporter (Fig. 2.4*A*). Along with the in silico predictions, this suggests that the serines near to Q647 are phosphorylated to activate MYOCD, and that Q647H may disrupt one or more of these phosphorylation events.

Wnt/GSK3β/ β-Catenin signaling is known to lead to cardiac valve stenosis in zebrafish when Wnt is hyperactivated or when GSK3β has been inhibited (114,115). GSK3β binds to serines that have already been phosphorylated by a priming kinase. After binding to the primed site GSK3b then proceeds to phosphorylate serines or threonines that are separated by four amino acids towards the N-terminus of the binding serine

(S/TxxxP-S). MYOCD serine 650 would be a predicted GSK3β phosphorylation site if S654 were first primed by another kinase. To test whether GSK3β played a role in the Q647H partial loss of function, we transiently coexpressed constitutively active GSK3β (S9A) along with WT and Q647H MYOCD^{935}. While this research was on going, it was recently shown that GSK3β is able to inhibit MYOCD by directly phosphorylating at six serines (S455, 459, 463, 624, 628, and 632, (108)).

Contrary to the initial hypothesis but in agreement with the published report, GSK3β overexpression inhibited WT MYOCD in a dose dependent manner on the SM22-Luc reporter (Fig. 2.4*B*). Surprisingly though, Q647H MYOCD displayed a different dose response curve where the lowest doses of GSK3β highly activated Q647H. Higher levels of GSK3β activated Q647H less and MYOCD Q647H was inhibited at the highest doses of GSK3β (Fig. 2.4*B)*. Inhibition of GSK3β by LiCl relieved both the activation and inhibition of WT and Q647H confirming that this differential effect was dependent upon GSK3β (Fig. 2.4*C*). We hypothesize that the Q647H mutation is disrupting a kinase-dependent activation signal that utilizes low levels of GSK3β activity, probably through other effecters. Higher levels of GSK3β activity though are able to directly phosphorylate MYOCD and leads to MYOCD inhibition. Without the S650/S654-dependent activation signal, MYOCD Q647H would have a lower basal activity in cells.

Cardiac But Not Smooth Muscle Myocardin K259R Is Hypomorphic and Has Reduced SRF Affinity

Since MYOCD is expressed in both cardiac and smooth muscle lineages that affect the outflow tract valves, we tested whether K259R affected the MYOCD$^{\Delta MHD}$ in a

similar fashion to the cardiac isoform. While Q647H MYOCD$^{\Delta MHD}$ was hypomorphic in comparison to WT MYOCD$^{\Delta MHD}$, in contrast to what was observed with MYOCD^{935}, K259R MYOCD$^{\Delta MHD}$ was functionally normal in luciferase reporter assays using the SM22_ promoter (Fig. 2.5*A*). Furthermore, WT and K259R MYOCD$^{\Delta MHD}$ showed similar SRF binding affinities, as assessed by CoIP (Fig. 2.5*B*) and EMSA (Fig. 2.5*C*).

The MYOCD MHD Inhibits MYOCD-Dependent Transcription in Vitro *by Binding to MYOCD and Blocking Its Interaction with SRF*

Based on the differences in functional consequences of MYOCD K259R between cardiac and smooth muscle isoforms, we investigated whether MYOCD's MHD acts in an autoinhibitory fashion by disrupting SRF-dependent MYOCD activation (116). Expression of amino acids 1–195 alone inhibited transactivation by MYOCD on the SRF-dependent reporters described earlier, and expression of amino acids 1–149 did so in a dose-dependent manner; however, amino acids 1–129 did not inhibit MYOCD activity (Fig. 3*A*). Truncation of the MHD amino terminus revealed that amino acids 1–30 were dispensable for inhibition of MYOCD transactivation (Fig. 2.6*A*). Thus, the minimal MYOCD autoinhibitory domain lies between amino acids 30 and 149.

MRTF-A's MHD has been well characterized as an actin-dependent regulator of nuclear localization (105,117); however, MYOCD is thought to be constitutively nuclear (95,105). Like MRTF-A, MYOCD contains two conserved RPEL motifs in the minimal inhibitory MHD. There is one evolutionarily divergent RPEL motif that is partially in the minimal inhibitory MHD, but due to its lack of conservation, it was discounted from the experiments. In previous reports, mutation of the RPEL motif's conserved arginines to alanine disrupted the MHD-dependent nuclear localization of MRTF-A (105). We found

that mutation of the two conserved RPEL motifs (R71A, R115A) had no effect on the MHD's ability to inhibit MYOCD activity, suggesting that the RPEL motifs are not necessary for autoinhibition (Fig. 2.6*B*). Another known motif within the MHD is the MEF2 binding site, located in the first 17 amino acids of MYOCD (118). Since amino acids 1–30 were not necessary for inhibition, the MEF2 binding domain may also be dispensable for inhibition of SRF-dependent MYOCD activity (Fig. 2.6*A*).

Since the RPEL and MEF2 binding motif were not necessary, and MHD1–129 was insufficient to inhibit MYOCD coactivation, we focused on amino acids 129–149. Sequence analysis identified no recognizable motifs, but revealed two acidic residues that are conserved from humans to amphibians: aspartate 130 (D130) and glutamate 135 (E135). Mutation of these two negatively charged residues to uncharged alanines (DE>AA) disrupted the autoinhibition (Fig. 2.6*B*).

Next, we investigated whether the MHD was a true autoinhibitory domain that directly binds to MYOCD via intramolecular interactions. In Co-IP experiments, truncated MHD that contained the minimal autoinhibitory domain bound to MYOCD, although the 30–149 construct had less affinity than the 1–149 construct (Fig. 2.6*C*). Furthermore, mutation of both D130 and E135 blocked MYOCD:MHD interactions, but mutation of the conserved RPEL motifs did not. This finding may explain why MHD containing DE>AA mutations was not inhibitory in the luciferase reporter assays.

Consistent with the hypothesis that MYOCD K259R is hypomorphic due to its increased autoinhibition, K259R MYOCD$^{\Delta MHD}$ displayed more MHD-dependent inhibition than WT MYOCD$^{\Delta MHD}$ (Fig. 2.6*D*).

The MYOCD MHD Inhibits MYOCD-Dependent Smooth Muscle Production and Cardiomyocyte Hypertrophy and Disrupts Normal Cardiac Morphogenesis

MYOCD has a limited capacity to transdifferentiate CH310T1/2 fibroblasts into smooth muscle cells (112). Since truncations of MYOCD lacking the MHD showed greater smooth muscle conversion than $MYOCD^{935}$, we hypothesized that this phenomenon might be explained by amino terminus autoinhibition. We therefore tested whether introduction of MHD1–149 would repress MYOCD-dependent smooth muscle conversion (Fig. 2.7*A,B*). $MYOCD^{\Delta MHD}$ converted approximately 40% of transfected 10T1/2 fibroblasts into SM-α-actin-positive cells within 7 days. Consistent with our *in vitro* reporter assay results, MHD1-149 inhibited the conversion efficiency by about 50% (Fig. 2.7*A,B*). Neither the RPEL motifs nor the MEF2 binding domain was necessary, but the two acidic residues (D130, E135) were required for effective inhibition (Fig. 2.7*B*). We next tested the mRNA transcript levels of multiple MYOCD target genes by quantitative RT-PCR to determine if MHD-dependent inhibition affected genes other than SM-α-actin. MHD-dependent inhibition extended to multiple other direct MYOCD targets such as *SM22α*, *ANF*, and *smooth muscle calponin* (Fig. 2.7*C*).

We determined whether the MHD affects MYOCD activity in cardiomyocytes. MYOCD induces a hypertrophic response in primary cardiomyocytes (107,108), and a dominant-negative MYOCD (DN-MYOCD) inhibited hypertrophic responses to chemicals such as PE. We hypothesized the MHD might mimic that effect. Indeed, WT but not DE>AA MHD 1–149 inhibited PE-induced cardiomyocyte hypertrophy, as

assessed by measurements of cell surface area (Fig. 2.8*A,B*). With the *in vitro* experiments above, this observation suggests that the inhibition of hypertrophy was dependent on SRF/MYOCD and independent of MEF2, since the DE>AA mutant still retained the MEF2 binding domain. The hypertrophic response is normally accompanied by an increase in expression of the ANF, BNP and Sk-a-actin transcripts and a decrease in GSK3β expression (107,108). Consistent with the calculations of surface area, DN-MYOCD and WT MHD inhibited the PE-induced changes in hypertrophic gene expression to a greater extent than the mutant MHD (Fig. 2.8*C*). Strikingly, the WT MHD was almost as effective as DN-MYOCD at inhibiting the hypertrophic response in cardiomyocytes, indicating that autoinhibition is very effective at regulating MYOCD activity (Fig. 2.8*C*).

To test whether the MHD would have any effect *in vivo,* we transgenically overexpressed MHD1-149 in the developing heart under control of the β-myosin heavy chain (β-MHC) promoter (β-MHC-MHD^{WT}, (119)). β-MHC-MHD^{WT} mice did not survive to weaning, and embryonic day (e)17.5 embryos had a thin myocardium with muscular and membranous ventricular septal defects (VSDs, n=2), although gross heart failure was not evident (Fig. 2.8*D*). These cardiac defects were not observed in transgenic embryos expressing the mutant MHD (β-MHC-MHD$^{DE>AA}$, n=2), which failed to inhibit MYOCD *in vitro* (Fig. 2.8*D*). Both transgenic mouse lines, MHD^{WT} and MHD$^{DE>AA}$, were non-viable suggesting that only some of the effect of the MHD is directly through inhibition of MYOCD-dependent SRF target genes.

The Histone Acetyltransferase, p300, Acetylates MYOCD To Regulate MHD Autoinhibition

In vitro, transfected MYOCD protein is responsive to extracellular hypertrophic stimuli on synthetic promoters apparently without affecting steady state protein levels (107). MYOCD is sumoylated by the PIAS1 ligase and associates with the histone acetyltransferase (HAT), p300, which acetylates proteins (109,120). Both of these activities are dependent upon lysine residues, and in these instances arginine is not able to replace the post-translationally modified lysines (109,120). Therefore, MYOCD may be post-translationally modified at K259 to directly or allosterically disrupt MHD binding to MYOCD. We hypothesized that K259 is a site of acetylation by p300 and that K259R may disrupt that acetylation.

DNA binding proteins, including histones and multiple transcription factors, are post-translationally acetylated by p300 (121). Acetylation can result in either activation (122) or repression of transcription factor activity (123). To determine if MYOCD is directly acetylated, we overexpresssed MYOCD and p300 in the presence of deacetylase inhibitors and then immunoprecipitated MYOCD. Using an antibody for pan-acetylated-lysines revealed that, as we hypothesized, WT MYOCD$^{\Delta MHD}$ was directly acetylated. Furthermore, we observed approximately similar levels of acetylation in K259R as compared to WT MYOCD$^{\Delta MHD}$, although we did see slight hyperacetylation of K259R compared to wildtype in some experiments (Fig. 2.9*A,* Data not shown). Truncations of MYOCD that lacked the basic domain showed reduced acetylation, but truncations lacking the transactivation domain – where p300 binds to MYOCD – showed higher levels of acetylation as compared to WT (Fig. 2.9*A*). Full length MRTF-B was also acetylated and the mutation R288K showed slightly higher levels of acetylation as compared to WT (Fig. 2.9*B*).

It was shown previously that p300 could increase and HDAC5 could decrease MYOCD-dependent activity (124). We next tested whether WT or K259R MYOCD^{935} responded differently to p300 and HDAC5 in the SM22-Luc reporter assay. WT MYOCD responded in a dose dependent manner to both p300 and HDAC5 (Fig. 2.9*C*). K259R MYOCD also responded in a dose dependent manner, until the highest concentrations of p300 where there was a response plateau (Fig. 2.9*C*). Because K259R responded in a dose dependent manner to HAT activity, we hypothesized that MHD-dependent autoinhibition was stronger in K259R and that autoinhibition would act antagonistically to p300. We found that the transcriptional activity of MYOCD was dependent upon the relative levels of p300 and MHD1-149, such that the MHD could counteract p300-dependent MYOCD activation in a dose dependent manner and vice versa (Fig. 2.9*D*). Furthermore, preliminary results show that p300 is able to inhibit the binding between MHD1-149 and MYOCD in a dose dependent manner (Fig. 2.9*E*). This suggests that p300 and MHD-dependent autoinhibition exert opposing influences on each other, in part through their actions on MYOCD. More experiments will be necessary to determine how K259R MYOCD is both acetylated and hypomorphic in the reporter assays shown.

DISCUSSION

This study shows that MYOCD has the potential for dynamic intramolecular and post-translational regulation of the SRF-dependent gene program. Two human mutations, K259R and Q647H, resulted in attenuated activation of a cardiac isoform of Myocardin. The Q647H sequence variation was statistically enriched in Caucasian and Hispanic

patients with congenital outflow tract valve disease. The Q647H variation is located near multiple potential kinase phosphorylation sites and disrupts a potential GSK3β-dependent signal that activates MYOCD.

In contrast to the full-length cardiac isoform, the K259R mutation in a smooth muscle isoform that lacked the amino terminus displayed no appreciable difference from WT *in vitro*. This observation led to the discovery that the amino terminus acted as an inhibitor of SRF-dependent Myocardin activity. Neither the MEF2 binding site nor the RPEL motifs in the amino terminus were necessary for this effect, we did find that two evolutionarily conserved acidic residues within the amino terminus were necessary for MHD-dependent inhibition. In conjunction with our observation that mutation of arginine 288 to lysine, in MRTF-B, was able to increase transcriptional activity, this suggests that autoinhibition is a novel mechanism for regulating the activity of the Myocardin family.

Interestingly, inclusion of amino acids 149–195 in the MHD constructs increased the binding affinity and inhibitory activity towards MYOCD. Of those 46 amino acids only 7 are conserved with amphibians and 5 of those are acidic (e.g., D130 and E135; data not shown). It is hypothetically possible for a direct interaction between the MHD's acidic residues and lysine 259 or even the entire lysine-rich basic domain. Alternatively, the increased length of the arginine side chain, compared to lysine, may disrupt MYOCD folding in a way that blocks SRF binding. As was already mentioned, post-translational modification probably will also play a role. Ultimately though, the protein structure of MYOCD will need to be solved to see what role the MHD plays as an inhibitor of MYOCD's activity in cardiac tissue.

We found that MYOCD was acetylated directly by p300, that K259R was slightly hyperacetylated, and that p300 was able to counteract the effects of MHD binding and autoinhibition. Superficially this data appears to be contradictory, but there are possible explanations as to how K259R is hyperacetylated and still hypomorphic. One possible explanation is that because K259R is hypomorphic in MYOCD^{935}, but not MYOCD$^{\Delta MHD}$, the hyperacetylation that is observed in K259R MYOCD$^{\Delta MHD}$ may be a compensatory mechanism by the cell to attempt to increase MYOCD-dependent activity that the MHD normally blocks. Multiple avenues of evidence support this hypothesis, 1) mutant MRTF-B is both hyperacetylated and more active than WT in reporter assays, 2) K259R MYOCD shows stronger response to MHD-dependent autoinhibition compared to WT, and 3) p300 and the MYOCD MHD counter one another. Alternatively, the MHD and autoinhibition may be involved in a negative feedback loop that the cell uses to repress MYOCD-activation. In such a case the K259R mutation would be hyperactive early and repress its own activity at the timepoint when we assay for activity. Given that MYOCD can be inhibited by overexpression of SRF (95), this feedback loop is a formal possibility. To test these possibilities it will necessary to check the acetylation state of WT and K259R MYOCD^{935} as well as K259R MYOCD lacking the transactivation domain. Hypothetically, overexpression of the MHD may inhibit p300-dependent MYOCD acetylation. It will also be necessary to determine what residues in the MYOCD protein are directly acetylated. Since MYOCD is still acetylated even when the basic domain is deleted it is unlikely that K259 is a site of direct acetylation. There is also always the possibility that p300 may not be the only HAT to acetylate MYOCD since

deletion of the p300 binding domain in the TAD actually resulted in more acetylation of MYOCD.

VSDs were observed in β-MHC-MHD^{WT} embryos, but were not observed in animals overexpressing the mutant MHD. The lack of VSDs in mutant MHD transgenics suggests that the inhibition of endogenous MYOCD could have caused a portion of the morphogenetic defects caused by WT MHD. On the other hand, MHD mutations that cannot inhibit SRF-dependent MYOCD activity did not rescue all of the defects that were observed. This implies that other inherent, or even off-target effects of the MHD could be behind the neonatal lethality. It is formally possible that overexpression of the MHD bound and sequestered endogenous free actin or disrupted the Myocardin/MEF2 transcriptional complex. Although these possibilities confound further interpretation of the transgenic results, we simply conclude that overexpression of the MHD elicited effects in vivo through a mechanism that was dependent on the conserved acidic residues.

Outflow tract valves are composed of both the second heart field and neural crest (5). MYOCD-null mutant embryos only survive to embryonic day 10.5, before the formation of cardiac valves, precluding the ability to examine MYOCD's role in these tissues (100). Selective ablation of the MYOCD gene from neural crest resulted in patent ductus arteriousus, but had no effect on valve morphogenesis (103) suggesting that MYOCD may play a role in the second heart field. To determine whether the K259R mutation contributed to the CCVM in our patient or cosegregated with the true disease-causing mutation as part of a haplotype block, it will be necessary to generate a mouse model of K259R, which we have begun. If the knock-in mouse has defects similar to those in our patient, such as pulmonic stenosis or other outflow tract defects, it would

also provide a valuable tool for understanding valve development. Most genes that are known to play a role in valve development (e.g., vascular endothelial growth factor, nuclear factor of activated T cells 1, and Notch1) are expressed in the endocardium of the prevalve tissue and respond to paracrine signals, such as transforming growth factor-β family members, that are released from the muscle tissue surrounding the valves (125) (10). Since MYOCD is expressed in the myocardium, it may be well situated to induce these paracrine signals (95). Alternatively, Myocardin expression is induced by transforming growth factor-β and acts as a tumor suppressor in precancerous mesenchyme (126). Thus, MYOCD may be involved in guiding early cardiac mesenchymal progenitors into fully differentiated valve tissue and any reduction in its activity could result in overproduction of undifferentiated valve progenitors and thickened valves.

FOOTNOTES

*This study was supported by NIH R01 HL080592 and UT Southwestern Cardiovascular Training Grant NIH 5-T32-HL007360.

ACKNOWLEDGEMENTS

We would like to thank Drs. E.N. Olson for advice, reagents, and generous help throughout the project, Drs. D.Z. Wang, and G. Amarasinghe for technical assistance.

FIGURES AND LEGENDS

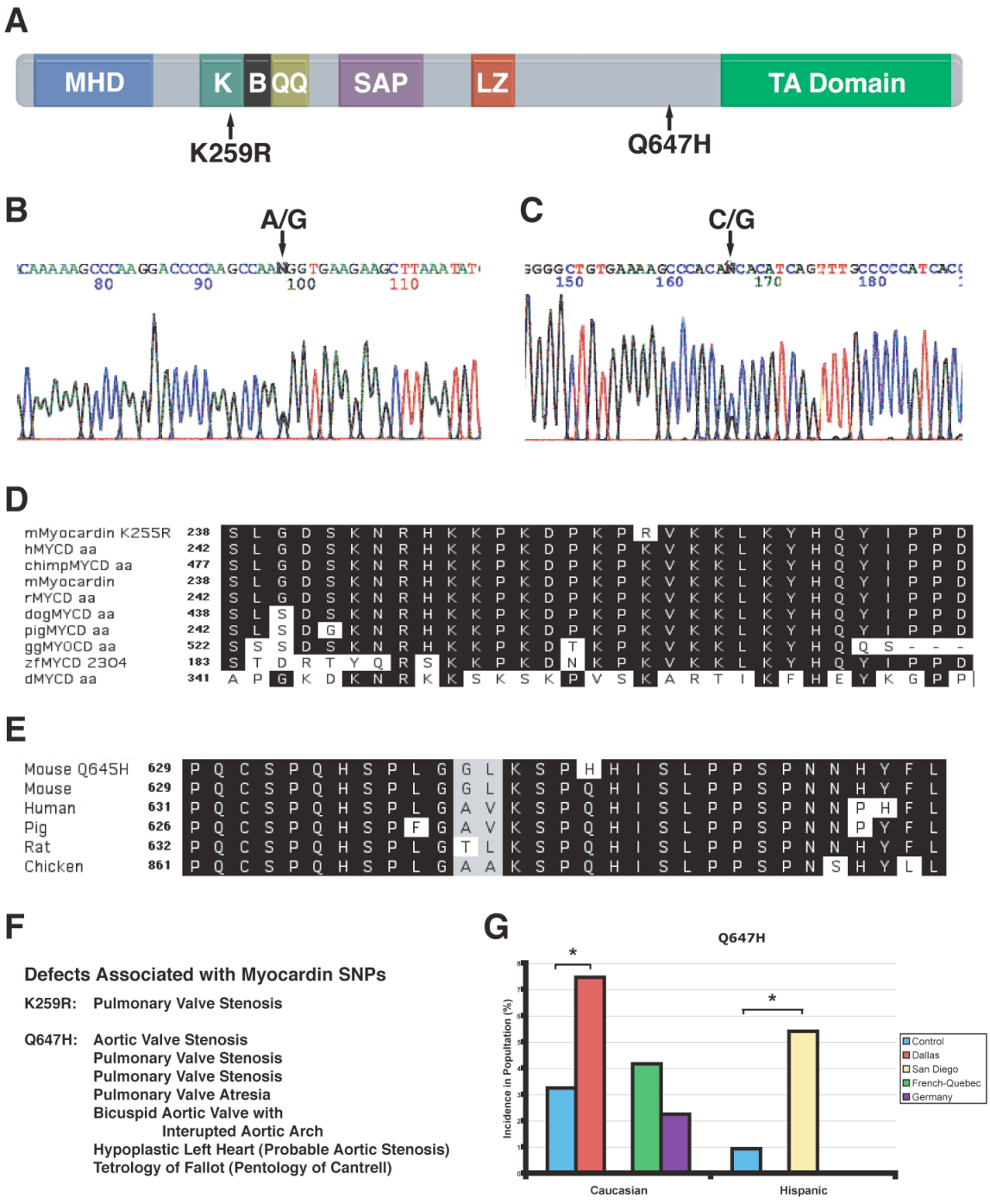

FIGURE 2.1. **Discovery of Evolutionarily Conserved Myocardin Sequence Variations Associated With Outflow Tract Valve Disease.** *A,* schematic of MYOCD[935] showing the locations of known domains and the K259R and Q647H sequence variations. MHD, MYOCD homology domain; K, lysine rich basic domain; B, ELK1-like B-box; QQ, polyglutamine tract; SAP, SAF/Acinus/PIAS domain; LZ, leucine zipper; TA, transactivation. *B and C,* Chromatographs showing heterozygous non-sense

mutations (*B*) K259R or (*C*) Q647H in MYOCD. *D and E*, Sequence alignment showing evolutionary conservation of MYOCD (*D*) K259R and (*E*) Q647H in humans, chimpanzees, etc., MRTF-B has an arginine at aligned position for MYOCD K259. *F*, List of the CCVM that was diagnosed in the eight patients that had outflow tract diseases. One patient (not shown) had a cardiac conduction defect that is probably not related to an outflow tract abnormality. *G*, Incidence of Q647H in various cohorts with subsets of outflow tract disease. Groups are divided by self-reported racial identity. Dallas and San Diego cohorts consist of predominately aortic/pulmonic valve stenosis, French-Canadian cohort is a familial case of bicuspid aortic valve, German cohort is a large cohort of patients diagnosed with adult onset aortic valve disease (predominately valve calcification). Statistical analysis is a two-tailed Chi-square analysis, with expected values calculated from the control population. *,$p<0.05$.

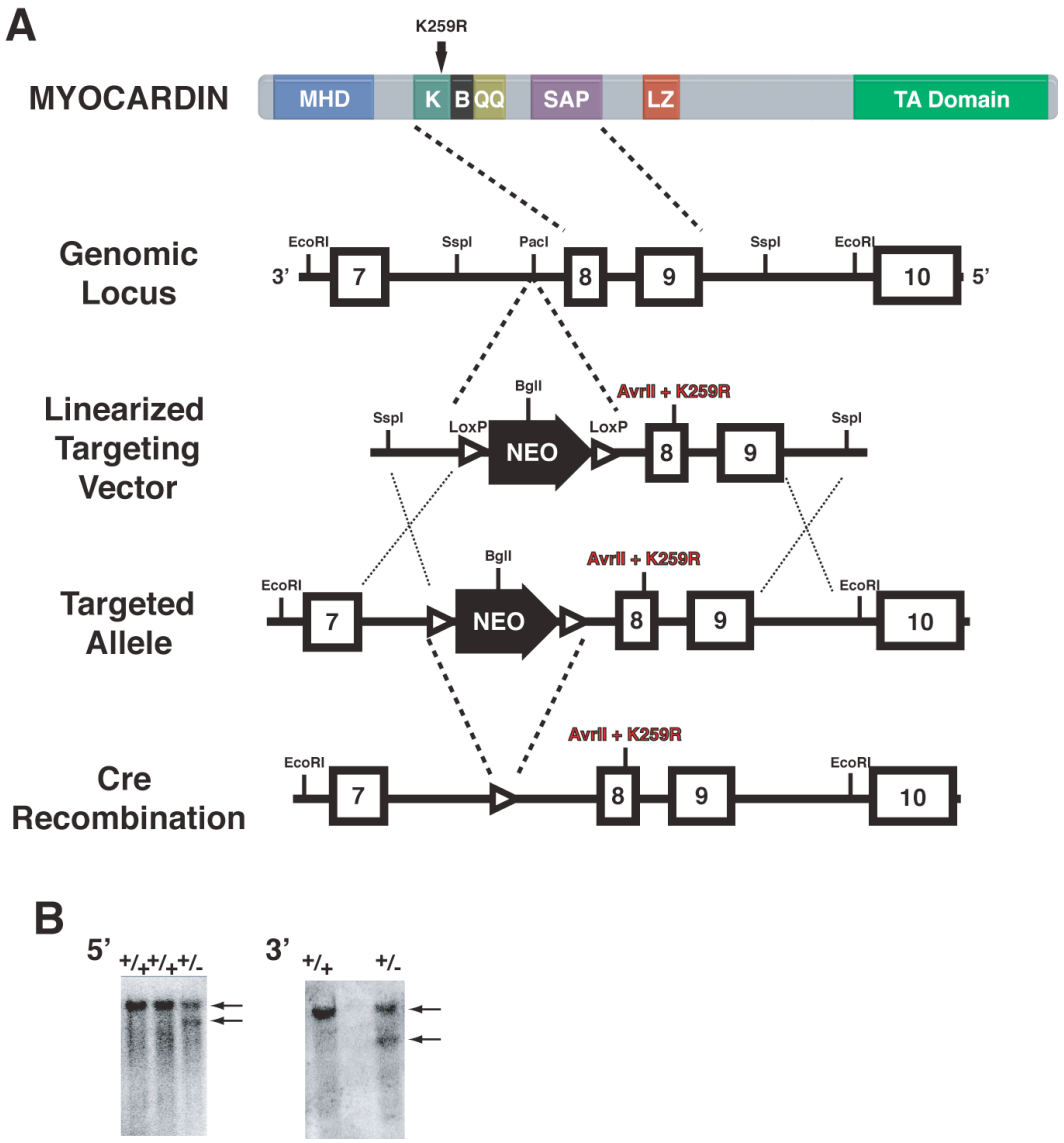

FIGURE 2.2. **Generation of Mice with Targeted Knock-In of MYOCD K259R.** *A*, Targeting strategy for homologous recombination of K259R in the endogenous MYOCD locus. A floxed-Neomycin resistance cassette (NEO) was inserted into a PacI site 3' to exon 8. The wildtype and mutant targeted allele (before and after excision of NEO) are shown with the targeting vector. Inserted mutation and AvrII restriction site for genotyping are indicated in red. *B*, Genomic Southern analysis of ES cell colonies with targeted (-/-) and untargeted (+/+) MYOCD K259R alleles.

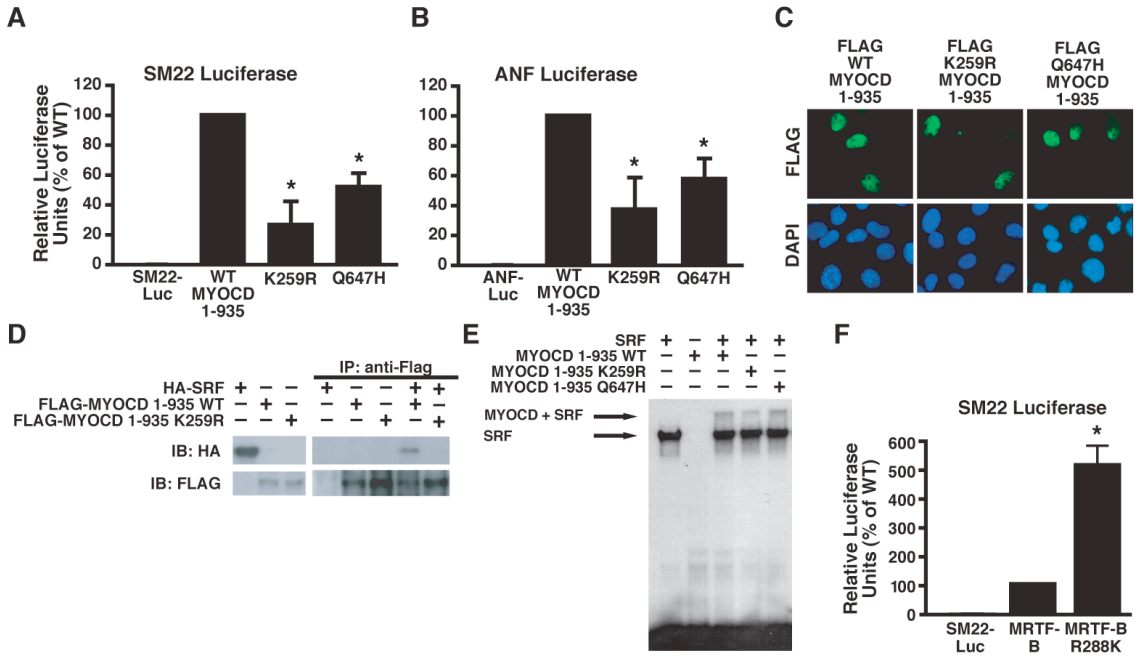

FIGURE 2.3. **Cardiac MYOCD K259R and Q647H are Hypomorphic *In vitro* and K259R has Reduced SRF Binding Affinity.** *A and B,* effect of the K259R mutation on MYOCD^{935} coactivation of the SM22_–Luc (*A*) and ANF–Luc (*B*) promoters *C,* nuclear co-localization of FLAG-tagged WT and K259R MYOCD^{935} *D,* HA-tagged SRF (HA-SRF) coimmunoprecipitates with WT but not K259R FLAG-tagged MYOCD^{935}. *E,* EMSA with ^{32}P-labeled c-fos CArG-box oligonucleotide. SRF impedes oligonucleotide, and MYOCD forms a ternary complex with SRF to further impede mobility. K259R MYOCD showed a weaker ability to form the ternary complex. *F,* effect of the R288K mutation on MRTF-B coactivation of the SM22_–Luc promoter R288 corresponds to same codon as K259 in MYOCD. Values are the mean ± SD of three experiments in triplicate. Statistical differences were calculated using the Student's t-test. *, $p<0.05$ vs WT MYOCD.

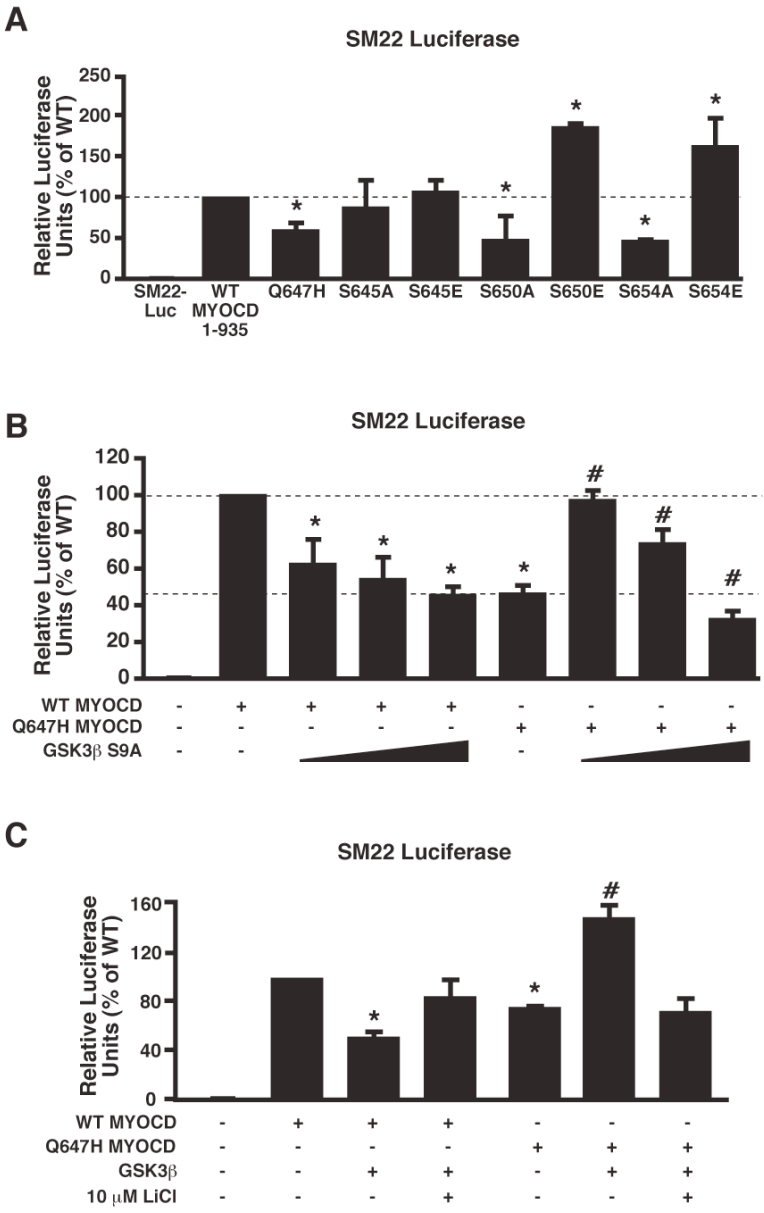

FIGURE 2.4. **MYOCD Q647H is Located Near Putative Phosphorylation Sites and Dysregulates GSK3β-Dependent Signals.** *A*, Mutation of putative phosphorylation sites near Q647H and their effect on MYOCD in the SM22-luciferase reporter. Serine 645 shows no difference with either mutation, but serine 650 and 654 both are hyperactive with phosphomimetic glutamates (S>E) and hypomorphic with non-phosphorylatable alanines (S>A). *B and C*, Effect of GSK3β on WT and Q647H MYOCD in the SM22-luciferase reporter. GSK3β can inhibit WT MYOCD in a dose dependent fashion but low levels of GSK3β will activate Q647H (*B*) with less activation and inhibition at higher concentrations. Lithium Chloride (LiCl) is able to inhibit both of these activities (*C*). Values are the mean ± SD of three experiments in triplicate. Statistical differences were calculated using the Student's t-test. *, $p<0.05$ vs WT MYOCD, #, $p<0.05$ vs Q647H MYOCD.

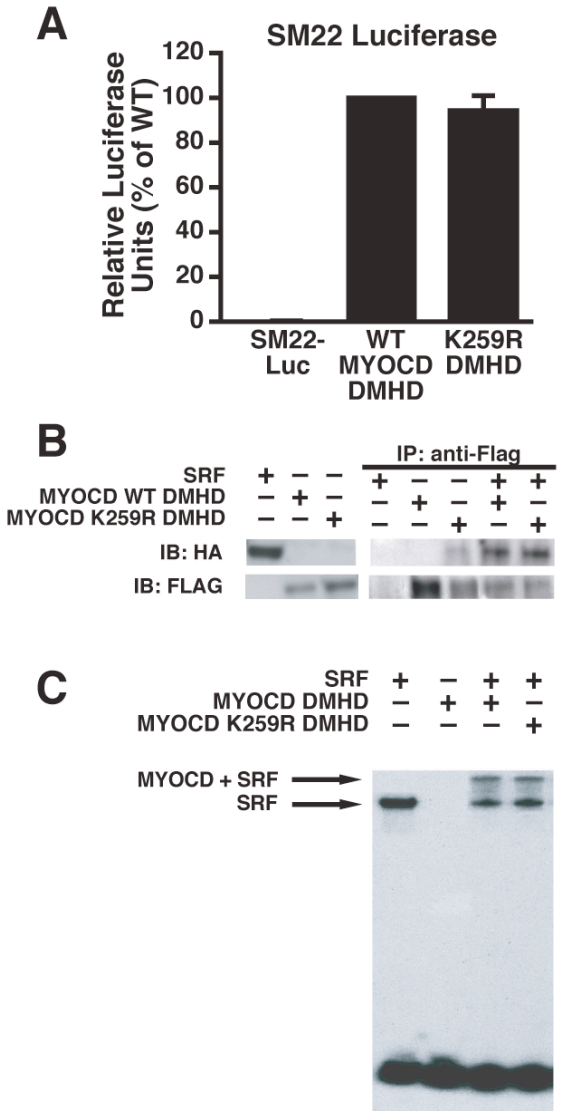

FIGURE 2.5. **Loss of MYOCD MHD rescues K259R.** *A,* WT and K259R MYOCD$^{\Delta MHD}$ activate SM22-Luciferase similarly. *B and C,* MYOCD::SRF binding experiments. *B*, CoIP showing similar levels of binding of HA-tagged SRF with WT and K259R FLAG-tagged MYOCD$^{\Delta MHD}$. *C,* EMSA of ^{32}P labeled c-fos CArG-box oligonucleotide. WT and K259R MYOCD$^{\Delta MHD}$ show similar levels of SRF ternary complex formation. Values are the mean ± SD of three experiments in triplicate.

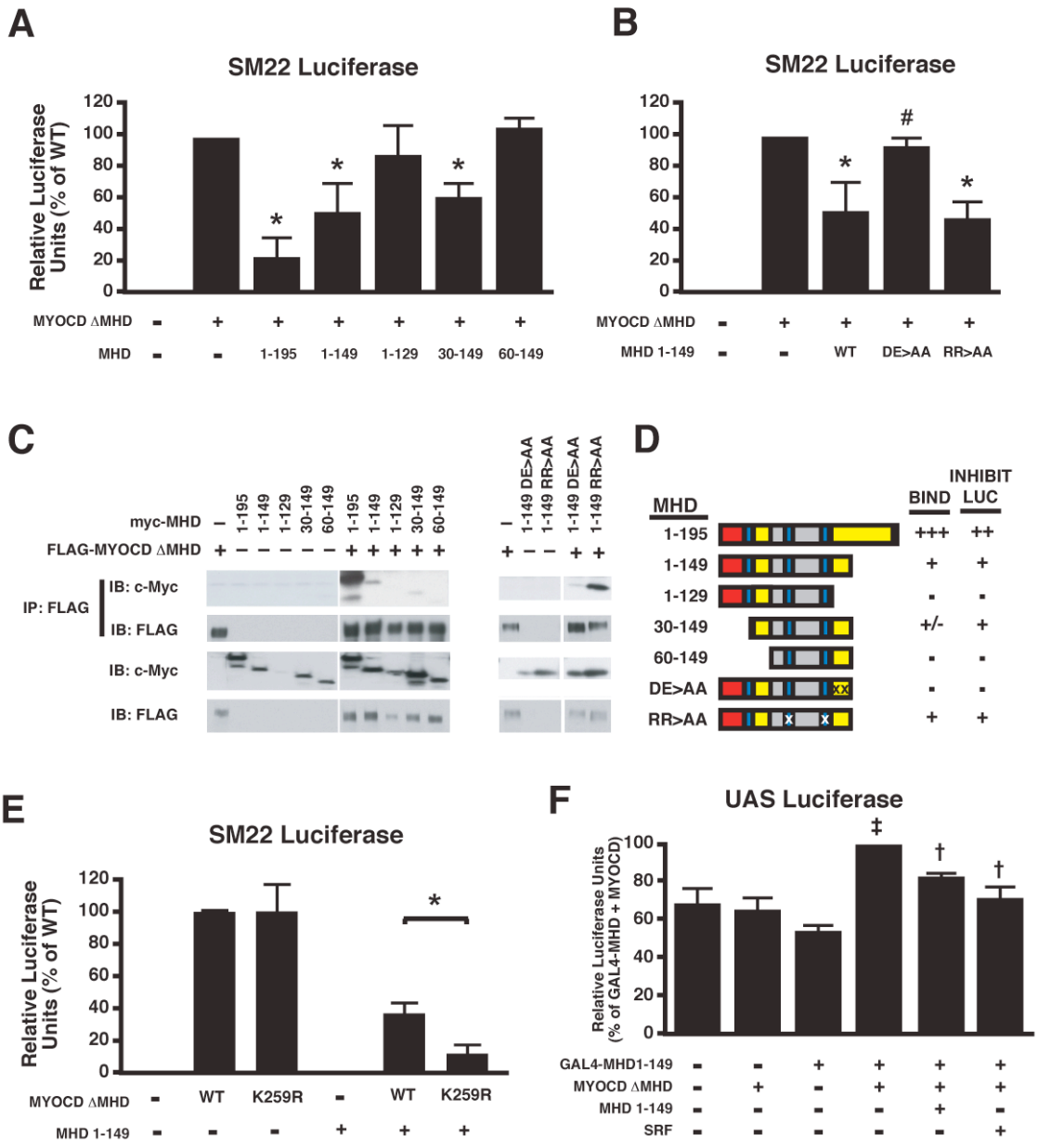

FIGURE 2.6. **The MYOCD MHD acts as an autoinhibitory domain by binding to and repressing MYOCD-dependent *in vitro* activity**. *A*, truncation of MHD to determine minimal inhibitor of MYOCD dependent activation of the SM22 promoter. *B*, mutation of conserved acidic residues D130,E135>AA but not RPEL motif R72,R115>AA relieved MHD inhibition. *C*, Co-IP of myc-tagged MHD truncations with FLAG tagged MYOCD$^{\Delta MHD}$ to determine minimal binding domain. *D*, schematic summarizing the ability of MHD truncations to bind to and inhibit MYOCD *in vitro*. *Red box*, MEF2 binding motif; *blue box*, RPEL motifs; *yellow box*, MHD inhibitory motifs. *X's* indicate point mutations. *E*, MHD-dependent inhibition is stronger for K259R than for WT MYOCD$^{\Delta MHD}$. *F*, Mammalian two-hybrid assay between MYOCD and the MHD. GAL4-MHD1-149 fusion protein interacts with MYOCD$^{\Delta MHD}$ to activate the UAS-

Luciferase reporter. Both extra free MHD1-149 and SRF are able to inhibit this interaction. Values are the mean ± SD of three experiments in triplicate. Statistical differences were calculated using the Student's t-test. *, $p<0.05$ vs MYOCD; #, $p<0.05$ vs WT MHD 1-149; ‡, $p<0.05$ vs GAL4-MHD149; †, $p<0.05$ vs GAL4-MHD149 and $MYOCD^{\Delta MHD}$.

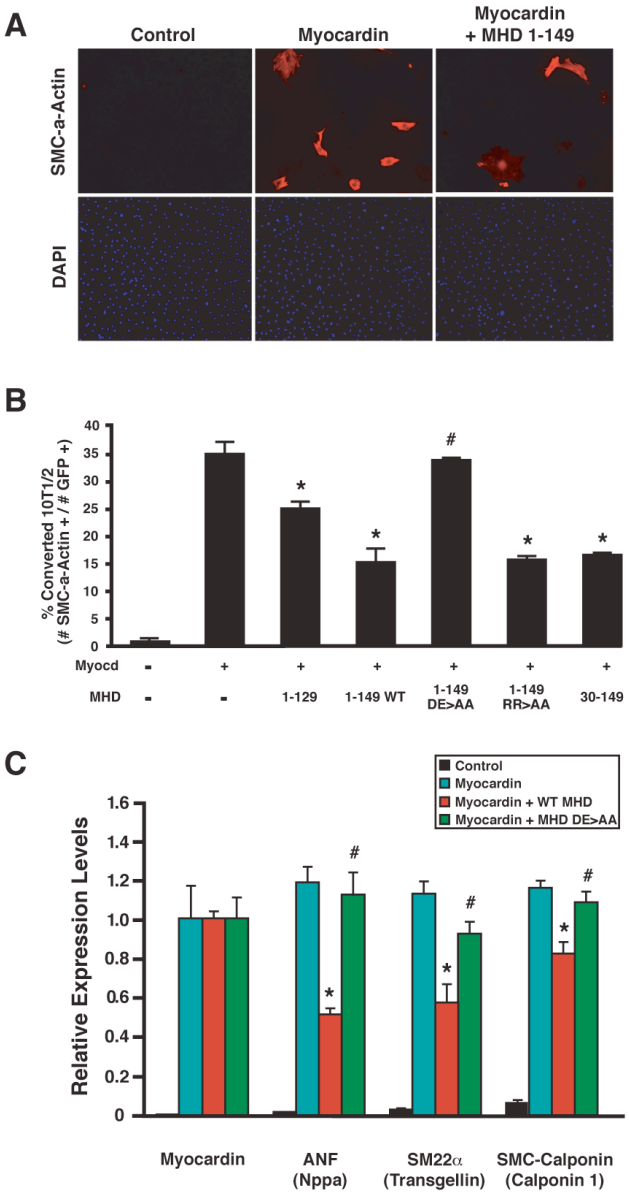

FIGURE 2.7. **The MHD of MYOCD inhibits MYOCD-dependent conversion of fibroblasts into smooth muscle cells.** *A*, 10T1/2 cells transfected with MYOCD with or without MHD were subjected to conversion protocol for 7 days and stained for SM-_-actin: TRITC, red, nuclei: DAPI, blue. *B,* double blind count of the number of transfected fibroblasts that converted in to SM-_-actin-positive cells. CMV-GFP was used as an internal control for transfection efficiency. For each conversion condition, experiments were performed three times in duplicate, and GFP-positive and TRITC-positive cells were counted in four randomly selected fields. Values are mean ± S.E.M. (n=8 fields of cells). *C*, quantitative RT-PCR for MYOCD-dependent genes: ANF, Sm22_, and smooth muscle calponin. Cotransfection of WT but not DE>AA MHD inhibited MYOCD-dependent gene expression. Values are the mean ± SD of two biological replicates in technical duplicates. Statistical differences were calculated using the Student's t-test. *, $p<0.05$ vs MYOCD, #, $p<0.05$ vs WT MHD 1-149.

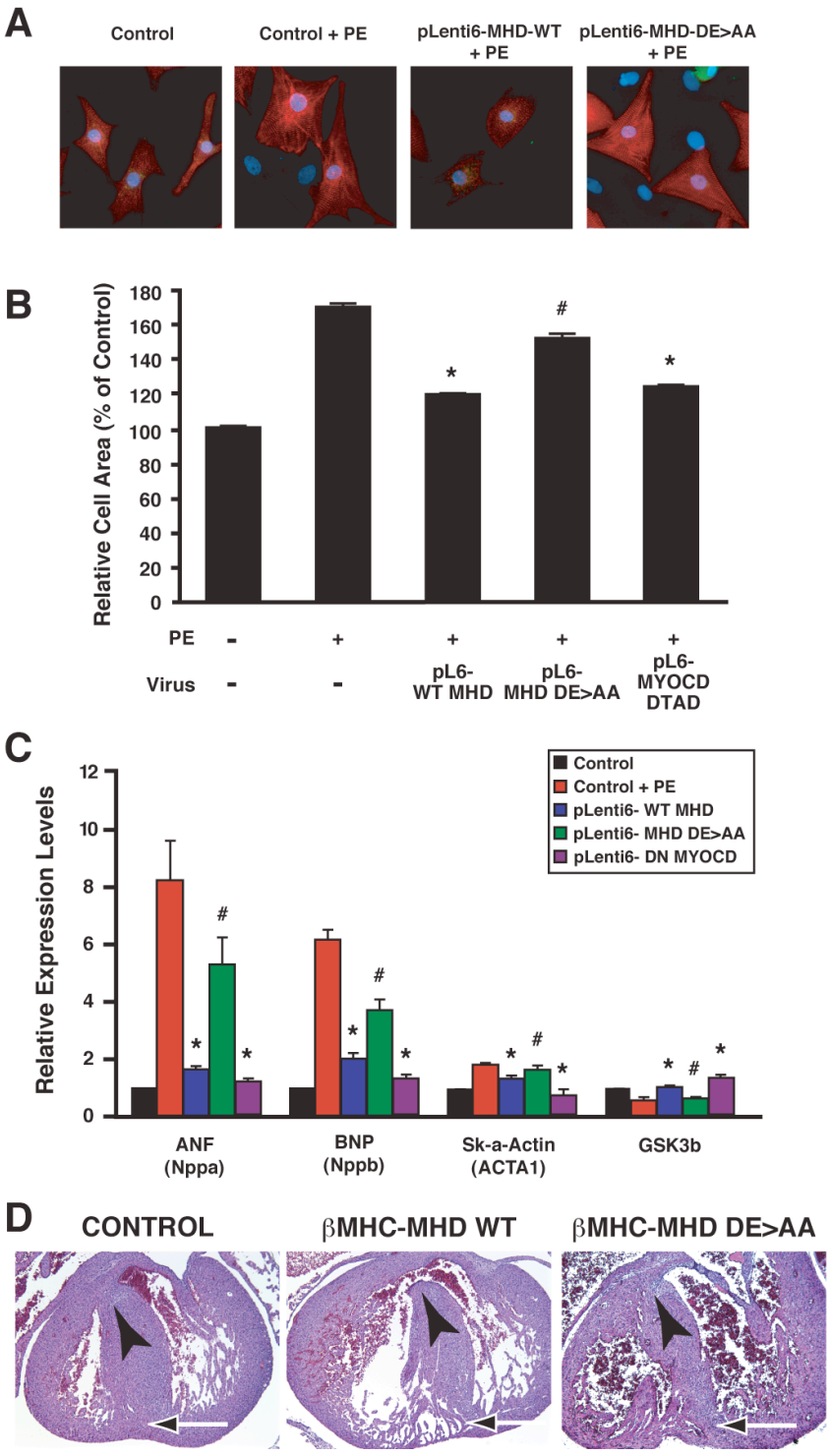

FIGURE 2.8. **The MYOCD MHD inhibits PE-dependent cardiomyocyte hypertrophy.** *A and B,* MHD inhibition of phenylephrine (PE)-dependent cardiomyocyte hypertrophy. A. Immunocytochemistry of neonatal rat cardiomyocytes subjected to PE (20 μM) for two days after being infected for one day with lentivirus that overexpresses WT (WT) or mutant (DE>AA) MHD, or dominant negative MYOCD (DN-MYOCD). α-

Actinin: TRITC, red, Nuclei: DAPI, blue. *B*, double-blind calculation of α-Actinin positive cell surface area of infected cardiomyocytes. Fields of cells in each condition were randomly selected and area calculations were made using Image-Pro 5.0 Software. Values are mean ± SEM) compared to the control, which is assigned a value of 100 (n=80). *C*, quantitative RT-PCR for hypertrophy-dependent genes: ANF, BNP, Skeletal muscle α-actin, and GSK3β. Infection with lentivirus overexpressing DN-MYOCD and WT-MHD but not DE>AA MHD inhibited the hypertrophy-dependent gene expression. *D*, Transverse sections of transgenic mice overexpressing the MHD under control of the βMHC promoter. Transgenic mice with βMHC driving WT MHD (middle panel) show signs of muscular (arrow) and membranous VSD (arrowhead) that were not seen in control mice (left panel) or transgenic mice that overexpress mutant MHD (DE>AA, right panel). Error bars represent SD of three biological replicates in technical duplicate. Statistical differences were calculated using the Student's t-test. *, $p<0.05$ vs PE alone, #, $p<0.05$ vs PE with WT MHD.

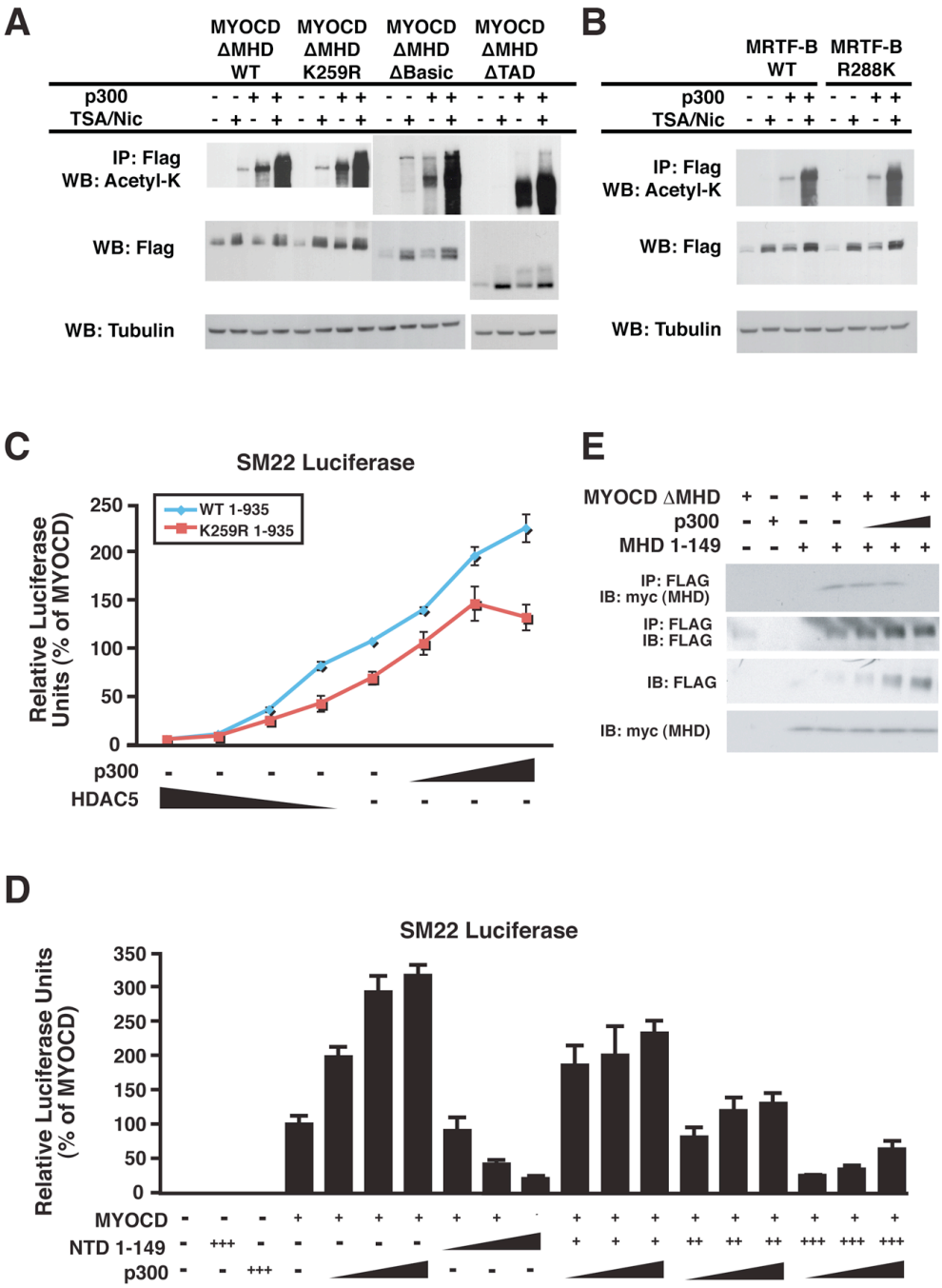

FIGURE 2.9. **p300 Acetylates MYOCD Directly to Inhibit MHD-Dependent Autoinhibition and Binding.** *A and B*, Immunoprecipitation of MYOCD and MRTF-B in the presence of HDAC inhibitors and the histone acetyltransferase, p300. Western analysis of acetylated lysines (Acetyl-K) revealed that MYOCD K259R showed similar levels of acetylation compared to WT in the absence of the MHD (*A*). Truncation of the basic domain attenuated acetylation while loss of the TA domain, the p300 binding site, resulted in increased acetylation. *B*, MRTF-B R288K acetylation was increased compared to WT. *C*, Effect of activation by p300 and inhibition by HDAC5 on WT and K259R

MYOCD^{935} coactivation of the SM22_–Luc promoter. K259R was hypomorphic compared to WT MYOCD when transfected alone, but K259R and WT responded proportionately to HDAC and p300, except at the highest doses of p300. *D*, Contradictory action between MHD-dependent autoinhibition and p300. MYOCD (100 ng) was cotransfected with p300 (250 ng, 500 ng, or 750 ng) or MHD (50 ng, 100 ng, or 200 ng) respectively. *E*, Myc tagged MHD1-149 coimmunoprecipitates with MYOCD but binds with less affinity in the presence of increasing amounts of p300.

Table 1:

Gene	Alias	Assay ID#
GAPDH		Mm99999915_g1
MYOCD		Mm01325104_m1
Nppa	ANF	Mm01255748_g1
Nppb	BNP	Mm00435304_g1
ACTA1	Skeletal Muscle Actin	Mm00808218_g1
GSK3β		Mm00444911_m1
Cnn1	Smooth Muscle Calponin	Mm00487035_g1
Transgellin	SM22α	Mm00441660_m1

Table 2.1. **List of Taqman Assays Used.**

CHAPTER 3: MUTATIONS IN NOTCH1 CAUSE AORTIC VALVE DISEASE

Vidu Garg[1,5], Alecia N. Muth[1,7], Joshua F. Ransom[1,7], Marie K. Schluterman[1], Robert Barnes[3,4], Isabelle N. King[1,5,7], Paul D. Grossfeld[6] and Deepak Srivastava[1,2,4,5,7]

[1]Departments of Pediatrics, [2]Molecular Biology and [3]Internal Medicine, and [4]the McDermott Center for Human Growth and Development, , University of Texas Southwestern Medical Center, Dallas, Texas. [5]Children's Medical Center, Dallas, Texas. [6]Department of Pediatrics, Division of Cardiology, University of California, San Diego [7]Gladstone Institute of Cardiovascular Disease and Department of Pediatrics, University of California, San Francisco

ABSTRACT

Calcification of the aortic valve is the third leading cause of heart disease in adults(127). The incidence increases with age, and it is often associated with a bicuspid aortic valve present in 1-2% of the population(128). Despite the frequency, neither the mechanisms of valve calcification nor the developmental origin of a two, rather than three, leaflet aortic valve is known. Here, we show that mutations in the signaling and transcriptional regulator NOTCH1 cause a spectrum of developmental aortic valve anomalies and severe valve calcification in non-syndromic autosomal-dominant human pedigrees. Consistent with the valve calcification phenotype, Notch1 transcripts were most abundant in the developing aortic valve of mice, and Notch1 repressed the activity of Runx2, a central transcriptional regulator of osteoblast cell fate. The hairy-related family of transcriptional repressors (Hrt), which are activated by Notch1 signaling, physically interacted with Runx2 and repressed Runx2 transcriptional activity independent of histone deacetylase activity. These results suggest that NOTCH1 mutations cause an early developmental defect in the aortic valve and a later de-repression of calcium deposition that causes progressive aortic valve disease.

INTRODUCTION

Abundant evidence suggests a major inherited component to the etiology of aortic valve disease in children and adults(129) 4(130). The most severe type of aortic valve obstruction in children results in failure of the fetal left ventricle to grow, a condition known as hypoplastic left heart syndrome. About 10% of relatives of hypoplastic left heart syndrome patients have bicuspid aortic valve, often undiagnosed, suggesting a common genetic etiology with phenotypic heterogeneity(131). The valve calcification often observed in bicuspid aortic valve is a result of inappropriate activation of osteoblast-specific gene expression(132), but the mechanism is unknown.

MATERIALS AND METHODS:

Clinical phenotype evaluation and DNA collection— The congenital heart disease families and individuals were ascertained for genetic linkage analyses at Children's Medical Center, Dallas (University of Texas Southwestern Medical Center) and the University of California, San Diego. Clinical evaluations and genetic studies were performed in accordance with human subject guidelines after informed consent according to the protocol approved by the individual Institutional Review Boards. Family members were studied by history, physical examination, 12-lead electrocardiogram, and echocardiography. Medical records were reviewed for individuals who had died. Cardiologists reviewed all phenotypic information. Genomic DNA for genetic analyses was extracted from peripheral lymphocytes.

Genetic linkage analysis—Autosomal genome linkage analysis was performed with 372 polymorphic DNA markers at approx10-cM intervals (ABI Mapping Set v2.5).

Markers were genotyped in all family members, and linkage analysis was performed with GENEHUNTER as described(44,133). In brief, initial linkage analysis of family A, assuming 90% penetrance and a disease allele frequency of 1.5%, demonstrated the highest LOD score on chromosome 9q34-35. Phenotypic analysis assuming 100% penetrance yielded a single peak at 9q34-35 and a maximum LOD score of 3.5.

Identification of NOTCH1 mutations—All NOTCH1 exons were sequenced bidirectionally to search for sequence variations in the probands of families A and B. Exons containing R1108X and H1505del mutations were amplified by PCR for each additional family member and sequenced bidirectionally. Sequences of the 42 primer pairs for the 34 NOTCH1 exons are available on request. PCR amplification was performed with the BD Biosciences Advantage GC Genomic PCR kit following the manufacturer's instructions, with annealing at 60 °C. Screening of identified human NOTCH1 mutations was performed with allelic discrimination assays and the ABI Prism 7900 HT Sequence Detection System using TaqMan probes on DNA from participants in the Dallas Heart Study, as described(134).

Radioactive-section in situ hybridization—35S-labelled antisense riboprobes were synthesized with T7 RNA polymerase (MAXIScript, Ambion) from 400-bp partial mouse Notch1 cDNA or plasmids encoding Hrt1 and Hrt2. With these riboprobes, radioactive-section in situ hybridization was performed on paraffin-embedded sections of E11.5, E13.5 and E17.5 mouse embryos, as described(135).

Luciferase assays—COS7 cells were transfected using Fugene 6 (Roche) according to the manufacturer's instructions. The reporter plasmid (250 ng), p6OSE2 luciferase(136), and CMV beta-galactosidase expression plasmid (50 ng) to control for

transfection efficiency were transfected along with Runx2 expression plasmid (100 ng) and Hrt1, Hrt2, Notch1 intracellular domain and Hrt2 deletion expression plasmids (300-1,000 ng). Hrt2 deletion constructs were generated as described(137) and protein levels of mutants kept constant. To inhibit HDAC activity, trichostatin A diluted to 0.1 μM in dimethyl sulphoxide (DMSO) was added 24 h before collecting cell lysates. Simultaneous duplicate experiments with an identical amount of DMSO served as a control. Immunoblots verified appropriate protein expression. Luciferase activity was measured 40 h after transient transfection as described(137) and was normalized to LacZ expression to generate relative luciferase activity (Fig. 3a) or expression of Hrt and Runx2 proteins (Fig. 3e). At least three independent experiments were performed in duplicate.

Quantitative RT-PCR—Total RNA from COS7 cells collected 40 h after transfection with empty vector and Notch1 intracellular domain expression plasmid was purified with the Trizol method (Invitrogen). Total RNA (1 μg) was reverse transcribed using the Superscript First Strand Synthesis System for RT-PCR (Invitrogen). PCR analysis was performed using primers specific for Hrt1 and Hrt2. Glyceraldehyde 3-phosphate dehydrogenase (G3PDH) RNA was amplified as a loading control. An annealing temperature of 56 °C was used for PCR analysis. Negative controls for each sample used non-reverse-transcribed RNA.

GST pull-down assay—Mouse GST-Hrt2 fusion proteins were purified with glutathione Sepharose 4 Fast Flow beads (Roche) for 12 h and washed twice in binding buffer (300 mM NaCl, 50 mM Tris-HCl, pH 8.0, 1 mM EDTA, 1% Triton X-100, 1% NP-40, 0.1% SDS, 0.5 mM dithiothreitol). 35S-labelled Runx2 protein was synthesized

using the T7 TNT coupled reticulocyte lysate system (Promega) according to the manufacturer's instructions. Labeled protein was incubated with GST fusion protein (2 μg) for 8-10 h at 4 °C in binding buffer with 1 mg of nonfat dried milk to compete for nonspecific interactions. Bound proteins were analyzed by SDS-PAGE and autoradiography.

RESULTS

We identified a family of European-American descent spanning five generations with 11 cases of congenital heart disease (Fig. 3.1*A*). Clinical evaluations demonstrated autosomal-dominant inheritance of congenital heart disease. Nine affected family members had aortic valve disease (Fig. 3.1*B,G*). In eight, an abnormal aortic valve was the only cardiac malformation; six had bicuspid aortic valve, and seven developed calcific aortic stenosis, including three cases in the setting of a three leaflet valve. One family member (IV-4) had an associated abnormal mitral valve, resulting in mitral stenosis, and a ventricular septal defect. An isolated ventricular septal defect or tetralogy of Fallot with a bicuspid pulmonary valve was identified in two other affected family members (III-4 and IV-1, respectively). Four family members have required aortic valve replacement for severe calcification. No cardiac conduction abnormalities, neurological deficits, or other birth defects were identified. Detailed clinical phenotype information for this family is shown in Supplementary Fig. 3.4*A*.

A genome-wide scan of available family members revealed linkage of the congenital heart disease phenotype to a single locus on chromosome 9q34-35 between D9S1826 and D9qter (logarithm of odds (LOD) score, 3.5, theta = 0), spanning

approximately 3 megabases (approx9 cM) (for haplotype data, see Supplementary Fig. 3.5). Review of 30 known (and 57 predicted) genes revealed NOTCH1, which encodes a transmembrane receptor (2,556 amino acids) that functions in a highly conserved intracellular signaling pathway involved in cellular differentiation, cell fate and lateral inhibition(138). Direct sequencing of NOTCH1 in an affected patient revealed a heterozygous C-to-T transition of nucleotide 3322 that predicted a premature stop codon instead of arginine at position 1108 in the extracellular domain (Fig. 3.1*C*). All affected subjects who were clinically evaluated had the R1108X mutation, suggesting autosomal-dominant inheritance of the disease phenotype with complete penetrance (Fig. 3.1*A*). The mutant allele was not detected in unaffected family members or in 1,136 unrelated subjects of diverse ethnicity (Supplementary Fig. 3.6), making it unlikely that R1108X is a rare polymorphism. In the proband (the index case), sequencing of 100 additional regulatory genes essential for, or expressed during, cardiac development identified no other linked mutations, consistent with a monogenic etiology (V.G. and D.S., unpublished observations).

Direct sequencing of NOTCH1 in a smaller, unrelated Hispanic family with aortic valve disease revealed a second mutation that segregated with three affected family members, all with bicuspid aortic valve (Fig. 3.1*D,E*). The proband (III-1) also had mitral valve atresia, hypoplastic left ventricle and double-outlet right ventricle; his sibling (III-2) and mother (II-1) had aortic valve calcification and stenosis. Family member II-2 had an ascending aortic aneurysm (Fig. 3.1*E*; see also Supplementary Fig. 3.4*B*) but no aortic valve disease. A single base pair deletion at position 4515 that segregated with aortic valve disease in this family was not found in 1,138 ethnically diverse controls (Fig. 3.1*F*;

see also Supplementary Fig. 3.6). This deletion resulted in a frameshift mutation (H1505del) that predicted a severely altered protein containing 74 incorrect amino acids at the carboxy terminus of the extracellular domain followed by a premature stop codon (Fig. 3.1*F*). These NOTCH1 mutations generate truncated transcripts that probably undergo nonsense-mediated decay(139) and provide compelling genetic evidence that NOTCH1 haploinsufficiency results in human congenital heart disease, although dominant-negative effects cannot formally be ruled out.

To determine whether Notch1 expression during development correlates with the predominant phenotype in humans, we performed in situ hybridization at multiple stages during cardiogenesis, focusing on Notch1 transcripts in cardiac valves and their precursors in mice. At mouse embryonic day (E) 11.5, Notch1 messenger RNA transcripts were abundant in the outflow tract mesenchyme, which gives rise to the valves, and in the endocardium (Fig. 3.2*A-D*). By E13.5, when septation of the common arterial trunk occurs, Notch1 was expressed at high levels in the endothelial layer (Fig. 3.2*E-H*) and mesenchyme of aortic valve leaflets (Fig. 3.2*G,H*), possibly explaining the increased dose sensitivity of the aortic valve. These findings suggest a role for Notch signaling in the morphological development of the aortic valve. Disruption of Notch1 in mice results in death by E9.5 from vascular endothelial defects, precluding analysis of the aortic valve(140), but in fish and frogs Notch1 appears to be important for early valve development(141).

NOTCH1 encodes a large protein containing an extracellular domain with 36 tandem epidermal growth factor (EGF)-like repeats and three cysteine-rich Notch/LIN-12 repeats, an intracellular domain with six ankyrin repeats, and a transactivation domain.

The Notch signaling pathway is highly conserved across species(138). Notch receptors (1-4) interact with Delta(1-4) or jagged(1, 2)/serrate, resulting in two independent cleavages, first by a metalloprotease(142,143) and then by presenilin(144,145), that release the Notch intracellular domain from the membrane, in a manner similar to that first described for sterol response element binding protein(146). Notch intracellular domain translocates to the nucleus, where it interacts with the DNA-binding protein CSL (CBF-1, suppressor of hairless, and Lag-1) to activate downstream target genes, including members of the hairy/enhancer of split (Hes) family of transcriptional repressors. This pathway participates in cell fate determination and differentiation during organogenesis throughout the embryo and is regulated by glycosylation of the extracellular EGF-like repeats in Notch1 (147).

Although haemodynamic alterations induced by bicuspid aortic valve may contribute to calcification, several family members with tricuspid aortic valves also developed calcification. This observation, along with the severity of calcification, led us to test whether NOTCH1 may directly affect calcium deposition. A proposed cellular mechanism by which valvular calcification develops is via differentiation of valvular cells into osteoblast-like cells(132), including upregulation of genes, such as osteopontin(148). Expression of osteopontin, osteocalcin and other osteoblast-specific genes is directly regulated by upstream cis-elements that bind to the transcription factor Runx2(136). Because Runx2 is upregulated in mouse and rabbit models of valvular calcification(149,150), we investigated whether Notch1 normally represses Runx2 activation. In the fibroblast cell line COS7, constitutively active Notch1 intracellular domain repressed Runx2-induced activation of luciferase through a multimerized Runx2-

binding cis-element normally present upstream of osteocalcin (Fig. 3.3*A*). Although Runx2 can be inhibited by histone deacetylase (HDAC) activity(151), Notch1-mediated repression of Runx2 was unaffected by the potent HDAC inhibitor trichostatin A, suggesting that it was HDAC-independent.

Notch directly activates the hairy family of transcriptional repressors, the central mediators of Notch's effects on gene expression. The heart and vasculature are enriched in the hairy-related transcriptional repressors Hrt1 and Hrt2, which mediate the Notch signal(135,152). Hrt1 and Hrt2, also known as Hey1 and Hey2, were co-expressed in the endothelial lining of the murine aortic valve leaflet at E17.5, as well as in the endocardium and vascular endothelium (Fig. 3*B-D*). As with Notch1, Hrt1 and Hrt2 inhibited Runx2 activation of the osteocalcin enhancer. Using Hrt2 truncation mutants, we determined that the basic helix-loop-helix (bHLH) domain of Hrt2 is necessary for full Hrt2-mediated repression of Runx2 (Fig. 3*E,F*). Moreover, semi-quantitative RT-PCR demonstrated upregulation of Hrt1 and Hrt2 transcripts in COS7 cells transfected with Notch1 intracellular domain (Fig. 3*G*). In glutathione S-transferase (GST) pull-down studies performed to investigate the mechanism of Hrt2-mediated repression, Hrt2 and Runx2 specifically interacted (Fig. 3.3*H*), consistent with the repression we observed and the reported in vitro interaction between Hes1 and Runx2 (153). The bHLH domain of Hrt2 can recruit HDACs(154); however, as with Notch1, Hrt repression of Runx2 activation was not dependent on HDAC activity (Fig. 3.3). These data suggest that Hrt proteins repress Runx2 through a physical interaction, and may mediate Notch1 repression of Runx2.

NOTCH Inhibits MYOCD-Dependent miR-1 Expression

We hypothesized that NOTCH1 and MYOCD may epistatically interact in valve tissue because of two additional facts. First, NOTCH1 and multiple members of the NOTCH signaling pathway are linked to both Aortic and Pulmonic valve disease (36,83,155) similar to our findings with the MYOCD mutations. In this same line, the Runx2 pathway inhibits MYOCD-dependent control of smooth muscle differentiation (156). Secondly, the NOTCH:JAGGED1 pathway was recently shown to activate smooth muscle genes synergistically with MYOCD but no physical interaction was shown (157). Because hypomorphic alleles of MYOCD or NOTCH can lead to OFT valve disease, we hypothesized that MYOCD would activate NOTCH1-dependent target genes that are involved in OFT development. The NOTCH1 intracellular domain is known to activate a luciferase reporter driven by the Hrt2 promoter (33). WT MYOCD^{935} was able to weakly activate Hrt2-Luc, but in conjunction with the NOTCH1 intracellular domain was able to synergistically induce activation of Hrt2-Luc much more (Fig. 3.7*A*). MYOCD induction of Hrt2 and Hrt2 inhibition of MYOCD may be a mechanism used by MYOCD to regulate MYOCD and/or NOTCH-dependent activity in various boundaries in the body, such as between OFT valve endocardium and the surrounding muscle.

Previous reports have shown that MYOCD and SRF are able to activate enhancers that drive expression of the muscle specific microRNA cluster, miR-1/miR-133a (119). It was striking that the enhancers for the two separate clusters drove expression in either the atria (miR-1-1/miR-133a-2) or in the ventricles (miR-1-2/miR-133a-1). This expression was reminiscent of the expression patterns of Hrt1 and Hrt2, which had atrial and ventricular specific expression respectively in early development (158). We hypothesized

that since NOTCH was able to inhibit some MYOCD target genes that NOTCH may also regulate microRNA tissue specificity through Hrt-mediated inhibition, such as when Hrt2 inhibits atrial gene expression (159). As hypothesized, Hrt1 and Hrt2 were able to inhibit MYOCD dependent transcription of luciferase driven by the miR-1-2 promoter (Fig. 3.7*B*). Furthermore, whole heart tissue from embryonic Hrt2 null mice showed a small but consistent increase in total miR-1 and miR-133 expression levels (Fig. 3.7*C*). These data suggest that NOTCH1 can regulate MYOCD in a context dependent manner and that NOTCH1 can regulate the expression of the microRNA-1/133a cluster.

DISCUSSION:

Somatic NOTCH1 mutations have been identified in human blood cancers(160), but the discovery of NOTCH1 mutations as a cause of aortic valve calcification and aortic valve anomalies represents the first demonstration of NOTCH1 germline mutations in human disease. The families reported here provided insights into the cause of a common human developmental malformation (bicuspid aortic valve) and revealed a potential mechanism mediated by NOTCH1 mutations that may predispose to endothelial dysfunction and inflammation underlying abnormal cardiovascular calcification events. Further studies of the NOTCH1 signaling pathway in the adult calcific process may identify preventative and pharmacological approaches to slow this age-related disease.

Whereas the role of NOTCH1 in preventing aortic valve calcification is relevant for adult-onset disease, its essential function in normal development of the valve is equally intriguing. Bicuspid and even unicuspid aortic valves typically contain a ridge where the valve leaflets did not separate in utero (Fig. 3.1*G*). In extreme cases, blood

flow may be so restricted that the left ventricle fails to grow, resulting in hypoplastic left heart syndrome, the most frequent cause of death in children with congenital heart disease. As bicuspid aortic valve and hypoplastic left heart syndrome may represent extremes of the aortic valve disease spectrum, the discovery of NOTCH1 as a cause of bicuspid aortic valve and a hypoplastic left ventricle in the same family suggests that NOTCH1 mutations may be the genetic basis for hypoplastic left heart syndrome in some patients. Future studies of NOTCH1 mutations in this population may reveal those at risk for a subset of severe congenital heart lesions.

ACKNOWLEDGEMENTS

The authors thank the families for their participation; the Divisions of Pediatric Cardiology and Pediatric Cardiothoracic Surgery at Children's Medical Center Dallas for assistance with clinical information; McDermott Center for Human Growth and Development for assistance with linkage analysis and allelic discrimination assays; Dallas Heart Study participants and investigators for DNA samples; members of the Molecular Histology Core laboratory for radioactive-section in situ hybridization; J. C. Cohen and H. H. Hobbs for discussions and critical review of this manuscript; K. Ivey for graphics assistance; C. Butler, A. Garg and D. Srivastava for assistance with blood collection; G. Karsenty for Runx2 expression and p6OSE2 reporter plasmids; and L. Kedes for the GST-Hrt2 expression plasmid.

FOOTNOTES

This work was supported by grants from NICHD/NIH and March of Dimes Birth Defects Foundation to V.G., and NHLBI/NIH, March of Dimes Birth Defects Foundation and the Donald W. Reynolds Cardiovascular Clinical Research Center to D.S. J.F.R. was supported by a training grant from NIH; I.N.K. is an NICHD/NIH fellow of the Pediatric Scientist Development Program; and D.S. is an Established Investigator of the American Heart Association.

FIGURES AND LEGENDS

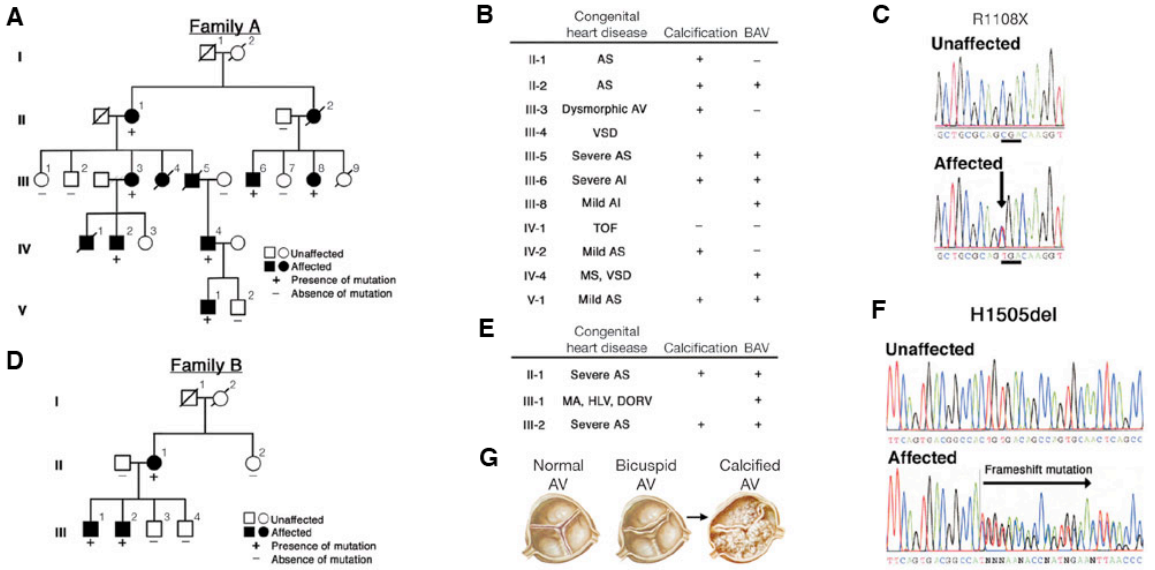

Figure 3.1**: NOTCH1 mutations segregate with familial aortic valve disease.**
A, Kindred with five generations (indicated with Roman numerals) affected by congenital heart disease and valve calcification. Participating members of each generation are indicated numerically. Deceased family members (slash) were unavailable for mutation analysis. Squares, males; circles, females. B, Cardiac phenotype in affected family members. AI, aortic insufficiency; AS, aortic stenosis; AV, aortic valve; BAV, bicuspid aortic valve; TOF, tetralogy of Fallot; VSD, ventricular septal defect. C, Sequence chromatogram of affected family members. D, Kindred with three members affected by congenital heart disease. E, Cardiac phenotype of family B. DORV, double-outlet right ventricle; HLV, hypoplastic left ventricle; MA, mitral atresia; MS, mitral stenosis. F, Sequence chromatogram of affected members in family B. G, Schematic of normal trileaflet aortic valve, bicuspid aortic valve and calcified aortic valve.

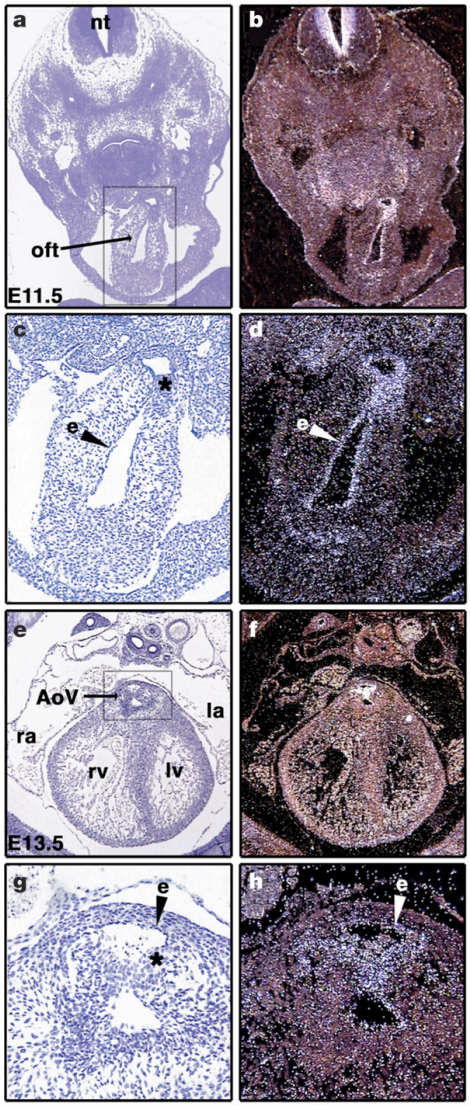

Figure 3.2**: Cardiac expression of mouse Notch1 mRNA by radioactive-section in situ hybridization.**
A-D, Transverse sections of E11.5 mouse embryos through endocardium (arrowhead) and endocardial cushions (asterisk) of the outflow tract (oft). C, D, High-magnification images of A, B, as depicted by box in A. e, endocardium; nt, neural tube. E-H, Transverse sections through E13.5 embryonic heart. G, H, High-magnification of aortic valve (AoV) region outlined by box in E. The asterisk indicates AoV mesenchyme. Sections in A, C, E and G are bright-field images of B, D, F and H, respectively. la, left atrium; lv, left ventricle; ra, right atrium; rv, right ventricle.

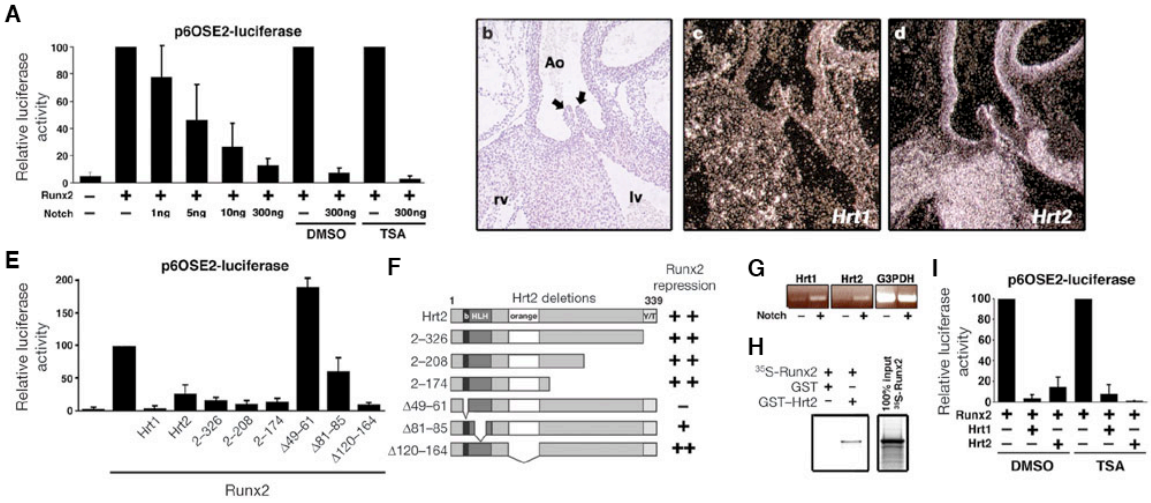

Figure 3.3**: Notch1, Hrt1 and Hrt2 repress Runx2 transcriptional activity.**
A, Relative luciferase activity in COS7 cells transfected with Flag-Runx2 and Runx2-dependent osteocalcin enhancer (p6OSE2) luciferase reporter with or without co-transfection of the indicated concentrations of Myc-Notch1 intracellular domain, in the presence of trichostatin A (TSA) or vehicle (DMSO). B-D, Coronal section in situ hybridization through aortic valve (arrows) of E17.5 mouse embryos (C, D). Panel B is a bright-field image. Ao, aorta; lv, left ventricle; rv, right ventricle. E, Relative luciferase activity directed by Runx2 with co-transfection of Hrt1, Hrt2 or Hrt2 mutant proteins. Numbers indicate amino acid positions of mutant proteins. F, Schematic and summary of Hrt2 mutant protein effects on Runx2. B, basic domain; HLH, helix-loop-helix domain; orange, orange domain; Y/T, YXPW-TEIGAF motif. G, Semi-quantitative RT-PCR of Hrt1, Hrt2 and G3PDH in COS7 cells with or without transfection of Notch intracellular domain. H, Pull-down assays with GST-Hrt2 fusion protein and 35S-labelled Runx2. I, Relative luciferase activity of Runx2 with Hrt1 or Hrt2 in the presence of trichostatin A or DMSO control. Luciferase data are shown as percentage of Runx2 activation (normalized to 100%); mean plus minus s.d. are shown.

	CHD	Aortic Valve Morphology	Surgery	Aortic Valve Replacement	Other congenital anomalies/diseases	Cause of Death
I-1	U	U	-	-	U	Colon CA at 66 yo
I-2	U	U	-	-	U	MI at 62 yo
II-1	AS, AI, dilated asc aorta	three leaflet	+	Yes, 65 yo	HTN, hyperlipidemia, CVA, breast CA	
II-2	AS	BAV	+	Yes, 76 yo	HTN	CVA after AVR
III-1	Normal		-			
III-2	Normal		-			
III-3	abnormal AV	three leaflet	-	-	uterine CA	
III-4	VSD	U	-	-	scoliosis	Eisenmenger
III-5	AS, dilated asc aorta	BAV	+	Yes, 26 yo	retinal embolism	sudden death
III-6	AI	BAV	+	Yes, 33 yo	HTN, depression	
III-7	Normal					
III-8	AI	BAV	-	-	U	
III-9	U	U	-	-	U	MVA
IV-1	TOF, bicuspid PV	three leaflet	+	-	s/p Waterston shunt	after surgery
IV-2	AS	three leaflet	-	-	seizure disorder	
IV-3	U	U	-	-	U	
IV-4	VSD, MS, parachute MV	BAV	+	-	s/p VSD closure; s/p MVR	
V-1	AS, dilated asc aorta	BAV	-	-		
V-2	Normal					

Supplementary Figure 1B

	CHD	Aortic Valve Morphology	Surgery	Aortic Valve Replacement	Other congenital anomalies/diseases	Cause of Death
I-1	U	U	-	-	U	
I-2	U	U	-	-	U	
II-1	AS	BAV	+	Yes	AA, s/p AoR	
II-2	Normal	three leaflet	+	No	AA, s/p AoR, s/p PM	
III-1	MA, HLV, DORV	BAV	+	-	s/p palliative surgery	
III-2	AS	BAV	+	Yes		
III-3	Normal					
III-4	Normal					

Abbreviations: AS=aortic stenosis; AI=aortic insufficiency; AVR=aortic valve replacement; AoR=aortic root replacement; AA=ascending aortic aneurysm; BAV=bicuspid aortic valve; CHD=congenital heart disease; DORV=double outlet right ventricle; HLV=hypoplastic left ventricle; MA=mitral atresia; MVR=mitral valve replacement; MS=mitral stenosis; MV=mitral valve; PM=pacemaker; PDA=patent ductus arteriosus; TOF=tetralogy of Fallot; VSD=ventricular septal defect; CA=cancer; CVA=cerebrovascular accident; HTN=hypertension; MI=myocardial infarction; MVA=Motor Vehicle Accident; U=unknown.

Supplementary Figure 3.4**: Clinical phenotype of Family A and Family B.**
1A and 1B show the detailed clinical phenotypes of individuals in Families A and B respectively, as described in Fig. 1. Key for abbreviations is shown. Shaded rows represent unaffected family members who did not have a *NOTCH1* mutation.

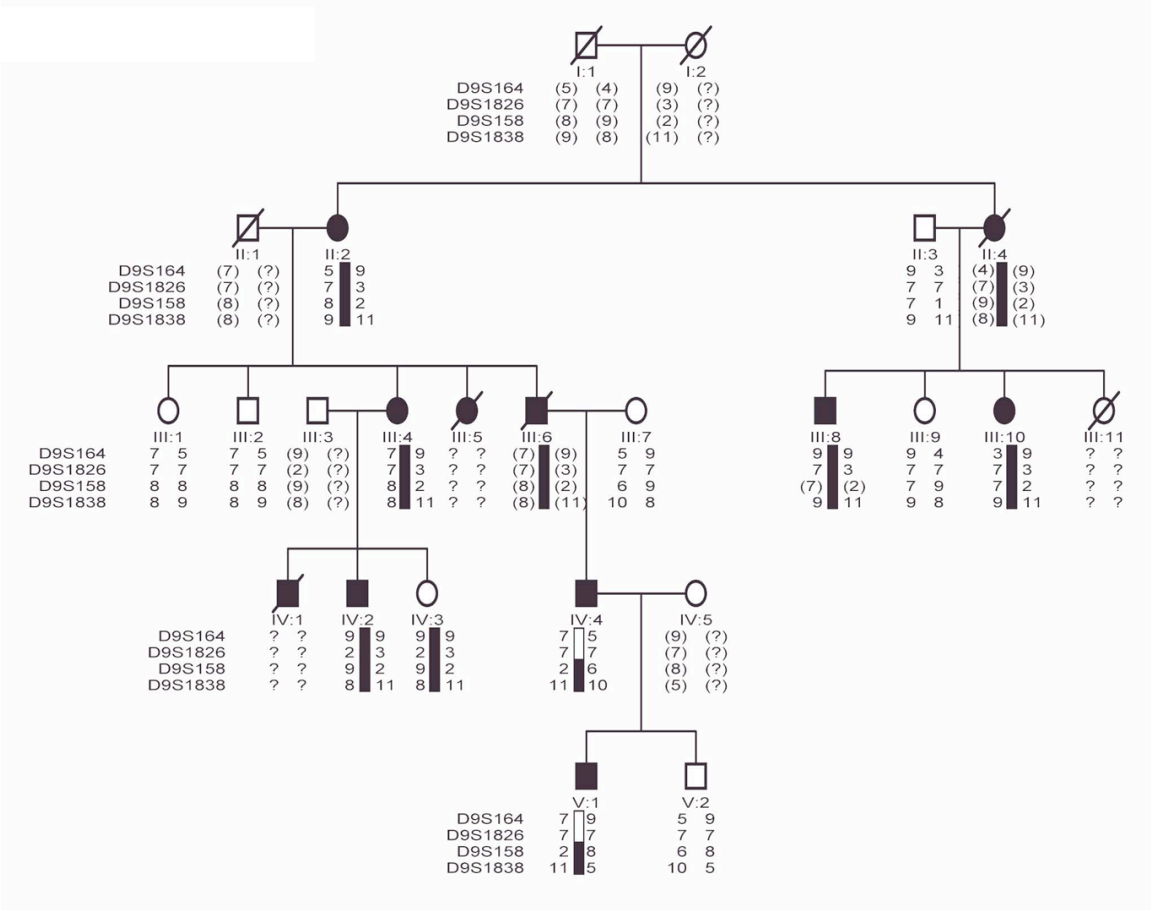

Supplementary Figure 3.5**: Pedigree of Family A with haplotype data.**
Mapping within linked region on chromosome 9q. The region between markers D9S158 and D9S1838 was shared among affected individuals as shown by black colored box. Parentheses indicate predicted haplotypes while the haplotype was unable to be determined in those marked with "?".

NOTCH1 Genetic Abnormality	Ethnicity of Identified Family	Overall SNP Frequency in Control Population	Ethnicity	SNP Frequency by Ethnicity
R1108X	European-American (Family A)	0/1136	European-American African-American Hispanic Other	0/349 0/543 0/217 0/27
H1505del	Hispanic (Family B)	0/1138	European-American African-American Hispanic Other	0/350 0/544 0/217 0/27

Supplementary Figure 3.6**: Ethnicity data for *NOTCH1* polymorphisms.**
For each genetic abnormality identified in *NOTCH1*, the ethnicity of the family is shown. The allele frequencies of the genetic abnormalities in each ethnic population are also shown.

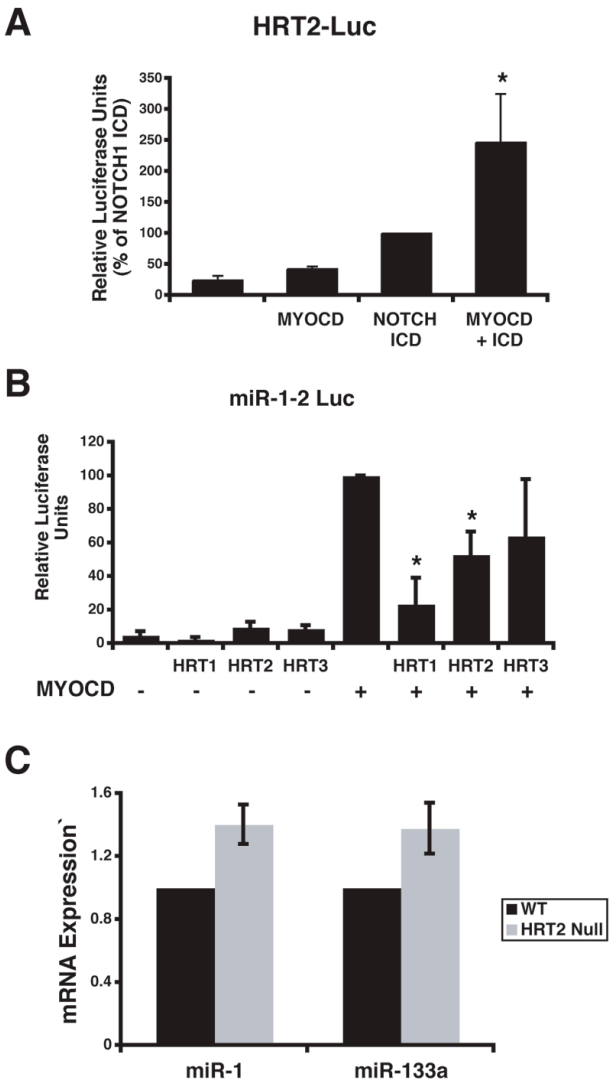

Figure 3.7**: MYOCD and NOTCH1 Synergistically Interact and HRT1/2 Inhibits MYOCD-Dependent miR-1 expression**
A, effect of MYOCD^{935} cotransfected with the NOTCH1 intracellular domain (ICD) on HRT2–Luc. *B*, effect of HRT1, 2, or 3 cotransfected with MYOCD on miR-1-2-Luc. *C*, quantitative RT-PCR for total microRNA in the miR-1 and miR-133a family. Whole heart mRNA was collected from E13.5 HRT2 null embryos and WT littermate controls. *, $p<0.05$ vs control.

Chapter 4: Dysregulation of Cardiogenesis, Cardiac Conduction and Cell Cycle in Mice Lacking microRNA-1-2

Yong Zhao[1,2,3]*, Joshua F. Ransom[1,2,3]*, Ankang Li[6,7], Vasanth Vedantham[1,4], Morgan von Drehle[1], Alecia N. Muth[1], Takatoshi Tsuchihashi[1,2,3], Michael T. McManus[5], Robert J. Schwartz[6], Deepak Srivastava[1,2,3,#]

[1]Gladstone Institute of Cardiovascular Disease, [2]Department of Pediatrics (Cardiology), [3]Department of Biochemistry & Biophysics, [4]Department of Internal Medicine (Cardiology), and [5]Diabetes Center, University of California, San Francisco; [6]Institute of Biosciences and Technology, Texas A & M Health Science Center; and [7]Graduate Program in Cardiovascular Sciences, Baylor College of Medicine

*Contributed equally to this work

ABSTRACT

MicroRNAs (miRNAs) are genomically encoded small RNAs used by organisms to regulate the expression of proteins generated from messenger RNA transcripts. The in vivo requirement of specific miRNAs in mammals through targeted deletion remains unknown, and reliable prediction of mRNA targets is still problematic. Here, we show that miRNA biogenesis in the mouse heart is essential for cardiogenesis. Furthermore, targeted deletion of the muscle-specific miRNA, miR-1-2, revealed numerous functions in the heart, including regulation of cardiac morphogenesis, electrical conduction, and cell cycle control. Analyses of miR-1 complementary sequences in mRNAs upregulated upon *miR-1-2* deletion revealed an enrichment of miR-1 "seed matches" and a strong tendency for potential miR-1 binding sites to be located in physically accessible regions. These findings indicate that subtle alteration of miRNA dosage can have profound consequences in mammals and demonstrate the utility of mammalian loss-of-function models in revealing physiologic miRNA targets.

INTRODUCTION

Many complex cellular, developmental, and homeostatic processes depend on precise spatiotemporal regulation of protein levels, some of which function as "rheostats" to execute programs in a quantitative fashion. The dose-sensitivity of proteins involved in the development and maintenance of organs is highlighted by the numerous human diseases caused by heterozygous mutations that result in haploinsufficiency (http://www.ncbi.nlm.nih.gov/entrez/query.fcgi?db=OMIM). This is particularly true for the heart. The heart is one of the most conserved organs at the molecular level (161-163) and is the organ most affected by disease in childhood and adult populations (164). Human heart disease can involve abnormalities in morphogenesis, muscle maintenance and function, and cardiac rhythm. Damage to heart muscle is typically irreversible as cardiomyocytes terminally exit the cell cycle postnatally and have little or no regenerative capacity, despite niches of cardiac progenitors that may contribute to basal turnover of myocytes (165-169). Networks of transcription factors regulate heart development and maintenance in a dose-dependent manner, but the effects of translational regulation on the titration of these pathways are largely unknown.

MicroRNA (miRNA)-mediated control of protein expression is likely a widely used mechanism for post-transcriptional regulation of important cellular pathways (170-174). Nearly 500 mammalian miRNAs are transcribed in the nucleus and undergo successive processing events by the enzymes Drosha and Dicer to ultimately yield mature miRNAs of ~20–22 nucleotides (172,173,175). Mature miRNAs typically bind to target mRNAs by partial sequence matching after becoming incorporated into the RNA-induced silencing complex (RISC), resulting in degradation of the mRNA transcript and/or

translational inhibition. Disruption of miRNAs in *Caenorhabditis elegans* and *Drosophila* suggest several ways by which miRNAs may control cellular events. In some cases, they function to "fine-tune" physiologic events, but in others they function as molecular "switches" (176-184). miRNAs can also function in a "fail-safe" mechanism to silence mRNAs that are unwanted in specific cell lineages (185,186). In mice, interference with miRNA biogenesis by tissue-specific deletion of *Dicer* revealed a requirement of miRNA function during limb outgrowth, (187) and in development of skin progenitors (188). However, the in vivo requirement of specific miRNAs in mammals through targeted deletion remains unknown.

We and others have described muscle-specific miRNAs, such as the bicistronic miR-1 and miR-133 cluster, and miR-206. miR-1 and –133 are expressed in cardiac and skeletal muscle and are transcriptionally regulated by the myogenic differentiation factors MyoD, Mef2, and serum response factor (SRF) (176,178,189-192). An ancient genomic duplication likely resulted in two distinct loci for the miR-1/miR-133 cluster in vertebrates, with identical mature sequences derived from the duplicated loci. In *Drosophila*, deletion of the single *miR-1* gene (*dmiR-1*), expressed specifically in cardiac and somatic muscle, results in a defect in muscle differentiation or maintenance (176,178). *dmiR-1* targets the Notch ligand, Delta, a known regulator of cardiogenesis and myogenesis in flies (178). In contrast, overexpression of miR-1 in mouse cardiac progenitors has a negative effect on proliferation, where it targets the transcription factor Hand2, which is involved in myocyte expansion (189). Similar to the heart, miR-1 overexpression in cultured skeletal myoblasts promotes skeletal muscle differentiation, as does the related but skeletal muscle–specific miR-206 (191,193). miR-133

overexpression curiously prevents skeletal muscle differentiation, suggesting that differential processing from the bicistronic transcript may regulate cellular decisions of differentiation or proliferation (191). Although significant dysregulation of miRNA expression has been reported in cardiac disease (194,195), it remains unknown if the heart requires miRNA function for normal development or maintenance.

A major obstacle in understanding how miRNAs regulate cellular events has been identifying mRNAs that are directly targeted by a specific miRNA. While a few targets have been validated at the protein level for miR-1 and several other miRNAs, each miRNA likely targets tens of different mRNAs (196-199). Bioinformatic approaches rewarding a high-degree of Watson-Crick base-pairing at nucleotides 2–7 at the 5′ end of the miRNA (the so-called "seed match") and its mRNA target have been informative, but specificity remains a problem in efficiently identifying targets (197,198,200-202). We proposed that accessibility of the miRNA binding site within the mRNA, as defined by the local secondary structure and free energy characteristics of the mRNA, may be an important predictor of true miRNA:mRNA interactions (189). We had found that most validated miRNA targets exist in locally accessible regions of mRNAs, although mammalian targets have generally been validated in overexpression models that may not accurately reflect endogenous requirements (170). The true importance of target accessibility in mammalian physiologic settings has awaited generation of in vivo loss-of-function models to better ascertain criteria for miRNA:mRNA interactions at a genome-wide level.

In this report, we examine the effects of a global loss of miRNAs during cardiac development and use targeted deletion to examine the requirement of a specific miRNA,

miR-1-2. We demonstrate that the functions of miR-1 are dose-sensitive and that miR-1-2 regulates cardiac morphogenesis, cardiac conduction and the cardiac cell cycle. Using the loss-of-function model, we characterize miR-1-2 targets and evaluate the importance of miRNA target accessibility along with seed matching in determining miRNA targets.

MATERIALS AND METHODS

Generation of Dicer Conditional Null or miR-1-2 Null Mice — Dicer$^{flox/flox}$ *mice (187) and* Nkx2.5-Cre *mice (203) have been described previously and were intercrossed to generate* Nkx2.5-Cre*;* Dicer$^{flox/flox}$ *mice. Genotyping was performed as described. To generate* miR-1-2 *null mice, Sv129 embryonic stem (ES) cells were electroporated with the targeting vector.* Nde *I or* Sac *I digests of genomic DNA were used for Southern blot genotyping of 5′ or 3′ recombination, respectively. Two of the 1500 colonies screened were properly targeted and injected into C57BL6 blastocysts to generate high percentage chimeras that were bred to recover heterozygous mice with germline transmission.*

RNA in Situ Hybridization, Quantitative Real-Time PCR and RT-PCR Analysis — RNA in situ hybridizations of whole embryos were performed as described (Yamagishi et al., 2003). qPCR was performed using the ABI 7900HT (TaqMan, Applied Biosystems) per the manufacturer's protocols. Primer sets for *Mib1* spanned exons 19–20 (Taqman: Mm00523008_m1) or exons 12–13; sequences are in Supplementary Methods. Expression levels were normalized to Gapdh expression. Semi-quantitative RT-PCR was done in the linear range of amplification. Statistical analysis was performed using the two-tailed student's t-test.

Immunohistochemistry and Western blot Analysis — Histological sectioning and

hematoxylin & eosin staining were performed according to standard practices. Immunohistochemistry was performed on paraffin embedded sections (7 μm) as described in Supplement Material. Western blots were performed as described previously (189) on heart tissues from P10 mice. Irx5 antibody (kindly provided by C.C. Hui) was used at 1:100 dilution; goat polyclonal Hand2 (Santa Cruz Biotechnology) at 1:100 dilution, and Dicer C-20 antibody (Santa Cruz Biotechnology) at 1:100 dilution.

Quantification of Cardiomyocyte Cell Numbers — Cardiomyocytes from adult hearts were isolated as previously described using an alkaline dissociation method (204,205). Cell suspension (10 μl) was loaded onto a Fuchs-Rosenthal counting chamber (Hausser Scientific). Cardiomyocytes in the counting chamber were distinguished from fibroblasts by cytoplasmic size and the presence of sarcomeres. The numbers of cardiomyocytes per mm^2 of counting chamber were evaluated 8 times per heart (n=3).

Sequence Analysis and Free Energy Calculations — Mouse 3′ UTR sequences were retrieved from the RefSeq database (http://www.ncbi.nlm.nih.gov/RefSeq/). Bioinformatic analyses of miRNA binding sites were performed as described with ΔG's determined using mFold (Zhao et al., 2005). Determination of motif occurrence assessment is described in Supplementary Methods.

Noninvasive Assessment of Heart Function — Transthoracic echocardiography was used for noninvasive serial assessment of cardiac function in mice using a Vevo 770 ultrasound machine (VisualSonics). Cardiac electrophysiological function was assessed by surface electrocardiograms as described in Supplementary Methods. Mean, standard deviation, and standard error of the mean were calculated for each genotype, and all pairwise statistical comparisons were made with t-tests.

Cell Culture and Transfection Assays — Irx5 3′ UTR was cloned into a pGL-TK vector as described (189) and introduced into Cos cells with or without a plasmid containing miR-1. Luciferase assays were performed as described previously (189).

Microarray Analysis — Mouse genome-wide gene expression analysis was performed using Affymetrix mouse genome 430 2.0 array. RNA was extracted from E11.5 or P10 whole heart tissue using Trizol reagent (Invitrogen) per manufacturer's protocol. Microarray analysis was performed in triplicate from independent biologic samples according to the standard Affymetrix GeneChip protocol. Data was analyzed with GeneSpring software (Agilent Technologies). Details of statistical analyses can be found in Supplementary Materials.

RESULTS

Disruption of the *Dicer* Allele in Cardiac Progenitors

To assess the global requirement of miRNAs in the mouse heart, we deleted a floxed *Dicer* allele (187), using Cre-recombinase under control of the endogenous *Nkx2.5* regulatory region, which directs expression in cardiac progenitors by embryonic day (E) 8.5 (203). *Dicer*, which is essential for processing of pre-miRNAs into the mature form (206), was efficiently deleted in the heart, and the embryos died from cardiac failure by E12.5 (Figure 1). Embryos lacking Dicer in the developing heart exhibited pericardial edema and a poorly developed ventricular myocardium. Most markers of initial cardiac differentiation and patterning, such as Tbx5, Hand1, Hand2, and Mlc2v were normal (Figure 1). Microarray analysis of E11.5 hearts in triplicate, before obvious signs of dysfunction, revealed upregulation of several genes, such as the

endoderm marker alpha fetoprotein and the skeletal muscle–specific gene, fast skeletal troponin; numerous genes were also downregulated, including ones encoding the homeodomain only protein (Hop), myoglobin, and the potassium channel Kcnd2 (Supp. Figure 1). The early lethality in the *Dicer* mutant revealed an essential requirement for miRNA function in the developing heart.

One of the most abundant and specific miRNAs affected in the *Dicer* mutant heart was miR-1. miR-1-1 and miR-1-2 are both specific for cardiac and skeletal muscle and are co-transcribed as bicistronic messages with miR-133a-2 and miR-133a-1, respectively, but have unique expression patterns (189,191,207). Using PCR primers specific for each miRNA, we found that both were present in the embryonic and postnatal heart, although miR-1-2 expression began slightly earlier in the embryonic heart (Figure 1).

Targeted Deletion of *miR-1-2* in Mice

To define the in vivo function of a specific miRNA in mammals, we targeted the 21-nt mature *miR-1-2* sequence for deletion by homologous recombination in mouse embryonic stem (ES) cells. *miR-1-2* is transcribed as a 2.5-kilobase (kb) message containing miR-1-2 and miR-133a-1 sequences (191). The *miR-1-2*/*miR-133a-1* gene resides in a 14.6-kb genomic region between the 12th and 13th exons of the *Mind bomb1* (*Mib1*) locus, involved in Notch signaling (Koo et al., 2005) in an antisense orientation and is regulated by an independent SRF-dependent enhancer in the heart and MyoD-dependent enhancer in skeletal muscle (Figure 2) (189). Gene targeting was designed to remove the mature 21-nt *miR-1-2* sequence, while leaving the rest of the transcribed sequence, enhancer region, and *Mib1* exons intact (Figure 2).

Mice heterozygous for *miR-1-2* survived without any apparent abnormalities and reproduced efficiently. *miR-1-2* heterozygotes were intercrossed, and in the surviving homozygous mutants, we confirmed the absence of the miR-1-2 transcript with PCR primers specific for the pre-form of miR-1-2. The miR-133a-1 pre-form was transcribed intact, and we did not detect compensatory changes in miR-1-1 levels. Importantly, Mib1 transcript levels were unchanged in the *miR-1-2* mutant with efficient transcription through the targeted locus, as determined by quantitative real-time RT-PCR (qPCR) using primers crossing the 19^{th}-20^{th} exon (Figure 2). PCR across exons12 and 13 revealed normal splicing of exons surrounding the targeted locus (Figure 2). Thus, we specifically targeted the *miR-1-2* locus without affecting nearby genes.

Cardiac Morphogenetic Defects in *miR-1-2* Mutants

Genotyping of offspring from *miR-1-2* heterozygous intercrosses revealed 50% lethality by weaning (Figure 3). Mendelian ratios were observed in offspring until E15.5, but thereafter, death occurred at varying times, ranging from E15.5 to just after birth. The external anatomy of mutant embryonic hearts was unremarkable, except for occasional enlargement. Skeletal muscle was grossly normal. However, histologic analysis revealed a large ventricular septal defect (VSD) in half of the embryos (Figure 3). Failure of ventricular septation results in death within hours after birth in mice, but some *miR-1-2*$^{-/-}$ embryos also exhibited pericardial edema before birth, consistent with primary myocardial dysfunction in utero contributing to embryonic demise.

VSDs can result from dysregulation of myriad events during cardiogenesis, and it is likely that miR-1-2 regulates numerous genes during this process. Our previous studies demonstrated a highly conserved miR-1 binding site in the 3′-UTR

of a critical cardiac transcription factor, Hand2, that responded to overexpression of miR-1 by inhibiting translation (189). Precise dosage of Hand2 is essential for normal cardiomyocyte development and morphogenesis (208-214). The mRNA levels of Hand2 were unchanged in *miR-1-2* mutants, but the protein levels were increased approximately fourfold as seen by western blots (Figure 3), consistent with Hand2 being a physiologic miR-1 target in vivo.

Cardiac Electrophysiologic Defects in *miR-1-2* Mutants and miR-1-2 Regulation of Irx5

The *miR-1-2* homozygous mice that survived post-natally exhibited a range of phenotypes. In some cases (~15%), mice developed rapid dilation of the heart and ventricular dysfunction with evidence of atrial thrombi and death by 2–3 months of age. The rest were remarkably normal with no dysfunction by echocardiography nor evidence of scarring, but many suffered sudden death. Because abnormalities in cardiac conduction and repolarization often cause sudden death, we performed surface electrocardiography in mutant mice and their littermates. The average heart rate of mutants was significantly lower than wild-type littermates, and the normal delay between atrial and ventricular depolarization (the PR interval) was shortened (Figure 4). In addition, ventricular depolarization, manifested by the QRS complex, was significantly prolonged in the mutant hearts. Synchronous depolarization of ventricular myocytes is coordinated by rapid conduction through the atrioventricular bundle, bundle branches, and Purkinje fibers. The increased width and the morphology of the QRS complex in the mutants was typical of abnormal conduction along one of the bundle branches (bundle branch block), a finding that in humans can be associated with an increased risk of sudden death (215).

In our search for potential miR-1 targets that might explain aspects of the cardiac conduction abnormalities, we found that the 3′-UTR of Irx5 had a well-conserved miR-1 binding site (Figure 4) and was located in a region of very high free energy (5′ DG: –8.5; 3′ DG: –2.8), suggesting a locally accessible site. Irx5 belongs to the Iroquois family of homeodomain-containing transcription factors and regulates cardiac repolarization by repressing a key potassium channel, Kcnd2 (216). We therefore cloned the miR-1 binding site (5x) from the Irx5 3′-UTR or the entire Irx5 3′-UTR into the luciferase reporter 3′-UTR, with transcription of luciferase under control of a constitutively active thymidine kinase promoter. Introduction of these reporter plasmids into tissue culture cells resulted in high levels of luciferase activity. Addition of miR-1 into this system resulted in a significant reduction in luciferase activity, which was specific for miR-1, as introduction of miR-133 did not result in a significant change in activity (Figure 4). Since miRNAs can repress protein production by affecting either mRNA stability or translation, we assessed both mRNA and protein levels in *miR-1-2* mutant hearts. qPCR revealed a nearly twofold increase in Irx5 mRNA levels in *miR-1-2* null hearts compared to wild type, and western blots showed an approximately fivefold increase in Irx5 protein accumulation by densitometry (Figure 4). Consistent with the upregulation of Irx5, we found that transcripts of the Irx5 target gene *Kcnd2* were downregulated in the mutant hearts (Figure 4). These data provide compelling evidence that miR-1 regulates the cardiac electrical system and directly targets Irx5.

miR-1-2 Regulates Cardiac Cell Cycle and Karyokinesis

Although the vast majority of adult *miR-1-2* mutants had normal cardiac function, we often observed thickening of the walls of the heart by echocardiography. We

confirmed this observation by assessing the heart-to-body weight ratios of mice sacrificed at 4–6 months of age. The mutant mice had a significant increase in this ratio (Figure 5). Histologic analysis revealed no evidence of myocyte hypertrophy or fibrosis, suggesting that the increased weight may be due to hyperplasia. Dissociation of heart muscle in wildtype and mutants and assessment of cell number revealed a 20% increase in the number of cardiomyocytes in *miR-1-2* null mice (Figure 5). The normal variance among animals was minimal, and this represented a significant degree of hyperplasia ($p<0.001$). Closer histologic examination of the adult hearts revealed that many myocytes appeared to be undergoing nuclear division. Immunohistochemistry with antibodies recognizing phosphohistone H3 (PH3) (217), a marker for mitotic nuclei, and cardiac α-actinin to mark cardiomyocytes, revealed the unusual presence of mitotic adult cardiomyocytes (Figure 5). Post-natal mouse cardiomyocytes typically undergo a single round of nuclear and sometimes cellular division in the first two weeks of life, before terminally exiting the cell cycle (218,219). At post-natal day 10 (P10), we consistently found a significant increase in PH3-positive myocytes (~threefold, $p<0.02$), indicating increased proliferation in the *miR-1-2* mutants (Figure 5). PH3-positive myocytes—never observed in adult wild-type mice—were found in 2–3-month-old mutant animals, although the number of PH3-positive cells was highly variable ranging from a few cells to the large number of cells indicated in a highly affected adult *miR-1-2* mutant heart.

Enrichment of miR-1 Seed Matches among mRNAs Upregulated in *miR-1-2* Mutants

A major benefit of studying mice that lack a specific miRNA is the ability to investigate mRNAs that may be upregulated upon loss-of-function of the miRNA, a

subset of which may be direct miRNA targets. These would represent targets regulated at the level of mRNA stability rather than via translational inhibition (220). To address this, we performed mRNA expression microarray analyses of P10 wildtype and mutant hearts, well before any obvious dysfunction. 45 protein-coding genes were significantly upregulated and 25 downregulated in *miR-1-2* null hearts (Figure 6). The dysregulated genes clustered into several major categories, including upregulation of cardiac transcription factors, such as Irx5 (as described above), Irx4, Hrt2, Hand1 and Gata6. In addition, we observed upregulation of numerous cell-cycle regulators and concomitant downregulation of tumor suppressor genes (Figure 6). qPCR of candidate dysregulated genes validated over 80% of those tested, suggesting that the subtle dysregulation of numerous regulatory genes may contribute to the *miR-1-2* mutant cardiac irregularities. qPCR data of a subset of cell cycle and tumor suppressor genes and genes encoding cardiac transcription factors are consistent with the proliferative phenotype of the mutant (Figure 6).

If some of the mRNAs upregulated upon *miR-1-2* deletion were direct targets, we would expect a disproportionate percentage of sequence complementarity with miR-1 in their 3′-UTRs (221). We therefore analyzed the 3′-UTRs for Watson-Crick base-pairing with varying stretches of residues between nucleteotides 1 and 8 of miR-1, encompassing the seed match. We compared the occurrence of motifs that had sequence matching with 5′ or 3′ regions of miR-1 in mRNAs upregulated or downregulated in *miR-1-2* mutants with the frequency of such motifs in over 26,000 mRNA 3′-UTRs encoded by the mouse genome. We did the same analysis for enrichment of seed matches with a second miRNA, miR-124, as a control.

There was no statistical enrichment for miRNA complementarity among mRNAs downregulated in mutants. However, we observed significant enrichment for matches with miR-1 positions 1–8, 2–8, 2-7, and 1–7 among mRNAs upregulated in *miR-1-2* mutants (Figure 7, $p<0.001$). An upward slope in the graphical depiction (Figure 7B–D) of tabular data indicates enrichment of miR-1 seed matches in upregulated genes. Although nearly 50% of upregulated genes had 2-7 seed matches, the six nucleotide complementarity did not effectively discriminate between up- and downregulated genes. However, 12/45 upregulated mRNAs (27%) had a miR-1 match of at least seven nucleotides in the 5′ region compared to 2/25 in the downregulated group ($p<0.0001$). No enrichment of 3′-sequence matches was observed in the upregulated genes. As an important control, there was no enrichment for 5′ matches of miR-124 with the upregulated genes in the *miR-1-2* mutant (Figure 7).

Accessibility of miRNA Binding Sites Defined by Local Free Energy

The degree of Watson-Crick base-pairing, particularly in the 5′ end of the miRNA, is a major criterion in defining miRNA:mRNA interactions (197,198,201,222,223). However, many mRNA targets predicted by sequence matching fail validation tests in vivo (189,202). There is increasing recognition that contextual features may also govern this interaction (171,224-226). Earlier, we proposed physical accessibility of the mRNA target region as a potential contextual feature and found that nearly all miRNA targets validated at the level of protein regulation were found preferentially in regions of high free energy (ΔG) and unstable secondary structure (170,189). Quantification of the ΔG for 70 nucleotides flanking each side of the miRNA binding site and evaluation of the secondary structure of the target site itself allowed

establishment of potential criteria to enhance target prediction. Since few miRNA targets have been described in mammals, the validity of this model remains uncertain.

The generation of *miR-1-2* mutants provided an opportunity to test whether upregulated mRNAs that contain seed matches are more frequently located in high ΔG areas than would be expected randomly. We calculated the ΔG of 70 nt immediately flanking the 5′ and 3′ sides of each miR-1 binding site in mRNAs upregulated in *miR-1-2* mutants and determined if it was above or below the species average. The ratio of regions flanking miR-1 binding sites with higher than average free energy compared to those with lower than average free energy was quantified as the "free energy index." In mice, there is a relatively equal distribution of high or low ΔG regions among 70 nucleotide 3′-UTR fragments, resulting in an average index of 1.17 among 100 randomly selected sequences. However, among the mRNAs upregulated in the *miR-1-2* mutant, the index was 6.69, indicating significant enrichment of miR-1 binding sites that are located in more accessible regions (Figure 8 and Supp. Table 1; Supp. Fig. 2; $p < 0.01$).

We extended the evaluation of this index to other targets that have been validated in 1) miRNA loss-of-function models in vivo or 2) in reporter assays involving endogenous rather than overexpressed miRNAs, given the potential for non-physiologic interactions upon overexpression (202). The free energy index in validated *C. elegans* miRNA targets was 5.67 (species average, 0.92; $p < 0.001$), suggesting that these targets were also preferentially located in accessible regions as defined by free energy of flanking regions (Figure 8, Supp. Fig. 3). In *Drosophila* the index was 3.0 for validated targets (species average, 0.67), but the number of targets was insufficient for statistical analysis. Evaluation of a number of other miRNA targets validated at the protein level in

tissue culture or through overexpression studies revealed that they too were almost always in areas with at least one high ΔG flanking region (Supp. Table 2).

The recent in vivo experimental testing of 16 specific *C. elegans* lsy-6 target sites with perfect seed pairing revealed striking discordance between the predicted and validated lsy-6 binding sites, although the reason for this discrepancy was unclear (202). We tested the utility of the free energy index on the experimentally validated (2/16) or non-validated (14/16) lsy-6 targets. The index among non-validated sites was 1.33 (close to species average), while both validated sites were in very high ΔG regions (Figure 8). This evaluation suggests a strong predictive value of the index, at least in this setting, and may explain why certain lsy-6 predicted targets were not true targets in vivo based on target site accessibility.

DISCUSSION

In this report, we demonstrate that miRNA function in cardiac progenitors is necessary for cardiogenesis and show that disruption of just one of the two *miR-1* family members, *miR-1-2*, has profound consequences for development and maintenance of the heart. Mice lacking *miR-1-2* have a spectrum of abnormalities, including VSDs in a subset that suffer early lethality, cardiac rhythm disturbances in those that survive, and a striking myocyte cell-cycle abnormality that leads to hyperplasia of the heart with nuclear division persisting post-natally. Remarkably, a redundant *miR-1-1* locus did not compensate for loss of *miR-1-2*, at least for many aspects of its function. While it is likely that mice lacking both *miR-1-1* and *miR-1-2* will have even more profound abnormalities, the range of defects upon deletion of *miR-1-2* highlights the ability of miRNAs to

regulate multiple diverse targets in vivo. Using the loss-of-function model, we determined in vivo miR-1-2 targets, including the cardiac transcription factor, Irx5, and used this model to evaluate the importance of miRNA target accessibility and of seed matching in determining miRNA targets.

miR-1-2 Regulates Cardiac Morphogenesis

In animals and in humans, increases in copy number or gain-of-function mutations can be as consequential as loss-of-function, sometimes causing similar phenotypes (227-229). The sensitivity of the heart to gene or protein dosage is reflected in the nearly 1% of live human births that are affected by cardiac malformations, with ventricular septal defects being the most frequent (230). Interestingly, many genes that cause VSDs when deleted in mice were upregulated in the *miR-1-2* mutants. These included Hrt2/Hey2, a member of the hairy family of transcriptional repressors that mediates Notch signaling (135,152,231), which itself causes heart disease (Garg et al., 2005) and Hand1, a bHLH transcription factor involved in ventricular development and septation (211). Hand2, a close relative of Hand1, was not upregulated at the mRNA level but the Hand2 protein levels were increased, consistent with our previous report of miR-1 directly targeting Hand2 for translational repression (189). *Hand2* and *Hand1* are partially redundant and progressive loss of the four combined alleles cause increasingly severe heart defects suggesting that proper titration of Hand dosage is important for cardiogenesis (211,232). Gata6, a transcription factor partially redundant with Gata4 (233), was also upregulated. GATA4 heterozygosity in humans causes VSDs, suggesting this family of genes also plays a role in ventricular septation (44). Subtle dysregulation of

numerous developmental genes may contribute to the embryonic defects observed in *miR-1-2* mutants.

miR-1-2 Regulation of Cardiac Conduction

Disruptions in cardiac rhythm are frequent causes of sudden death in humans and frequently require placement of pacemakers and defibrillators (234). In *miR-1-2* mutants, we observed an abnormality in the propagation of cardiac electrical activity despite normal anatomy and function. Normally, depolarization and repolarization of cardiomyocytes are determined by the properties of a specialized network of cardiomyocytes, the cardiac conduction system (235). The transcriptional regulation of these cells requires precise dosages of several transcription factors (Cheng et al., 2003). One of these factors, Irx5, functions with the co-repressor Smyd1 to repress the potassium channel, Kcnd2 in an endocardial-to-epicardial transmural gradient within ventricular myocytes (216,236,237). Loss of Irx5 disrupts this pattern, resulting in ventricular repolarization abnormalities and predisposition to arrhythmias.

Of particular relevance to the findings in the *mir-1-2* mutants, combined loss of function of Irx5 and Irx4 causes prolongation of the PR interval (B.G. Bruneau, unpublished observations). We showed that *miR-1-2* mutants have the opposite phenotype, with a shortened PR interval, and that Irx5 is a direct target of miR-1. The increase in protein levels of Irx5 in *miR-1-2* mutants was greater than the increase in mRNA levels, raising the possibility that miR-1-2 may regulate both mRNA translation and stability via the Irx5 3'-UTR, although this may simply reflect an accumulation of protein. The increase in Irx5 protein levels in *miR-1-2* mutants corresponded to a decrease in the Irx5 target gene, *Kcnd2*, as expected, as well as increased Irx4 mRNA

levels. The decrease in Kcnd2 was also observed in *Dicer* mutant embryos, likely due to loss of miR-1.

In addition to the short PR interval, electrocardiography also revealed a broad QRS complex with features of bundle branch block, which can be associated with sudden death in humans, although the contribution of Irx5 dysregulation to this feature remains to be tested.

Cell-Cycle Dysregulation in *miR-1-2* Mutants

miR-1-2 mutants displayed an increase in mitotic nuclei at P10 that continued to varying degrees, even in the adult. The hyperplasia of mutant hearts and the upregulation of genes that promote the cell cycle were consistent with *miR-1-2*-mediated regulation of cell-cycle events in the mammalian heart. Manipulation of the cardiac cell cycle could potentially stimulate regenerative capacity of the heart but this has proved challenging given the stringent cell cycle control in cardiomyocytes (238). Karyokinesis in differentiated cardiomyocytes is not normally observed. In *miR-1-2* mutants, karyokinesis occurs in the adult heart, and the general molecular "threshold" for cell cycling may be lower, given the upregulation of cell-cycle genes and downregulation of tumor suppressors. While we observed an increased number of cardiomyocytes in the hearts of adult mutants, this is likely a result of the early increase in proliferation, as we do not have evidence that cytokinesis persists in the adult. Consistent with our findings, overexpression of miR-1 and the related miR-206 in skeletal myoblasts results in inhibition of DNA synthesis and withdrawal from the cell cycle (Kim et al., 2006). It will be interesting to determine if the cell cycle threshold is also affected in *miR-1-2*

mutant cardiac progenitor cells as they begin to differentiate into myocytes, possibly allowing greater expansion of such cells after injury.

Sequence Matching and Target Site Accessibility during miRNA:mRNA Interactions

Some features of miRNA-mRNA interactions have been revealed through elegant bioinformatics and experimental approaches (197,222,223,239), but the limited number of validated miRNA targets reflects our incomplete knowledge of the "rules" of miRNA target prediction. Base-pairing between nucleotides 2–7 of the miRNA and its target site is important. However, many conclusions regarding base-pairing have been drawn from overexpression of miRNAs, in which non-physiologic miRNA-mRNA interactions may occur and siRNA-like off-target effects may be observed (240,241).

The *miR-1-2*$^{-/-}$ mouse model described here provided a unique model to address the question of endogenous targets in a mammalian model. Our findings that mRNAs upregulated in hearts lacking *miR-1-2* were enriched for sequence matches with miR-1 nt 1–8, 1–7 or 2–8 was consistent with the concept of seed match significance. As suggested by previous studies, matches to only 2–7 occurred with higher frequency than would be expected in upregulated genes, but this feature was not useful in discriminating between up- and downregulated genes in the *miR-1-2*$^{-/-}$ model, suggesting that a 7-nt match may be more predictive .

Another potential feature of miRNA:target site interactions may involve local accessibility of the binding site. Significant portions of mRNA sequences are hidden, and only local single-strand regions are accessible for binding to single-strand RNA. Thus, complex RNA secondary structures may have inhibitory effects on miRNA-mRNA

interactions. In earlier work, we found that validated miRNA target sites typically had destabilizing elements or had high free energy in regions flanking the 5′ or 3′ ends of the target site (189). Several additional miRNA targets have been validated in vivo, and we continue to find that most miRNA binding sites reside in areas of high free energy. Analysis of upregulated mRNAs in *miR-1-2* mutants that contain miR-1 binding sites revealed a strong bias toward sites in areas of high free energy. We attempted to quantify this bias with a free energy index that allows determination of the likelihood that target sets are located in accessible areas and therefore may be more likely to be true targets. Analysis of putative *C. elegans* lsy-6 targets provided further evidence of flanking free energy as a criterion for target prediction (202). Indeed, insertion of a lsy-6 binding site into a favorable region of lin-28 allowed targeting by lsy-6, but introduction of an equally matched lsy-6 site into a free energy area of unc-54 did not result in effective targeting. Our findings suggest that RNA accessibility, as assessed by free energy of flanking regions, may be a critical feature of miRNA target recognition. The accessibility of an mRNA binding site may be a factor that is regulated by cells via RNA binding proteins or other mechanisms that modulate RNA secondary structure. This may be analogous to DNA-binding proteins that function as transcriptional regulators only when local chromatin modifications render *cis*-elements accessible for interaction with transcription factors. RNA accessibility as a criterion for target recognition, if upheld as more targets are identified and validated, has the potential to rapidly accelerate the pace of biological discovery related to miRNA biology, as specificity of target prediction has been one of the most significant obstacles in this nascent field.

FOOTNOTES

Microarray data has been submitted and can be accessed by GEO accession number GSE7333.

ACKNOWLEDGEMENTS

The authors thank K. Ivey for helpful discussions and critical review of the manuscript; B. Harfe (University of Florida, Gainesville, Florida) for generously providing *Dicer* mutant mice; W. Yu for technical assistance; G. Howard for editorial assistance; P. Ursell (UCSF) for assistance with pathological analyses; S. Morton and J. Morton for help with statistical analyses; B. Taylor for preparation of graphics and manuscript; and C.C. Hui (Hospital for Sick Children, Toronto) for the Irx5-specific antibody. Y.Z. (yzhao@gladstone.ucsf.edu) is a post-doctoral scholar of the California Institute of Regenerative Medicine. V. V. was supported by NIH (T32HL007731) D.S. is supported by grants from the NHLBI/NIH, March of Dimes Birth Defects Foundation and is an Established Investigator of the American Heart Association. This work was also supported by NIH/NCRR grant (C06 RR018928) to Gladstone Institutes.

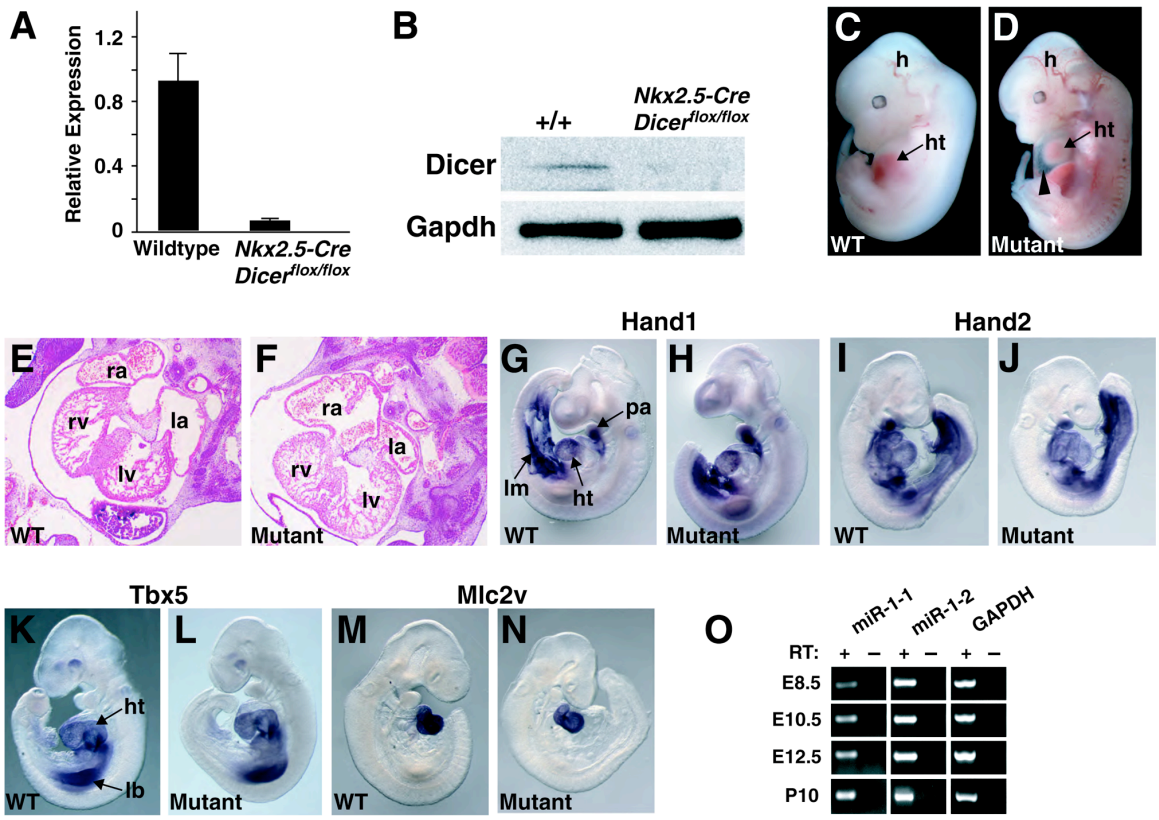

Figure 1**. miRNA Biogenesis Is Necessary for Cardiogenesis**
(A) Quantitative RT-PCR for relative mRNA levels of Dicer's RNAse III domain. (B) Protein level of Dicer in wild type (WT) or *Nkx2.5-Cre*; *Dicer*^{flox}/*Dicer*^{flox} embryos measured by western blot using an antibody that recognizes the RNAse III domain. (C,D) *Nkx2.5-Cre*; *Dicer*^{flox}/*Dicer*^{flox} (mutant) embryos showed developmental delay and pericardial edema (arrow) at E12.5. (E,F) Transverse sections of E11.5 embryos showing thin-walled myocardium in mutant. (G–N) Whole-mount in situ hybridization with indicated cardiac markers in wild type and mutant E9.5 embryos. (O) RT-PCR using primers specific for miR-1-1 or miR-1-2 in wild type hearts at E8.5, E10.5, E12.5 and P10 with or without reverse transcriptase (RT). ra, right atrium; la, left atrium; rv, right ventricle; lv, left ventricle; h, head; ht, heart; pa, pharyngeal arch; lm, lateral mesoderm; lb, limb bud.

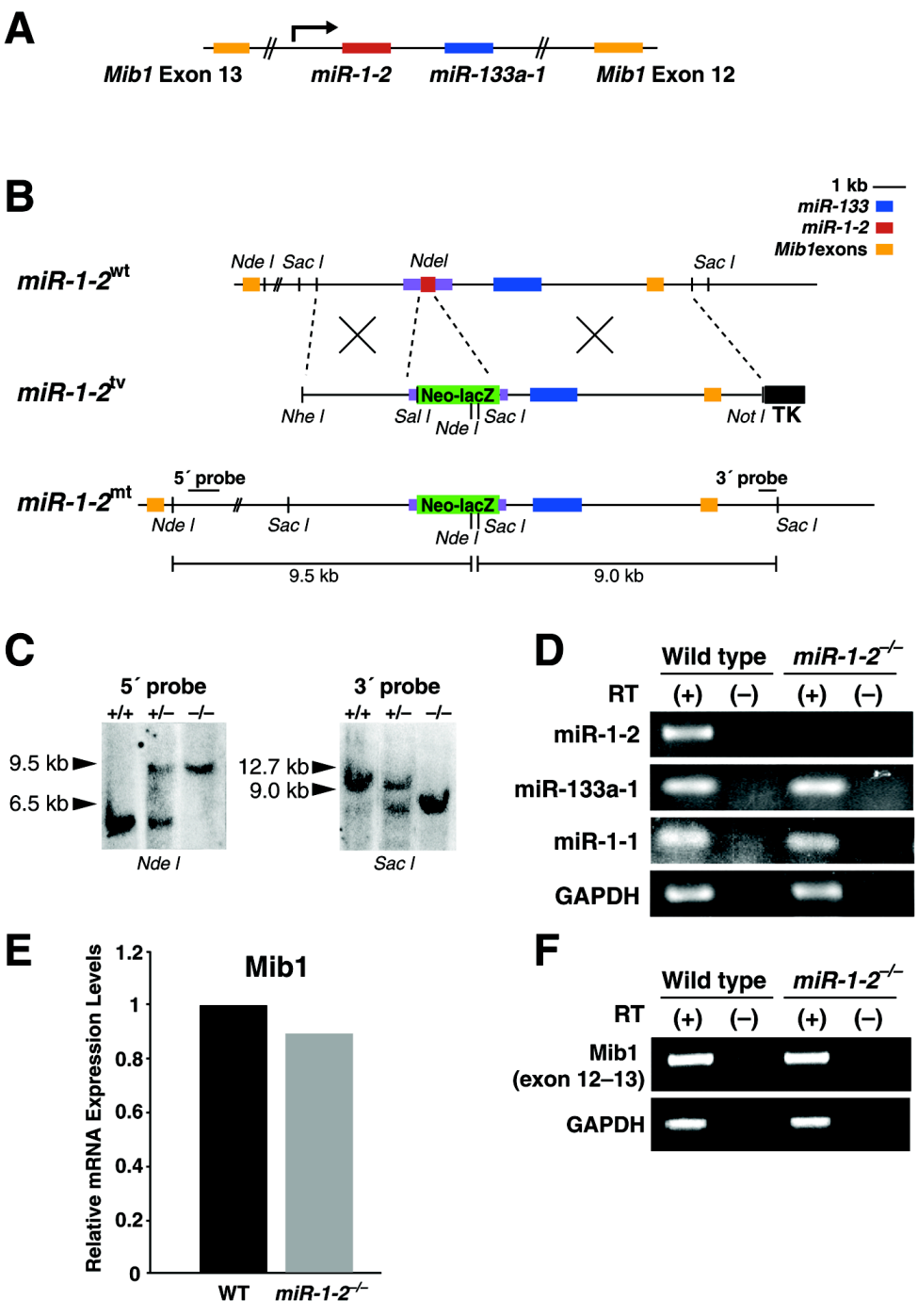

Figure 2**. Generation of Mice with Targeted Deletion of *miR-1-2***
(A) Schematic of the *miR-1-2* and *miR133a-1* locus between the 12th and 13th exons of *Mind bomb1* (*Mib1*); arrow indicates direction of transcription of the miRNAs, opposite of *Mib1* transcription. (B) Targeting strategy for deletion of *miR-1-2* by replacement of 21 nucleotides with the *Neomycin* (*Neo*) resistance cassette using homologous recombination. The wild type (wt) and mutant (mt) loci are shown with the targeting vector (tv). Mature miR-1-2 sequence is indicated in red, pre-miR-1-2 in purple. TK, thymidine kinase. (C) Genomic southern analysis of wild-type (+/+), *miR-1-2*

heterozygous (+/–) or homozygous (–/–) mice using 5´ or 3´ probes, after digesting genomic DNA with *Nde* I or *Sac* I, respectively. (D) RT-PCR of wild-type and *miR-1-2* null hearts showing specific loss of *miR-1-2* in comparison to *miR-133a-1* and absence of miR-1-1 upregulation. (E) Real-time qPCR results in WT or mutant hearts showing intact transcription of the *Mib1* gene using primers 3´ of the miRNA locus (exons 19–20). Data are presented as means +/- SEM.(F) RT-PCR using primers spanning exons 12 and 13 showing normal splicing across the targeted region.

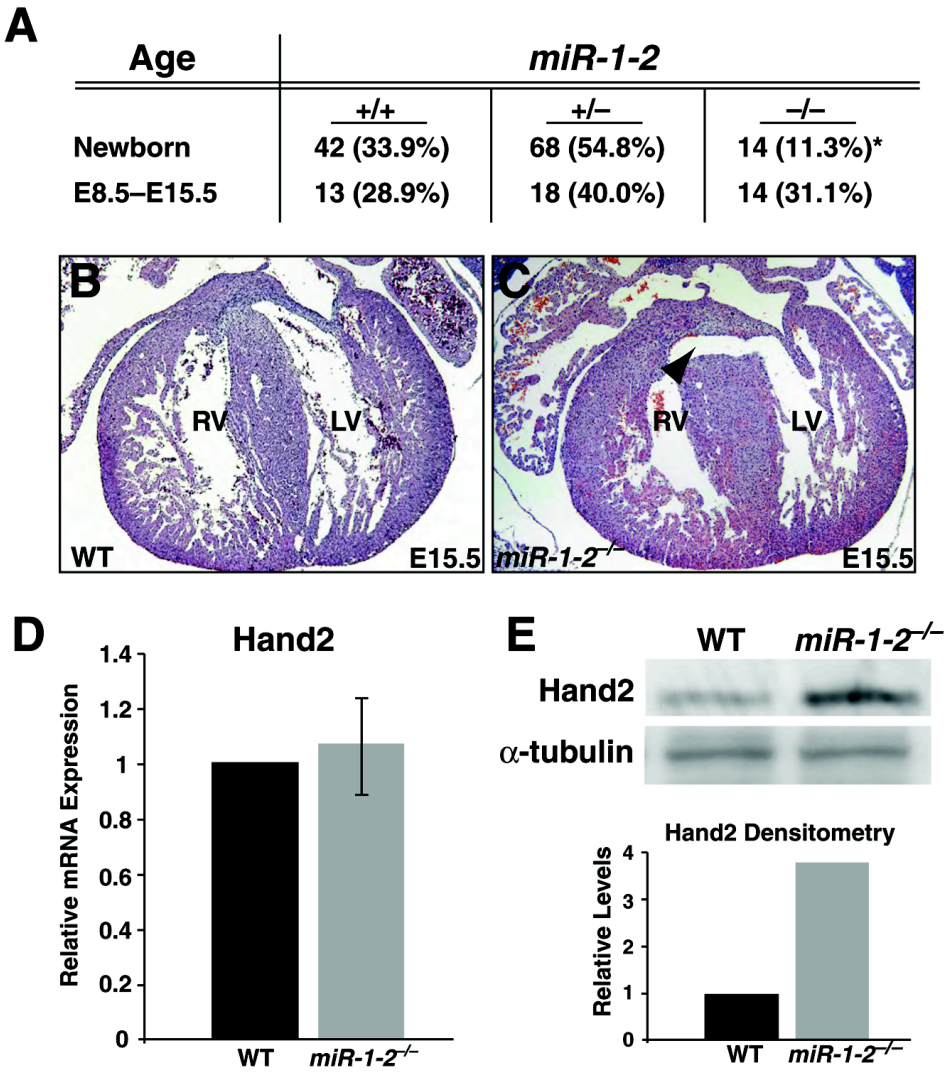

Figure 3**. Partial Penetrance of Cardiac Morphogenetic Defects in *miR-1-2* Mutants**
(A) Genotypes of mice from *miR-1*-2$^{+/-}$ intercrosses. Absolute numbers are shown with percentages in parenthesis. *p<0.025. (B, C) Transverse sections of wild type (WT) or *miR-1-2*$^{-/-}$ hearts at E15.5 showing ventricular septal defect (arrowhead). (D) qPCR of Hand2 showing similar levels of Hand2 mRNA in *miR-1-2* mutant and WT hearts. Data are presented as means +/- SEM. (E) Western blot of protein lysate from WT or mutant hearts showing increased Hand2 protein level in mutant, quantified by densitometry. rv, right ventricle; lv, left ventricle.

A

Parameter	*miR-1-2* +/+ (n = 7)	+/– (n = 9)	–/– (n = 12)	*P* value
Heart Rate (bpm)	459 ± 12	483 ± 11	411 ± 15*	0.03
PR Interval (msec)	35.5 ± 0.6	35.4 ± 0.6	33.4 ± 0.5*	0.03
QRS Interval (msec)	10.7 ± 0.3	10.8 ± 0.2	12.3 ± 0.3*	0.004
QT Interval (msec)	57 ± 2	55 ± 1	64 ± 1*	0.01
QTc	50 ± 2	50 ± 1	52 ± 1	0.3

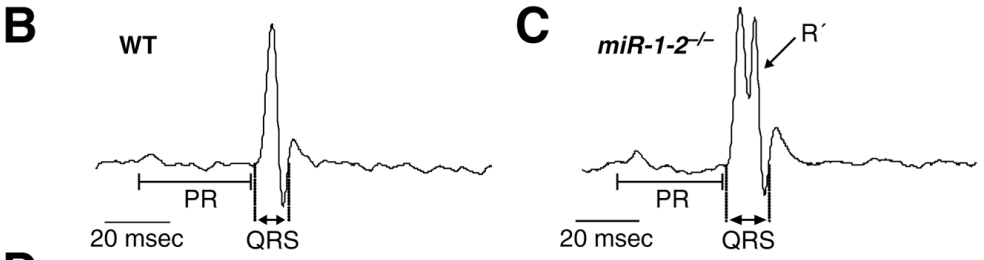

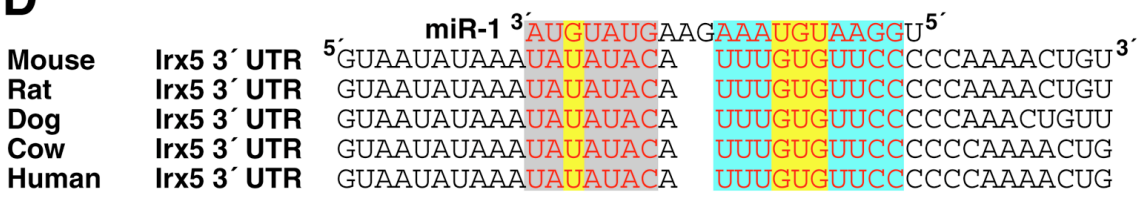

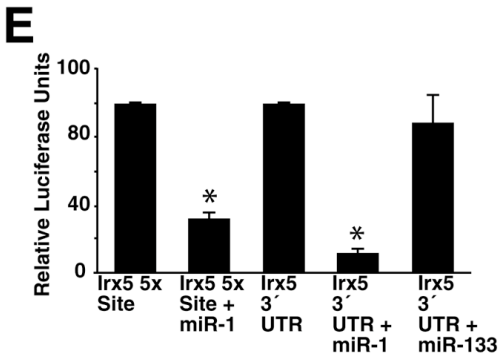

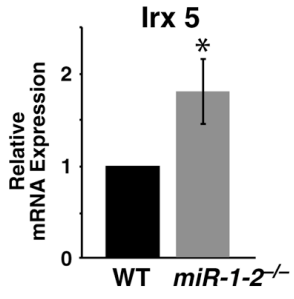

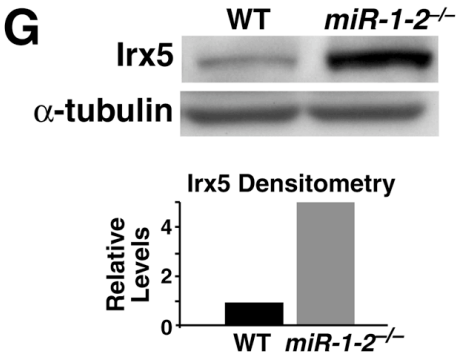

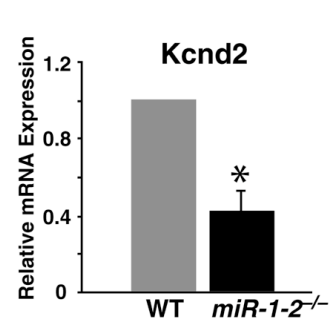

Figure 4**. Cardiac Electrophysiologic Defects in *miR-1-2* Mutants and miR-1-2 Regulation of Irx5**

(A) Electrocardiographic parameters of wild-type (+/+), *miR-1-2*$^{+/-}$, and *miR-1-2*$^{-/-}$ adult mice. $P<0.05$ was considered significant. bpm, beats per minute; msec, milliseconds. (B, C) Representative diagrams of electrocardiograms in lead II indicate the location of PR and QRS intervals. The second peak in the QRS complex (R') was observed in 58% of mutant and only 14% of wild-type mice ($p<0.05$). (D) Sequence alignment between miR-1 and the 3′-UTR of Irx5 in several species. 5′ seed matching is shown with Watson-Crick base pairing in blue and non-Watson-Crick G::U wobble in yellow; sequence matching in the 3′ end is boxed in light gray. (E) Luciferase activity in Cos cells with the Irx5 miR-1 binding site (5x) or 3′-UTR of Irx5 cloned into the luciferase 3′-UTR. Values relative to luciferase reporter alone are shown. Data are presented as means +/- SEM. (F) qPCR of Irx5 mRNA in WT or *miR-1-2* mutants showing 1.8-fold increase in mutants (n=3). (G) Western blot of protein lysates of postnatal day 10 (P10) WT or *miR-1-2* mutant hearts with Irx5- or a-tubulin specific antibodies showing an increase in Irx5 protein in mutants, quantified by densitometry. (H) qPCR of the Irx5 target gene, *Kcnd2*, showing downregulation in the *miR-1-2* mutant. Data are presented as means +/- SEM. * indicates $p< 0.05$.

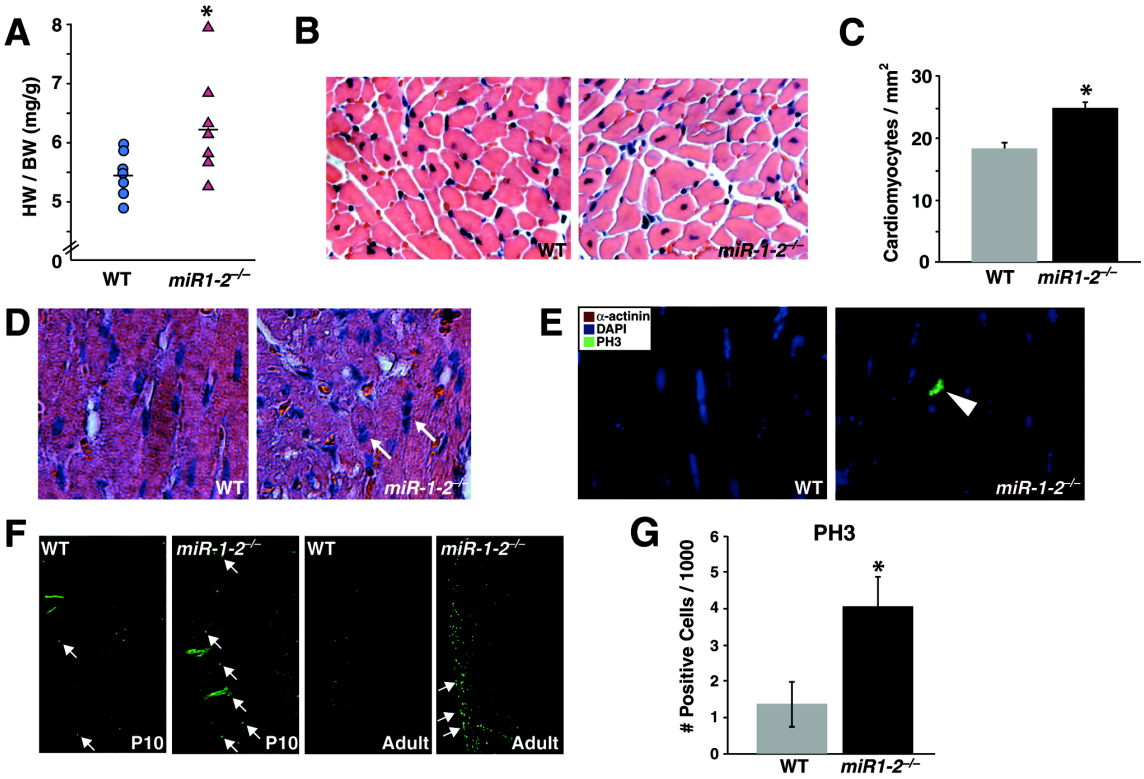

Figure 5**. Cardiomyocyte Hyperplasia and Proliferation in *miR-1-2* Mutants**
(A) The heart weight to body weight (HW/BW) ratio was greater in *miR-1-2*$^{-/-}$ adult mice than in wild-type (WT) mice with data from individual mice shown. Bars indicate averages, *p< 0.05. (B) Coronal sections stained with H & E showing similar cardiomyocyte diameter between adult WT and *miR1-2*$^{-/-}$ hearts and lack of hypertrophy. (C) Quantitation of cardiomyocyte number from dissociated WT or *miR-1-2*$^{-/-}$ adult hearts (n=3). (D) H & E of cardiac sections from adult hearts suggestive of mitotic nuclei in *miR-1-2*$^{-/-}$ animals (white arrows). (E) Immunohistochemistry using phosphohistone H3 (PH3, green), α-actinin (red) or DAPI (blue) antibodies demonstrating PH3-positive cardiomyocytes in the adult *miR-1-2* mutant. (F) Coronal sections of P10 and adult hearts showing an increase in the number of PH3^{+} nuclei in mutants compared to WT. (G) Quantification of PH3^{+} nuclei per section of P10 heart, showing average of multiple sections each from five WT or *miR-1-2* mutant mice. Data are presented as means +/- SEM. *p<0.05.

A

	Genes Dysregulated in *miR-1-2*$^{-/-}$	
	Upregulated	**Downregulated**
Cell cycle and/or associated with tumor	Gadd45b Trp53inp2 Runx1 Hlf protamine1 Rbbp9 Mt1 Netrin-1 Map2k5 Igsf4c Efna5 Efnb3	Lck Rad51l1 Arhgap20 Fbxw7 Lrrc3b
Cardiac growth and/or differentiation	Hrt2 Ror1 Gata6 Mov10l1	Nppb
Cardiac conduction system/ ventricular repolarization/ ion channels-associated gene	Irx5 Irx4 Cacna1c	Atp1a2 Kcnd2 Hamp1

B

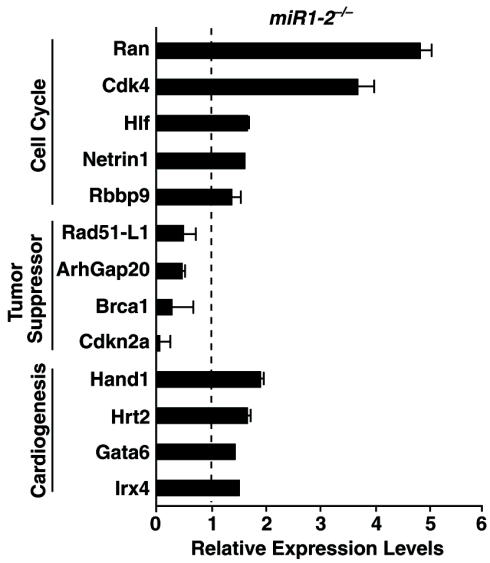

Figure 6**. Dysregulated Genes in *miR-1-2*$^{-/-}$ Hearts**
(A) Genes that were consistently up- or downregulated in the *miR1-2*$^{-/-}$ hearts at P10 by microarray analysis. (B) Validation of gene dysregulation in *miR-1-2*$^{-/-}$ P10 hearts compared to WT by qPCR. Data are presented as means +/- SEM. Dotted line indicates wild type expression levels for each gene set at one.

A

Motif Occurrence in 3´-UTRs

	Mouse mRNAs (n=26,968) (%)	Dysregulated mRNAs in *miR-1-2*$^{-/-}$ Upregulated (n=45) (%)	*P* value	Downregulated (n=25) (%)	*P* value
miR-1					
5´ region					
1–8 nt	2.1	8.8	0.0015	0.0	1.000
2–8 nt	5.9	20.0	0.0011	4.0	0.0714
1–7 nt	6.5	20.0	0.0002	4.0	0.8137
2–7 nt	18.0	48.9	0.0000	32.0	0.0661
3´ region					
14–21 nt	1.2	2.2	0.4192	0.0	1.0000
14–20 nt	4.0	8.9	0.1047	0.0	1.0000
15–21 nt	4.8	4.4	0.6427	12.5	0.1161
15–20 nt	17.1	20.0	0.3604	20.0	0.4294
miR-124					
5´ region					
1–8 nt	1.6	0.0	1.0000	4.0	0.3318
2–8 nt	7.8	8.9	0.4700	16.0	0.1262
1–7 nt	7.0	4.4	0.8325	8.0	0.5304
2–7 nt	77.1	53.3	0.9999	52.0	0.9986

B

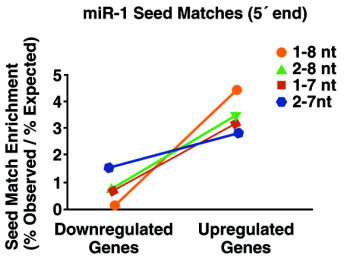

C

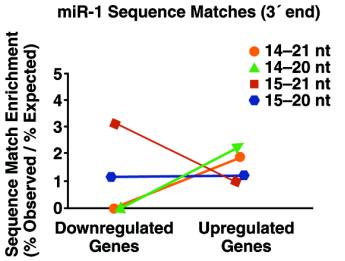

D

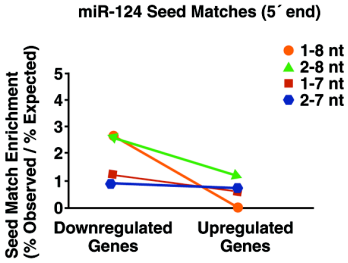

Figure 7**. Enrichment of miR-1 5´ Seed Matches among Genes Upregulated in *miR-1-2*$^{-/-}$ Hearts**

(A) Table showing the occurrence of miR-1 sequence matches in 3´-UTRs of all mRNAs of the mouse genome compared to genes up- or downregulated in *miR-1-2*$^{-/-}$ hearts at P10. The occurrence of motifs that had sequence matching with 5´ or 3´ regions of miR-1 is shown. Similar analysis for miR-124 was performed as a control. P values represent comparison with the genome-wide analysis. (B, C, D) Graphical depiction of the enrichment of miR-1 or miR-124 sequence matches among genes up- or downregulated in *miR-1-2* mutants versus the expected number from the mouse genome. A positive slope is indicative of enrichment of sequence matching in the upregulated vs downregulated genes.

A

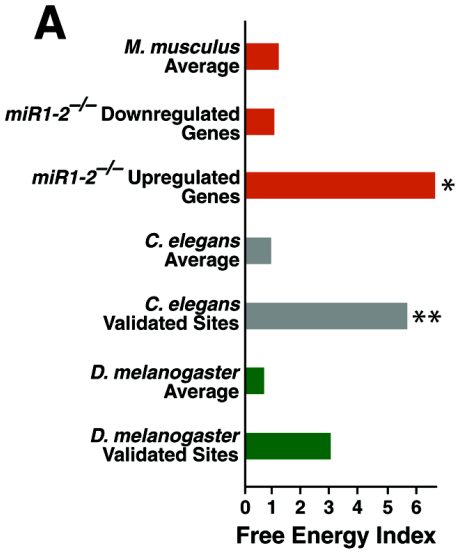

B

Organism	miRNA	Target	Site	5′ 70 bp (ΔG)	3′ 70 bp (ΔG)	Validation method
C. elegans (avg. ΔG=–7.2)	lin-4	*lin-14*	I	–7.7	–3.4	1
			II	–7.8	–1.5	
			III	–2.6	–4.2	
			IV	–5.0	–8.3	
			V	–4.2	–10.6	
			VI	–9.3	–8.7	
			VII	–3.2	–3.0	
		Lin-28	I	–0.6	–10.1	1
	let-7	*lin-41*	I	–0.6	–7.6	1
			II	–9.4	–7.2	
		daf-12	I	–1.6	–10.2	1
			II	–8.9	–1.1	
		pha-4	I	–10.1	–3.9	1
			II	–6.5	–6.6	
		lss-4	I	–17.6	–3.5	1
			II	–9.2	–1.8	
		lin-57	I	–1.5	–3.9	1
			II	–8.1	–8.8	
			III	–5.9	–4.7	
			IV	–2.3	–0.7	
			V	–0.3	–0.1	
			VI	–0.2	–0.3	
			VII	–0.7	–3.8	
			VIII	–0.3	–9.0	
		Ras	I	–1.4	–1.9	1
			II	–2.0	–6.5	
		Nhr-25	I	–6.5	–7.1	1
			II	–4.2	–1.0	
			III	–4.6	–0.5	
		Die-1	I	–15.8	–4.5	1
			II	–2.2	–0.4	
		T14B1.1	I	–7.7	–4.9	2
			II	–4.1	–0.2	
			III	–4.9	–0.3	
		C35E7.4	I	–2.8	–1.8	2
		UNC-129	I	–4.0	–0.7	2
	lsy-6	*cog-1*	I	–1.1	–1.7	1
	miR-273	*Die-1*	I	–3.8	–0.3	2
			II	–4.1	–5.5	
	miR-61	*Vav-1*	I	–0.7	–3.2	2
Drosophila (avg. ΔG=–8.5)	miR-7	*Yan*	I	–5.2	–1.5	1
			II	–4.5	–7.0	
	miR-278	*Expand*	I	–16.3	–6.1	1
			II	–6.6	–5.6	

C

Targets with complementary lsy-6 site	Validation in vivo	5′ 70 bp (ΔG)	3′ 70 bp (ΔG)
cog-1	Yes	–1.1	–1.7
Lin-28 (with lsy-6 binding site)	Yes	–0.3	–0.8
CO2B8.4	No	–6.0	–5.5
F55G1.12	No	–9.1	–5.6
T23E1.1	No	–6.9	–20.5
T14G12.2	No	–6.5	–6.9
Cct-1	No	–8.5	–8.4
T04C9.2	No	–9.9	–10.7
C27H6.3	No	–6.6	–13
C48.D5.2	No	–2.4	–11.7
T20G5.9	No	–11.4	–10.2
R07E3.5	No	–5.4	–7.6
F59A6.1	No	–6.9	–6.8
F40H3.4	No	–6.1	–6.3
ZK637.13	No	–6.5	–6.6
Unc54 (with lsy-6 binding site)	No	–1.5	–11.2

Figure 8**. Bias of miRNA Target Sites to "Accessible" Regions Defined by High Free Energy**

(A) Free energy index of miR-1 binding sites was defined by flanking regions (70 nucleotides) adjacent to either side of the binding site with calculated free energy (ΔG) above the species average divided by the number of flanking regions below the average. *p< 0.01, **p< 0.001. (B) List of miRNAs and their target sites within direct mRNA targets validated in vivo. The ΔG of 70 nt genes flanking each miRNA binding site on the 5′ or 3′ side is shown. Validation method by protein levels in loss-of-function models (1) or by repression of reporters by endogenous levels of miRNA activity (2) is indicated. (C) Analysis of free energy surrounding experimentally validated and non-validated *lsy-6* targets in vivo (202). The two validated targets were in much higher ΔG regions than either the *C. elegans* average (–7.2) or the non-validated targets, all of which were in low ΔG regions.

Supplementary Table 1

mRNA	Site	Flanking sequence ΔG (70 nt) 5′	3′
Upregulated in *miR-1-2*$^{-/-}$			
Speg	I	–22.9	–21.9
Bex4	I	–10.4	–5.4
Mapre2	I	–17.3	–7.0
Prps2	I	–6.5	–4.1
Slc25a23	I	–9.8	–12.4
	II	–2.3	–19.4
	III	–8.5	–15.4
Wdr40b	I	–10.2	–10.6
Gata6	I	–13.9	–10.2
Efna5	I	–8.6	–11.1
Gadd45b	I	–15.7	–2.3
Rbbp9	I	–15.4	–9.5
Sh3kbp1	I	–15.9	–8.9
Xpo6	I	–17.0	–19.2
	II	–15.8	–5.7
Downregulated in *miR-1-2*$^{-/-}$			
Kcnd2	I	–9.7	–4.8
Atpla2	I	–16.3	–21.5

Supplementary Table 2

Organism	miRNA	Target	Site	Flanking sequence ΔG (70 nt) 5′	3′
D. melanogaster	bantam	*Hid*	I	–3.4	–8.6
Ave. ΔG = –8.5			II	–9.5	–9.2
			III	–1.3	–4.1
			IV	–24.7	–19.2
			V	–8.6	-7.2
	miR-9a	*Sens*	I	–6.6	–8.8
			II	–6.8	–6.5
			III	–8.7	–6.2
	miR-1	*Delta*	I	–6.6	–3.2
M. musculus					
Ave. ΔG = 13.4	miR-196	*Hoxb8*	I	–12.8	–1.6
	miR-1	*Hand2*	I	–4.6	–13.1
H. sapiens					
Ave. ΔG = 13.2	Let-7	*Ras*	I	–7.2	–8.0
			II	–16.5	–4.8
			III	–13.6	–3.1

CHAPTER 5: DISCUSSION AND FUTURE DIRECTIONS

This work provides evidence for transcriptional, translational and post-translational regulation of heart development through multiple nodes. First, sporadic mutations in the transcription factor gene MYOCD were found to be associated with OFT valve disease. Both mutations were hypomorphic but for different reasons. Q647H disrupted putative kinase phosphorylation sites, while K259R disrupted SRF binding through a novel autoinhibitory domain. This autoinhibition was antagonized by the histone acetyltransferase, p300. Second, familial mutations in the NOTCH1 signal transduction pathway were found to be associated with aortic valve disease. These mutations revealed a role for NOTCH1 and its targets Hrt1/2 to repress calcification/bone formation in the valve leaflets. Notch signaling inhibits bone formation by repressing the osteoblast transcription factor RUNX2. Notch and Myocardin were also found to cooperate with or antagonize each other depending on the genomic location being targeted. One of the regions where Notch inhibits MYOCD was the promoters for microRNA-1. Finally, translational regulation in heart development was studied by the genetic perturbation of microRNAs in general and microRNA-1-2 specifically. The microRNA-processing enzyme Dicer was necessary for proper heart development and miR-1-2 was necessary for heart development, cardiac muscle cell cycle control, and proper cardiac conduction. Furthermore, microRNA target prediction rules were refined based upon the predicted secondary structure and accessibility of microRNA binding sites.

Valve Disease and Human Mutations

The two sequence variations in myocardin described here show potential association with a subset of CCVM, specifically stenosis in the outflow tract valves. Stenosis can occur whenever the valves are malformed and blood flow across the valves is impeded. This failure can occur either by decreasing the diameter of the arterial lumen above/below the valve or via a thickening of the valve leaflets directly. It is possible that myocardin mutations are responsible for only one of these specific subtypes of valve stenosis and that stronger statistical association would emerge from better characterization of the patient phenotype. The study of a MYOCD-dependent mouse model – either the K259R knock-in or MYOCD conditional deletion from the heart – may also provide a better understanding of how MYOCD is involved in OFT development. Since Q647H is more prevalent in the general population than K259R, it may also be worthwhile to generate a knock-in mouse of this mutation as well.

Unidirectional blood flow through the body is vital for oxygenation of the rest of the body. The formation of the valve leaflets is very tightly regulated, controlled by many known signaling pathways and through multiple morphogenetic events. Based on genetic studies in mice and other model organisms, the predominant areas where valvulogenesis is most likely to go afoul are at 1) preparation of extracellular matrix (ECM) in the valve cushions, 2) endothelial to mesenchymal transformation (EMT) and subsequent invasion of the valve ECM by these mesenchymal cells, 3) proliferation and differentiation of the mesenchyme (and other invading cells) into one of the multiple valve leaflet cell types, 4) thinning and remodeling of the valve leaflets through apoptosis and reorganization (125).

Based upon known properties of MYOCD though, I hypothesize that MYOCD will be involved in either EMT or in regulating the differentiation of valve tissue (126,242).

In the process of studying the Q647H mutation, it was shown that the serines at codon 650 and 654 could increase activity of MYOCD if they are mutated into phosphomimetic glutamates. Extrapolated from that, if Q647H disrupts phosphorylation at S650 and S654 and thus reduces MYOCD activity, then creating S650E and/or S654E in the Q647H background should rescue the partial loss of activity. Alternatively, the sequence surrounding Q647 (a.a. 644-KSP[Q/H]HISLPPSP-655) also provides clues as to how Q647H may reduce MYOCD activity. With three prolines surrounding Serine 654, it is highly predicted to be phosphorylated by a proline directed kinase, such as the MAPK family. This includes the ERK family of kinases that are known to be involved in Noonan's syndrome and cardiac valve stenosis through the RAS/MAPK pathway (28,87). It is hypothetically possible that ERK phosphorylates MYOCD at S654 to activate parts of the valve gene program and that Q647H would affect that activation signal. Q647H is also in the middle of a docking domain for p38, which is another class of kinases that are related to ERK and that, are known to activate MYOCD's cofactor, MEF2c (243). The docking domain consensus motif is Lysine-Xaa-Xaa-Xaa-Xaa-Hydrophobic-Xaa-Hydrophobic and **K***SPQH***I***S***L** perfectly matches the consensus. This docking domain may recruit MAPK family members that phosphorylate S654 to activate MYOCD, with Q647H disrupting the docking domain in this instance. Alternatively, the docking domain may recruit an inhibitory kinase with phosphorylation of S650 providing a negative charge to disrupt the hydrophobic residues. In this situation, Q647H could

enhance the docking domain or inhibit S650 phosphorylation. Mutation of the Lysine at codon 644 may reveal what, if any, role the putative docking domain plays.

The other kinase predicted to phosphorylate near Q647H, GSK3β, was able to inhibit WT MYOCD when overexpressed but showed activation of Q647H in the presence of low levels of GSK3β activity relative to the amount of MYOCD present. This suggests that Q647H blocks an activation signal that is dependent upon GSK3β, possibly through a secondary effect on another MYOCD inhibitor. How MYOCD may be regulated by MAPK does not elucidate a mechanism through which GSK3β generates this effect. GSK3β was previously shown to inhibit MYOCD by phosphorylating six of eight serines at S455,459,463,467,624,628,632, and 636, with an unknown priming kinase for S467/636 (108). Mutation of all eight serines in this motif (8xA) was able to block GSK3β dependent MYOCD inhibition. S650 is predicted to be GSK3β phosphorylation site in the event of a priming kinase that phosphorylates S654. It's possible that GSK3β both activates and inhibits MYOCD depending on the site of phosphorylation and depending on the activity of the priming kinases targeting S467/636 versus S654. If this were true, creation of 8xA with Q647H would be predicted to rescue MYOCD activity by relieving the GSK3β inhibitory signal. Conversely, mutating Q647H to also contain S654A should completely block the putative GSK3β activation signal. In other words, QS647,654HA would not be able to be activated in the presence of low (or any) levels of GSK3β. It will also be necessary to perform *in vitro* kinase assays to determine if serine 650 is phosphorylated by GSK3β directly. This would provide strong evidence for a GSK3β activation signal for MYOCD. Since activation of the Wnt/β-catenin pathway promotes valve stenosis and releases GSK3β from binding to β-catenin

(244), it is possible that Wnt (probably at low concentrations) may promote MYOCD activation in the presence of the correct priming kinase for GSK3β.

The MHD-dependent autoinhibition was also regulated by post-translational modifications, lysine acetylation. More work will be necessary to conclude how acetylation affects MYOCD autoinhibition. There is residual acetylation even when the p300 binding domain is removed from MYOCD, suggesting that p300 is recruited to MYOCD through another protein such as SRF. Possibly, the residual acetylation is due to another HAT other than p300, such as CBP (245). This seems plausible since CBP is associated with Notch pathway activation (246). Since deletion of the basic domain still resulted in partial acetylation, it seems less likely that K259 or the rest of the basic domain is a site of acetylation, but instead might be a binding/recruitment domain for a HAT. K259 acetylation cannot be ruled out though, until it has been determined which residues are acetylated within MYOCD. The $MYOCD^{\Delta MHD}$ isoform was used in the acetylation Western analysis because it is expressed at higher amounts compared to the $MYOCD^{935}$ isoform, but it will probably still be useful to compare the acetylation states of WT and K259R $MYOCD^{935}$. Once the acetylation patterns are known, mutation of the acetylated residues should help elucidate which residues are necessary for activation of transcription versus those involved in the relief from autoinhibition. It would also be fruitful to determine how deletion of the autoinhibitory domain without deleting the MEF2 binding motif would affect MYOCD activity.

Both MYOCD mutations will almost certainly affect valve formation through altered gene expression, so it will be eventually necessary to determine which MYOCD target genes are involved in valve development. More experimental evidence is needed,

but the preliminary results showing MYOCD can synergize with NOTCH1 to activate the Hrt2 promoter may be a link between the NOTCH and MYOCD gene programs. Multiple Notch pathway members are involved in OFT and valve development, making this a tantalizing avenue to follow up on (36,83,155). It will be necessary to more formally show that MYOCD binds to the promoter regions and activates the expression of Hrt1/2 *in vivo*. Also, since NOTCH specifically inhibited SRF-dependent MYOCD genes, it is possible that NOTCH is targeting the MYOCD:MEF2 pathway for synergistic activation. Alternatively, MYOCD is in a signaling feedback loop with the TGF-β/SMAD pathway (126,247,248), which may inhibit cell proliferation and promote differentiation in the valve tissue.

NOTCH and Hrt1/2 Repress Myocardin-Dependent miR-1/miR-133a Expression

Given the overlapping expression patterns of Hrt1/miR-1-1 and Hrt2/miR-1-2 and the preliminary results that the Notch pathway is able to inihibit MYOCD-dependent miR-1/miR-133a expression, there is probably an interesting and dynamic regulation of microRNAs by NOTCH, but more in depth analysis will be needed. Hrt2 can inhibit miR-1/miR-133a expression, but it needs to be formally shown that this is a Notch-dependent process. Overexpression of the NOTCH1-ICD in the context of MYOCD-dependent activation of the miR-1-2-Luc reporter would be the logical first step. Even though we observed Hrt-dependent repression of upstream miR-1 promoter (119), another MEF2-dependent promoter was also recently described (249) and it may be this or another unknown element that controls the miR-1 upregulation in the Hrt2 null hearts. One could also inhibit Notch activity with the γ-secretase inhibitor, DAPT, and determine if miR-1 is upregulated. Alternatively, utilization of the JAG1 expressing 10T1/2 cell line

created by Proweller et al. 2005 could be used to simulate Notch signaling when mixed with HL-1 cells transfected with MYOCD and miR-1-2-Luc. If Notch-dependent Hrt2 expression is necessary for inhibiting miR-1-2, then we would hypothesize that JAG1-10T1/2 cells would inhibit miR-1-2-Luc while normal 10T1/2 cells would not. While the Taqman miRNA primers are useful for studying mature miR expression, miR-1-1 and miR-1-2 cannot be differentiated because they have the same mature sequence. It would be more useful to look at each miR-1 cluster separately using primers specific to each cluster. Also, the Hrt1 and Hrt2 null mice will probably offer a useful way to study this regulation in more detail, but if our hypothesis is correct about tissue specific regulation then separating the ventricle from the atria should reveal a stronger deregulation of the separate clusters. Ultimately, it will be necessary to show that Hrt1 and/or Hrt2 are bound to the DNA promoters for the separate miR-1 clusters, which can probably be determined using either EMSA or chromatin immunoprecipitation (33,250).

microRNAs in Heart Development

MYOCD is able to activate the expression of both miR-1/133a clusters, and a MEF2-dependent enhancer has been described that drives miR-1-2 expression in the OFT pre-valve tissue but not the atrioventricular canal (249). No valve abnormalities were observed in miR-1-2 null mice, which suggests that miR-1 is not one of the MYOCD target genes that give rise to the valve abnormalities seen in the patients. Although, there is still the formal possibility that disruption of miR-1-1, miR-133a-1, miR-133a-2, or some combination of all four microRNAs will lead to improper valve development. On the other hand, miR-1-2 knockout mice displayed multiple heart defects that display the importance of gene dosage and translational regulation in heart development.

The best possible way to determine which miR-1 targets are responsible for the each of the three sets of defects will be to epistatically rescue the effect of miR-1 inhibition of mRNA translation. As shown, loss of miR-1-2 will lead to an upregualtion of its direct targets, so a proportionate reduction of miR-1 targets should counter-act the upregulation in miR-1-2 nullizygous animals. Breeding heterozygous mutations for miR-1 targets such as Hand2 or Delta-like 1 (78) into the miR-1-2 null background might rescue the embryonic lethality. miR-1-2-dependent conduction abnormalities may be rescued by partial loss of Irx5, although Cx43 (251) was recently shown to be a target and seems to be a better candidate based on its role in the cardiac conduction systerm (252). Currently, the only published miR-1 target that may account for the proliferating adult cardiomyocytes is Cdk9 (195) but no knockout mouse has been described. It might be possible to use primary rat cardiomyocytes with viral-mediated miR-1 inhibition using sponges (79) or antagomirs (253) to mimic the cardiomyocyte proliferative increase seen in the miR-1-2 null mice for the purpose of tesing Cdk9 or other targets.

Finally, the potential of accessibility for miRNA binding site(s) within a given mRNA is being experimentally studied and may play a key role in miRNA translational inhibition although possibily with a more complex set of rules than originally proposed (81,82). In silico prediction of mRNA secondary structure is immature, but experimentally determining the structure by either NMR or X-ray crytalography of any 3'UTR and hypothetical binding site will be very difficult due to the large size and flexibility of long mRNAs respestively. This also brings up the obvious possibility that if mRNA secondary structure affects accessibility then it also seems likely that tertiary structures will be able to affect miRNA:mRNA interactions as well.

There are many classes of RNA editing enzymes that may also be involved in the miRNA:mRNA targeting. Adenosine to Inosine conversion by ADARs has been shown to change which mRNA is targeted by miR-376 (254). APOBEC3G is best known for its ability to alter Cytidine to Uracil in HIV viral transcripts, but was also able to block miRNA repression without altering miRNA or mRNA sequence (255). In contrast to poly-adenosine tails classically added to the 3' end of mRNA molecules, the recently described poly-uracil polymerases (PUPs) are able to add poly-uracil tails to the 3' end of single stranded RNAs, including miRNAs (256). The addition of these extra nucleotides could alter the sequence recognition between a miRNA and its mRNA target adding yet another level of complexity. Finally, it is possible that RNA helicases could relax secondary structure to allow better access by miRNAs. One such cardiac specific RNA helicase, CHAMP, was able to inhibit both cardiomyocyte proliferation and hypertrophy *in vitro* (257). While this effect could be due multiple changes on any number of mRNA or miRNAs, it is interesting that miR-1 has been shown to be antagonistic to cardiomyocyte proliferation (111,119,178). Furthermore, overexpression of miR-133a was able to inhibit cardiac hypertrophy (258). Hypothetically, the CHAMP-dependent reduction in proliferation and hypertrophy could be due to increased 3'UTR accessibility for miR-1/133. Determining if CHAMP can increase miRNA-dependent inhibition of 3' UTRs in luciferase reporter assays could easily test this possibility.

As more miRNA targets are discovered the rules that govern miRNA:mRNA interactions will become better understood and lead to better *in silico* prediction tools. This will in turn probably help tease out the exceptions to these rules where novel regulatory events occur and an understanding of how the cell controls miRNA inhibition.

A more complete understanding of these rules and regulations of miRNA translational regulation will be necessary in the long run to realize the promise of miRNA/siRNA based therapies in patients.

CHAPTER 6: BIBLIOGRAPHY

1. Hoffman, J. I., and Kaplan, S. (2002) The incidence of congenital heart disease *J Am Coll Cardiol* **39**(12), 1890-1900
2. Garg, V. (2006) Molecular genetics of aortic valve disease *Curr Opin Cardiol* **21**(3), 180-184
3. Hoffman, J. I., Kaplan, S., and Liberthson, R. R. (2004) Prevalence of congenital heart disease *Am Heart J* **147**(3), 425-439
4. Brackley, K. J., Kilby, M. D., Wright, J. G., Brawn, W. J., Sethia, B., Stumper, O., Holder, R., Wyldes, M. P., and Whittle, M. J. (2000) Outcome after prenatal diagnosis of hypoplastic left-heart syndrome: a case series *Lancet* **356**(9236), 1143-1147
5. Srivastava, D. (2006) Making or breaking the heart: from lineage determination to morphogenesis *Cell* **126**(6), 1037-1048
6. Olson, E. N. (2006) Gene regulatory networks in the evolution and development of the heart *Science* **313**(5795), 1922-1927
7. Gittenberger-de Groot, A. C., Bartelings, M. M., Deruiter, M. C., and Poelmann, R. E. (2005) Basics of cardiac development for the understanding of congenital heart malformations *Pediatr Res* **57**(2), 169-176
8. Allen, H., Gutgesell, H., Clark, E., and Driscoll, D. (2001) *Moss and Adams' Heart Disease in Infants, Children, and Adolescents: Including the Fetus and Young Adult*, 6 Ed., Lippincott Williams & Wilkins
9. Buckingham, M., Meilhac, S., and Zaffran, S. (2005) Building the mammalian heart from two sources of myocardial cells *Nat Rev Genet* **6**(11), 826-835
10. Armstrong, E. J., and Bischoff, J. (2004) Heart valve development: endothelial cell signaling and differentiation *Circ Res* **95**(5), 459-470
11. Mikawa, T., Gourdie, R. G., Takebayashi-Suzuki, K., Kanzawa, N., Hyer, J., Pennisi, D. J., Poma, C. P., Shulimovich, M., Diaz, K. G., Layliev, J., et al. (2003) Induction and patterning of the Purkinje fibre network *Novartis Found Symp* **250**, 142-153; discussion 153-146, 276-149
12. Rentschler, S., Vaidya, D. M., Tamaddon, H., Degenhardt, K., Sassoon, D., Morley, G. E., Jalife, J., and Fishman, G. I. (2001) Visualization and functional characterization of the developing murine cardiac conduction system *Development* **128**(10), 1785-1792
13. Bruneau, B. G., Nemer, G., Schmitt, J. P., Charron, F., Robitaille, L., Caron, S., Conner, D. A., Gessler, M., Nemer, M., Seidman, C. E., et al. (2001) A murine model of Holt-Oram syndrome defines roles of the T-box transcription factor Tbx5 in cardiogenesis and disease *Cell* **106**(6), 709-721
14. Costantini, D. L., Arruda, E. P., Agarwal, P., Kim, K. H., Zhu, Y., Zhu, W., Lebel, M., Cheng, C. W., Park, C. Y., Pierce, S. A., et al. (2005) The homeodomain transcription factor Irx5 establishes the mouse cardiac ventricular repolarization gradient *Cell* **123**(2), 347-358
15. Zimmerman, E. F. (1991) Substance abuse in pregnancy: teratogenesis *Pediatr Ann* **20**(10), 541-544, 546-547

16. Starreveld-Zimmerman, A. A., van der Kolk, W. J., Elshove, J., and Meinardi, H. (1975) Teratogenicity of antiepileptic drugs *Clin Neurol Neurosurg* **77**(2), 81-95
17. Jerome, L. A., and Papaioannou, V. E. (2001) DiGeorge syndrome phenotype in mice mutant for the T-box gene, Tbx1 *Nat Genet* **27**(3), 286-291
18. Merscher, S., Funke, B., Epstein, J. A., Heyer, J., Puech, A., Lu, M. M., Xavier, R. J., Demay, M. B., Russell, R. G., Factor, S., et al. (2001) TBX1 is responsible for cardiovascular defects in velo-cardio-facial/DiGeorge syndrome *Cell* **104**(4), 619-629
19. Basson, C. T., Bachinsky, D. R., Lin, R. C., Levi, T., Elkins, J. A., Soults, J., Grayzel, D., Kroumpouzou, E., Traill, T. A., Leblanc-Straceski, J., et al. (1997) Mutations in human TBX5 cause limb and cardiac malformation in Holt-Oram syndrome *Nat. Genet.* **15**(1), 30–35
20. Li, Q., Newbury-Ecob, R., Terrett, J., Wilson, D., Curtis, A., Yi, C., Gebuhr, T., Bullen, P., Robson, S., Strachan, T., et al. (1997) Holt-Oram syndrome is caused by mutations in TBX5, a member of the Brachyury (T) gene family *Nat. Genet.* **15**(1), 21–29
21. Basson, C. T., Huang, T., Lin, R. C., Bachinsky, D. R., Weremowicz, S., Vaglio, A., Bruzzone, R., Quadrelli, R., Lerone, M., Romeo, G., et al. (1999) Different TBX5 interactions in heart and limb defined by Holt-Oram syndrome mutations *Proc. Natl. Acad. Sci. USA* **96**(6), 2919–2924
22. Satoda, M., Zhao, F., Diaz, G. A., Burn, J., Goodship, J., Davidson, H. R., Pierpont, M. E., and Gelb, B. D. (2000) Mutations in TFAP2B cause Char syndrome, a familial form of patent ductus arteriosus *Nat Genet* **25**(1), 42-46
23. Tartaglia, M., Mehler, E. L., Goldberg, R., Zampino, G., Brunner, H. G., Kremer, H., van der Burgt, I., Crosby, A. H., Ion, A., Jeffery, S., et al. (2001) Mutations in PTPN11, encoding the protein tyrosine phosphatase SHP-2, cause Noonan syndrome *Nat Genet* **29**(4), 465-468
24. Ion, A., Tartaglia, M., Song, X., Kalidas, K., van der Burgt, I., Shaw, A. C., Ming, J. E., Zampino, G., Zackai, E. H., Dean, J. C., et al. (2002) Absence of PTPN11 mutations in 28 cases of cardiofaciocutaneous (CFC) syndrome *Hum Genet* **111**(4-5), 421-427
25. Bahuau, M., Flintoff, W., Assouline, B., Lyonnet, S., Le Merrer, M., Prieur, M., Guilloud-Bataille, M., Feingold, N., Munnich, A., Vidaud, M., et al. (1996) Exclusion of allelism of Noonan syndrome and neurofibromatosis-type 1 in a large family with Noonan syndrome-neurofibromatosis association *Am J Med Genet* **66**(3), 347-355
26. Bahuau, M., Houdayer, C., Assouline, B., Blanchet-Bardon, C., Le Merrer, M., Lyonnet, S., Giraud, S., Recan, D., Lakhdar, H., Vidaud, M., et al. (1998) Novel recurrent nonsense mutation causing neurofibromatosis type 1 (NF1) in a family segregating both NF1 and Noonan syndrome *Am J Med Genet* **75**(3), 265-272
27. Rodriguez-Viciana, P., Tetsu, O., Tidyman, W. E., Estep, A. L., Conger, B. A., Cruz, M. S., McCormick, F., and Rauen, K. A. (2006) Germline mutations in genes within the MAPK pathway cause cardio-facio-cutaneous syndrome *Science* **311**(5765), 1287-1290
28. Niihori, T., Aoki, Y., Narumi, Y., Neri, G., Cave, H., Verloes, A., Okamoto, N., Hennekam, R. C., Gillessen-Kaesbach, G., Wieczorek, D., et al. (2006) Germline

KRAS and BRAF mutations in cardio-facio-cutaneous syndrome *Nat Genet* **38**(3), 294-296
29. Aoki, Y., Niihori, T., Kawame, H., Kurosawa, K., Ohashi, H., Tanaka, Y., Filocamo, M., Kato, K., Suzuki, Y., Kure, S., et al. (2005) Germline mutations in HRAS proto-oncogene cause Costello syndrome *Nat Genet* **37**(10), 1038-1040
30. Schubbert, S., Zenker, M., Rowe, S. L., Boll, S., Klein, C., Bollag, G., van der Burgt, I., Musante, L., Kalscheuer, V., Wehner, L. E., et al. (2006) Germline KRAS mutations cause Noonan syndrome *Nat Genet* **38**(3), 331-336
31. Li, L., Krantz, I. D., Deng, Y., Genin, A., Banta, A. B., Collins, C. C., Qi, M., Trask, B. J., Kuo, W. L., Cochran, J., et al. (1997) Alagille syndrome is caused by mutations in human Jagged1, which encodes a ligand for Notch1 *Nat. Genet.* **16**(3), 243–251
32. Oda, T., Elkahloun, A. G., Pike, B. L., Okajima, K., Krantz, I. D., Genin, A., Piccoli, D. A., Meltzer, P. S., Spinner, N. B., Collins, F. S., et al. (1997) Mutations in the human Jagged1 gene are responsible for Alagille syndrome *Nat. Genet.* **16**(3), 235–242
33. Nakagawa, O., McFadden, D. G., Nakagawa, M., Yanagisawa, H., Hu, T., Srivastava, D., and Olson, E. N. (2000) Members of the HRT family of basic helix-loop-helix proteins act as transcriptional repressors downstream of Notch signaling *Proc Natl Acad Sci U S A* **97**(25), 13655-13660
34. McDaniell, R., Warthen, D. M., Sanchez-Lara, P. A., Pai, A., Krantz, I. D., Piccoli, D. A., and Spinner, N. B. (2006) NOTCH2 mutations cause Alagille syndrome, a heterogeneous disorder of the notch signaling pathway *Am J Hum Genet* **79**(1), 169-173
35. Krantz, I. D., Smith, R., Colliton, R. P., Tinkel, H., Zackai, E. H., Piccoli, D. A., Goldmuntz, E., and Spinner, N. B. (1999) Jagged1 mutations in patients ascertained with isolated congenital heart defects *Am. J. Med. Genet.* **84**(1), 56–60
36. Garg, V., Muth, A. N., Ransom, J. F., Schluterman, M. K., Barnes, R., King, I. N., Grossfeld, P. D., and Srivastava, D. (2005) Mutations in NOTCH1 cause aortic valve disease *Nature* **437**(7056), 270–274
37. Schott, J. J., Benson, D. W., Basson, C. T., Pease, W., Silberbach, G. M., Moak, J. P., Maron, B. J., Seidman, C. E., and Seidman, J. G. (1998) Congenital heart disease caused by mutations in the transcription factor NKX2-5 *Science* **281**(5373), 108–111
38. Benson, D. W., Silberbach, G. M., Kavanaugh-McHugh, A., Cottrill, C., Zhang, Y., Riggs, S., Smalls, O., Johnson, M. C., Watson, M. S., Seidman, J. G., et al. (1999) Mutations in the cardiac transcription factor NKX2.5 affect diverse cardiac developmental pathways *J. Clin. Invest.* **104**(11), 1567–1573
39. Goldmuntz, E., Geiger, E., and Benson, D. W. (2001) NKX2.5 mutations in patients with tetralogy of fallot *Circulation* **104**(21), 2565–2568
40. Ikeda, Y., Hiroi, Y., Hosoda, T., Utsunomiya, T., Matsuo, S., Ito, T., Inoue, J., Sumiyoshi, T., Takano, H., Nagai, R., et al. (2002) Novel point mutation in the cardiac transcription factor CSX/NKX2.5 associated with congenital heart disease *Circ J* **66**(6), 561-563

41. McElhinney, D. B., Geiger, E., Blinder, J., Benson, D. W., and Goldmuntz, E. (2003) NKX2.5 mutations in patients with congenital heart disease *J Am Coll Cardiol* **42**(9), 1650-1655
42. Elliott, D. A., Kirk, E. P., Yeoh, T., Chandar, S., McKenzie, F., Taylor, P., Grossfeld, P., Fatkin, D., Jones, O., Hayes, P., et al. (2003) Cardiac homeobox gene NKX2-5 mutations and congenital heart disease: associations with atrial septal defect and hypoplastic left heart syndrome *J Am Coll Cardiol* **41**(11), 2072-2076
43. Pashmforoush, M., Lu, J. T., Chen, H., Amand, T. S., Kondo, R., Pradervand, S., Evans, S. M., Clark, B., Feramisco, J. R., Giles, W., et al. (2004) Nkx2-5 pathways and congenital heart disease; loss of ventricular myocyte lineage specification leads to progressive cardiomyopathy and complete heart block *Cell* **117**(3), 373–386
44. Garg, V., Kathiriya, I. S., Barnes, R., Schluterman, M. K., King, I. N., Butler, C. A., Rothrock, C. R., Eapen, R. S., Hirayama-Yamada, K., Joo, K., et al. (2003) GATA4 mutations cause human congenital heart defects and reveal an interaction with TBX5 *Nature* **424**(6947), 443–447
45. Ching, Y. H., Ghosh, T. K., Cross, S. J., Packham, E. A., Honeyman, L., Loughna, S., Robinson, T. E., Dearlove, A. M., Ribas, G., Bonser, A. J., et al. (2005) Mutation in myosin heavy chain 6 causes atrial septal defect *Nat. Genet.* **37**(4), 423–428
46. Molkentin, J., Kalvakolanu, D., and Markham, B. (1994) Transcription factor GATA-4 regulates cardiac muscle-specific expression of the alpha-myosin heavy-chain gene *Mol. Cell. Biol.* **14**(7), 4947–4957
47. McBride, K. L., Pignatelli, R., Lewin, M., Ho, T., Fernbach, S., Menesses, A., Lam, W., Leal, S. M., Kaplan, N., Schliekelman, P., et al. (2005) Inheritance analysis of congenital left ventricular outflow tract obstruction malformations: Segregation, multiplex relative risk, and heritability *Am J Med Genet A* **134**(2), 180-186
48. Stalmans, I., Lambrechts, D., De Smet, F., Jansen, S., Wang, J., Maity, S., Kneer, P., von der Ohe, M., Swillen, A., Maes, C., et al. (2003) VEGF: a modifier of the del22q11 (DiGeorge) syndrome? *Nat Med* **9**(2), 173-182
49. Dietz, H. C., Cutting, G. R., Pyeritz, R. E., Maslen, C. L., Sakai, L. Y., Corson, G. M., Puffenberger, E. G., Hamosh, A., Nanthakumar, E. J., Curristin, S. M., et al. (1991) Marfan syndrome caused by a recurrent de novo missense mutation in the fibrillin gene *Nature* **352**(6333), 337–339
50. Lee, B., Godfrey, M., Vitale, E., Hori, H., Mattei, M. G., Sarfarazi, M., Tsipouras, P., Ramirez, F., and Hollister, D. W. (1991) Linkage of Marfan syndrome and a phenotypically related disorder to two different fibrillin genes *Nature* **352**(6333), 330-334
51. Mizuguchi, T., Collod-Beroud, G., Akiyama, T., Abifadel, M., Harada, N., Morisaki, T., Allard, D., Varret, M., Claustres, M., Morisaki, H., et al. (2004) Heterozygous TGFBR2 mutations in Marfan syndrome *Nat Genet* **36**(8), 855-860
52. Lin, A. E., Birch, P. H., Korf, B. R., Tenconi, R., Niimura, M., Poyhonen, M., Armfield Uhas, K., Sigorini, M., Virdis, R., Romano, C., et al. (2000)

Cardiovascular malformations and other cardiovascular abnormalities in neurofibromatosis 1 *Am. J. Med. Genet.* **95**(2), 108–117
53. Li, Y., Bollag, G., Clark, R., Stevens, J., Conroy, L., Fults, D., Ward, K., Friedman, E., Samowitz, W., Robertson, M., et al. (1992) Somatic mutations in the neurofibromatosis 1 gene in human tumors *Cell* **69**(2), 275-281
54. Ewart, A. K., Morris, C. A., Atkinson, D., Jin, W., Sternes, K., Spallone, P., Stock, A. D., Leppert, M., and Keating, M. T. (1993) Hemizygosity at the elastin locus in a developmental disorder, Williams syndrome *Nat Genet* **5**(1), 11-16
55. Gebbia, M., Ferrero, G. B., Pilia, G., Bassi, M. T., Aylsworth, A., Penman-Splitt, M., Bird, L. M., Bamforth, J. S., Burn, J., Schlessinger, D., et al. (1997) X-linked situs abnormalities result from mutations in ZIC3 *Nat Genet* **17**(3), 305-308
56. Bamford, R. N., Roessler, E., Burdine, R. D., Saplakoglu, U., dela Cruz, J., Splitt, M., Goodship, J. A., Towbin, J., Bowers, P., Ferrero, G. B., et al. (2000) Loss-of-function mutations in the EGF-CFC gene CFC1 are associated with human left-right laterality defects *Nat Genet* **26**(3), 365-369
57. Ruiz-Perez, V. L., Ide, S. E., Strom, T. M., Lorenz, B., Wilson, D., Woods, K., King, L., Francomano, C., Freisinger, P., Spranger, S., et al. (2000) Mutations in a new gene in Ellis-van Creveld syndrome and Weyers acrodental dysostosis *Nat Genet* **24**(3), 283-286
58. Ruiz-Perez, V. L., Tompson, S. W., Blair, H. J., Espinoza-Valdez, C., Lapunzina, P., Silva, E. O., Hamel, B., Gibbs, J. L., Young, I. D., Wright, M. J., et al. (2003) Mutations in two nonhomologous genes in a head-to-head configuration cause Ellis-van Creveld syndrome *Am J Hum Genet* **72**(3), 728-732
59. Galdzicka, M., Patnala, S., Hirshman, M. G., Cai, J. F., Nitowsky, H., Egeland, J. A., and Ginns, E. I. (2002) A new gene, EVC2, is mutated in Ellis-van Creveld syndrome *Mol Genet Metab* **77**(4), 291-295
60. Vissers, L. E., van Ravenswaaij, C. M., Admiraal, R., Hurst, J. A., de Vries, B. B., Janssen, I. M., van der Vliet, W. A., Huys, E. H., de Jong, P. J., Hamel, B. C., et al. (2004) Mutations in a new member of the chromodomain gene family cause CHARGE syndrome *Nat Genet* **36**(9), 955-957
61. Lalani, S. R., Safiullah, A. M., Molinari, L. M., Fernbach, S. D., Martin, D. M., and Belmont, J. W. (2004) SEMA3E mutation in a patient with CHARGE syndrome *J Med Genet* **41**(7), e94
62. Muncke, N., Jung, C., Rudiger, H., Ulmer, H., Roeth, R., Hubert, A., Goldmuntz, E., Driscoll, D., Goodship, J., Schon, K., et al. (2003) Missense mutations and gene interruption in PROSIT240, a novel TRAP240-like gene, in patients with congenital heart defect (transposition of the great arteries) *Circulation* **108**(23), 2843-2850
63. Basson, C. T., Huang, T., Lin, R. C., Bachinsky, D. R., Weremowicz, S., Vaglio, A., Bruzzone, R., Quadrelli, R., Lerone, M., Romeo, G., et al. (1999) Different TBX5 interactions in heart and limb defined by Holt-Oram syndrome mutations *Proc Natl Acad Sci U S A* **96**(6), 2919-2924
64. Krantz, I. D., Smith, R., Colliton, R. P., Tinkel, H., Zackai, E. H., Piccoli, D. A., Goldmuntz, E., and Spinner, N. B. (1999) Jagged1 mutations in patients ascertained with isolated congenital heart defects *Am J Med Genet* **84**(1), 56-60

65. Benson, D. W., Silberbach, G. M., Kavanaugh-McHugh, A., Cottrill, C., Zhang, Y., Riggs, S., Smalls, O., Johnson, M. C., Watson, M. S., Seidman, J. G., et al. (1999) Mutations in the cardiac transcription factor NKX2.5 affect diverse cardiac developmental pathways *J Clin Invest* **104**(11), 1567-1573
66. Goldmuntz, E., Geiger, E., and Benson, D. W. (2001) NKX2.5 mutations in patients with tetralogy of fallot *Circulation* **104**(21), 2565-2568
67. Arron, J. R., Winslow, M. M., Polleri, A., Chang, C. P., Wu, H., Gao, X., Neilson, J. R., Chen, L., Heit, J. J., Kim, S. K., et al. (2006) NFAT dysregulation by increased dosage of DSCR1 and DYRK1A on chromosome 21 *Nature* **441**(7093), 595-600
68. International_HapMap_Consortium. (2005) A haplotype map of the human genome *Nature* **437**(7063), 1299-1320
69. Clayton, D. G., Walker, N. M., Smyth, D. J., Pask, R., Cooper, J. D., Maier, L. M., Smink, L. J., Lam, A. C., Ovington, N. R., Stevens, H. E., et al. (2005) Population structure, differential bias and genomic control in a large-scale, case-control association study *Nat Genet* **37**(11), 1243-1246
70. Feuk, L., Carson, A. R., and Scherer, S. W. (2006) Structural variation in the human genome *Nat Rev Genet* **7**(2), 85-97
71. Basson, C. T., Bachinsky, D. R., Lin, R. C., Levi, T., Elkins, J. A., Soults, J., Grayzel, D., Kroumpouzou, E., Traill, T. A., Leblanc-Straceski, J., et al. (1997) Mutations in human TBX5 [corrected] cause limb and cardiac malformation in Holt-Oram syndrome *Nat Genet* **15**(1), 30-35
72. Li, Q. Y., Newbury-Ecob, R. A., Terrett, J. A., Wilson, D. I., Curtis, A. R., Yi, C. H., Gebuhr, T., Bullen, P. J., Robson, S. C., Strachan, T., et al. (1997) Holt-Oram syndrome is caused by mutations in TBX5, a member of the Brachyury (T) gene family *Nat Genet* **15**(1), 21-29
73. Schott, J. J., Benson, D. W., Basson, C. T., Pease, W., Silberbach, G. M., Moak, J. P., Maron, B. J., Seidman, C. E., and Seidman, J. G. (1998) Congenital heart disease caused by mutations in the transcription factor NKX2-5 *Science* **281**(5373), 108-111
74. Pashmforoush, M., Lu, J. T., Chen, H., Amand, T. S., Kondo, R., Pradervand, S., Evans, S. M., Clark, B., Feramisco, J. R., Giles, W., et al. (2004) Nkx2-5 pathways and congenital heart disease; loss of ventricular myocyte lineage specification leads to progressive cardiomyopathy and complete heart block *Cell* **117**(3), 373-386
75. Garg, V., Kathiriya, I. S., Barnes, R., Schluterman, M. K., King, I. N., Butler, C. A., Rothrock, C. R., Eapen, R. S., Hirayama-Yamada, K., Joo, K., et al. (2003) GATA4 mutations cause human congenital heart defects and reveal an interaction with TBX5 *Nature* **424**(6947), 443-447
76. van Rooij, E., Sutherland, L. B., Liu, N., Williams, A. H., McAnally, J., Gerard, R. D., Richardson, J. A., and Olson, E. N. (2006) A signature pattern of stress-responsive microRNAs that can evoke cardiac hypertrophy and heart failure *Proc Natl Acad Sci U S A* **103**(48), 18255-18260
77. Hobert, O. (2008) Gene regulation by transcription factors and microRNAs *Science* **319**(5871), 1785-1786

78. Ivey, K. N., Muth, A., Arnold, J., King, F. W., Yeh, R. F., Fish, J. E., Hsiao, E. C., Schwartz, R. J., Conklin, B. R., Bernstein, H. S., et al. (2008) MicroRNA Regulation of Cell Lineages in Mouse and Human Embryonic Stem Cells *Cell Stem Cell* **2**(3), 219-229
79. Ebert, M. S., Neilson, J. R., and Sharp, P. A. (2007) MicroRNA sponges: competitive inhibitors of small RNAs in mammalian cells *Nat Methods* **4**(9), 721-726
80. van Rooij, E., Sutherland, L. B., Qi, X., Richardson, J. A., Hill, J., and Olson, E. N. (2007) Control of stress-dependent cardiac growth and gene expression by a microRNA *Science* **316**(5824), 575–579
81. Kertesz, M., Iovino, N., Unnerstall, U., Gaul, U., and Segal, E. (2007) The role of site accessibility in microRNA target recognition *Nat Genet* **39**(10), 1278-1284
82. Grimson, A., Farh, K. K., Johnston, W. K., Garrett-Engele, P., Lim, L. P., and Bartel, D. P. (2007) MicroRNA targeting specificity in mammals: determinants beyond seed pairing *Mol Cell* **27**(1), 91-105
83. Li, L., Krantz, I. D., Deng, Y., Genin, A., Banta, A. B., Collins, C. C., Qi, M., Trask, B. J., Kuo, W. L., Cochran, J., et al. (1997) Alagille syndrome is caused by mutations in human Jagged1, which encodes a ligand for Notch1 *Nat Genet* **16**(3), 243-251
84. Oda, T., Elkahloun, A. G., Pike, B. L., Okajima, K., Krantz, I. D., Genin, A., Piccoli, D. A., Meltzer, P. S., Spinner, N. B., Collins, F. S., et al. (1997) Mutations in the human Jagged1 gene are responsible for Alagille syndrome *Nat Genet* **16**(3), 235-242
85. Garg, V., Muth, A. N., Ransom, J. F., Schluterman, M. K., Barnes, R., King, I. N., Grossfeld, P. D., and Srivastava, D. (2005) Mutations in NOTCH1 cause aortic valve disease *Nature* **437**(7056), 270-274
86. Tartaglia, M., Cotter, P. D., Zampino, G., Gelb, B. D., and Rauen, K. A. (2003) Exclusion of PTPN11 mutations in Costello syndrome: further evidence for distinct genetic etiologies for Noonan, cardio-facio-cutaneous and Costello syndromes *Clin Genet* **63**(5), 423-426
87. Fragale, A., Tartaglia, M., Wu, J., and Gelb, B. D. (2004) Noonan syndrome-associated SHP2/PTPN11 mutants cause EGF-dependent prolonged GAB1 binding and sustained ERK2/MAPK1 activation *Hum Mutat* **23**(3), 267-277
88. Krenz, M., Yutzey, K. E., and Robbins, J. (2005) Noonan syndrome mutation Q79R in Shp2 increases proliferation of valve primordia mesenchymal cells via extracellular signal-regulated kinase 1/2 signaling *Circ Res* **97**(8), 813-820
89. Chen, B., Bronson, R. T., Klaman, L. D., Hampton, T. G., Wang, J. F., Green, P. J., Magnuson, T., Douglas, P. S., Morgan, J. P., and Neel, B. G. (2000) Mice mutant for Egfr and Shp2 have defective cardiac semilunar valvulogenesis *Nat Genet* **24**(3), 296-299
90. Rajagopal, S. K., Ma, Q., Obler, D., Shen, J., Manichaikul, A., Tomita-Mitchell, A., Boardman, K., Briggs, C., Garg, V., Srivastava, D., et al. (2007) Spectrum of heart disease associated with murine and human GATA4 mutation *J. Mol. Cell. Cardiol.*, (e-pub ahead of print: doi:10.1016/j.yjmcc.2007.1006.1004)
91. Schluterman, M. K., Krysiak, A. E., Kathiriya, I. S., Abate, N., Chandalia, M., Srivastava, D., and Garg, V. (2007) Screening and biochemical analysis of

GATA4 sequence variations identified in patients with congenital heart disease *Am. J. Med. Genet. A* **143**(8), 817–823
92. Service, R. F. (2006) Gene sequencing. The race for the $1000 genome *Science* **311**(5767), 1544-1546
93. Nora, J. J., and Nora, A. H. (1988) Update on counseling the family with a first-degree relative with a congenital heart defect *American journal of medical genetics* **29**(1), 137-142
94. Wessels, M. W., Berger, R. M., Frohn-Mulder, I. M., Roos-Hesselink, J. W., Hoogeboom, J. J., Mancini, G. S., Bartelings, M. M., Krijger, R., Wladimiroff, J. W., Niermeijer, M. F., et al. (2005) Autosomal dominant inheritance of left ventricular outflow tract obstruction *Am. J. Med. Genet. A* **134**(2), 171–179
95. Wang, D., Chang, P. S., Wang, Z., Sutherland, L., Richardson, J. A., Small, E., Krieg, P. A., and Olson, E. N. (2001) Activation of cardiac gene expression by myocardin, a transcriptional cofactor for serum response factor *Cell* **105**(7), 851-862
96. Wang, D. Z., Li, S., Hockemeyer, D., Sutherland, L., Wang, Z., Schratt, G., Richardson, J. A., Nordheim, A., and Olson, E. N. (2002) Potentiation of serum response factor activity by a family of myocardin-related transcription factors *Proc Natl Acad Sci U S A* **99**(23), 14855-14860
97. Wang, D. Z., and Olson, E. N. (2004) Control of smooth muscle development by the myocardin family of transcriptional coactivators *Curr Opin Genet Dev* **14**(5), 558-566
98. Cen, B., Selvaraj, A., and Prywes, R. (2004) Myocardin/MKL family of SRF coactivators: key regulators of immediate early and muscle specific gene expression *J Cell Biochem* **93**(1), 74-82
99. Parmacek, M. S. (2007) Myocardin-related transcription factors: critical coactivators regulating cardiovascular development and adaptation *Circ Res* **100**(5), 633-644
100. Li, S., Wang, D. Z., Wang, Z., Richardson, J. A., and Olson, E. N. (2003) The serum response factor coactivator myocardin is required for vascular smooth muscle development *Proc Natl Acad Sci U S A* **100**(16), 9366-9370
101. Oh, J., Richardson, J. A., and Olson, E. N. (2005) Requirement of myocardin-related transcription factor-B for remodeling of branchial arch arteries and smooth muscle differentiation *Proc Natl Acad Sci U S A* **102**(42), 15122-15127
102. Li, S., Chang, S., Qi, X., Richardson, J. A., and Olson, E. N. (2006) Requirement of a myocardin-related transcription factor for development of mammary myoepithelial cells *Mol Cell Biol* **26**(15), 5797-5808
103. Huang, J., Cheng, L., Li, J., Chen, M., Zhou, D., Lu, M. M., Proweller, A., Epstein, J. A., and Parmacek, M. S. (2008) Myocardin regulates expression of contractile genes in smooth muscle cells and is required for closure of the ductus arteriosus in mice *J Clin Invest* **118**(2), 515-525
104. Creemers, E. E., Sutherland, L. B., Oh, J., Barbosa, A. C., and Olson, E. N. (2006) Coactivation of MEF2 by the SAP domain proteins myocardin and MASTR *Mol Cell* **23**(1), 83-96

105. Miralles, F., Posern, G., Zaromytidou, A. I., and Treisman, R. (2003) Actin dynamics control SRF activity by regulation of its coactivator MAL *Cell* **113**(3), 329-342
106. Wang, Z., Wang, D. Z., Hockemeyer, D., McAnally, J., Nordheim, A., and Olson, E. N. (2004) Myocardin and ternary complex factors compete for SRF to control smooth muscle gene expression *Nature* **428**(6979), 185-189
107. Xing, W., Zhang, T. C., Cao, D., Wang, Z., Antos, C. L., Li, S., Wang, Y., Olson, E. N., and Wang, D. Z. (2006) Myocardin induces cardiomyocyte hypertrophy *Circ Res* **98**(8), 1089-1097
108. Badorff, C., Seeger, F. H., Zeiher, A. M., and Dimmeler, S. (2005) Glycogen synthase kinase 3beta inhibits myocardin-dependent transcription and hypertrophy induction through site-specific phosphorylation *Circ Res* **97**(7), 645-654
109. Wang, J., Li, A., Wang, Z., Feng, X., Olson, E. N., and Schwartz, R. J. (2007) Myocardin sumoylation transactivates cardiogenic genes in pluripotent 10T1/2 fibroblasts *Mol Cell Biol* **27**(2), 622-632
110. Ruwhof, C., and van der Laarse, A. (2000) Mechanical stress-induced cardiac hypertrophy: mechanisms and signal transduction pathways *Cardiovascular research* **47**(1), 23-37
111. Zhao, Y., Ransom, J. F., Li, A., Vedantham, V., von Drehle, M., Muth, A. N., Tsuchihashi, T., McManus, M. T., Schwartz, R. J., and Srivastava, D. (2007) Dysregulation of cardiogenesis, cardiac conduction, and cell cycle in mice lacking miRNA-1-2 *Cell* **129**(2), 303-317
112. Wang, Z., Wang, D. Z., Pipes, G. C., and Olson, E. N. (2003) Myocardin is a master regulator of smooth muscle gene expression *Proc Natl Acad Sci U S A* **100**(12), 7129-7134
113. Farese, R. V., Jr., Ruland, S. L., Flynn, L. M., Stokowski, R. P., and Young, S. G. (1995) Knockout of the mouse apolipoprotein B gene results in embryonic lethality in homozygotes and protection against diet-induced hypercholesterolemia in heterozygotes *Proceedings of the National Academy of Sciences of the United States of America* **92**(5), 1774-1778
114. Lee, H. C., Tsai, J. N., Liao, P. Y., Tsai, W. Y., Lin, K. Y., Chuang, C. C., Sun, C. K., Chang, W. C., and Tsai, H. J. (2007) Glycogen synthase kinase 3 alpha and 3 beta have distinct functions during cardiogenesis of zebrafish embryo *BMC developmental biology* **7**, 93
115. Hurlstone, A. F., Haramis, A. P., Wienholds, E., Begthel, H., Korving, J., Van Eeden, F., Cuppen, E., Zivkovic, D., Plasterk, R. H., and Clevers, H. (2003) The Wnt/beta-catenin pathway regulates cardiac valve formation *Nature* **425**(6958), 633-637
116. Peterson, J. R., and Golemis, E. A. (2004) Autoinhibited proteins as promising drug targets *J Cell Biochem* **93**(1), 68-73
117. Zaromytidou, A. I., Miralles, F., and Treisman, R. (2006) MAL and ternary complex factor use different mechanisms to contact a common surface on the serum response factor DNA-binding domain *Mol Cell Biol* **26**(11), 4134-4148

118. Creemers, E. E., Sutherland, L. B., McAnally, J., Richardson, J. A., and Olson, E. N. (2006) Myocardin is a direct transcriptional target of Mef2, Tead and Foxo proteins during cardiovascular development *Development* **133**(21), 4245-4256
119. Zhao, Y., Samal, E., and Srivastava, D. (2005) Serum response factor regulates a muscle-specific microRNA that targets Hand2 during cardiogenesis *Nature* **436**(7048), 214-220
120. Cao, D., Wang, Z., Zhang, C. L., Oh, J., Xing, W., Li, S., Richardson, J. A., Wang, D. Z., and Olson, E. N. (2005) Modulation of smooth muscle gene expression by association of histone acetyltransferases and deacetylases with myocardin *Mol Cell Biol* **25**(1), 364-376
121. Imhof, A., Yang, X. J., Ogryzko, V. V., Nakatani, Y., Wolffe, A. P., and Ge, H. (1997) Acetylation of general transcription factors by histone acetyltransferases *Curr Biol* **7**(9), 689-692
122. Boyes, J., Byfield, P., Nakatani, Y., and Ogryzko, V. (1998) Regulation of activity of the transcription factor GATA-1 by acetylation *Nature* **396**(6711), 594-598
123. Fukuoka, M., Daitoku, H., Hatta, M., Matsuzaki, H., Umemura, S., and Fukamizu, A. (2003) Negative regulation of forkhead transcription factor AFX (Foxo4) by CBP-induced acetylation *International journal of molecular medicine* **12**(4), 503-508
124. Cao, D., Wang, Z., Zhang, C. L., Oh, J., Xing, W., Li, S., Richardson, J. A., Wang, D. Z., and Olson, E. N. (2005) Modulation of smooth muscle gene expression by association of histone acetyltransferases and deacetylases with myocardin *Mol. Cell Biol.* **25**(1), 364–376
125. Schroeder, J. A., Jackson, L. F., Lee, D. C., and Camenisch, T. D. (2003) Form and function of developing heart valves: coordination by extracellular matrix and growth factor signaling *J Mol Med* **81**(7), 392-403
126. Milyavsky, M., Shats, I., Cholostoy, A., Brosh, R., Buganim, Y., Weisz, L., Kogan, I., Cohen, M., Shatz, M., Madar, S., et al. (2007) Inactivation of myocardin and p16 during malignant transformation contributes to a differentiation defect *Cancer Cell* **11**(2), 133-146
127. AHA. (2004) Heart Disease and Stroke Statistics—2004 update. In., American Heart Association, Dallas, TX
128. Hoffman, J. I., and Kaplan, S. (2002) The incidence of congenital heart disease *J. Am. Coll. Cardiol.* **39**(12), 1890–1900
129. Cripe, L., Andelfinger, G., Martin, L. J., Shooner, K., and Benson, D. W. (2004) Bicuspid aortic valve is heritable *J. Am. Coll. Cardiol.* **44**(1), 138–143
130. Horne, B. D., Camp, N. J., Muhlestein, J. B., and Cannon-Albright, L. A. (2004) Evidence for a heritable component in death resulting from aortic and mitral valve diseases *Circulation* **110**(19), 3143–3148
131. Loffredo, C. A., Chokkalingam, A., Sill, A. M., Boughman, J. A., Clark, E. B., Scheel, J., and Brenner, J. I. (2004) Prevalence of congenital cardiovascular malformations among relatives of infants with hypoplastic left heart, coarctation of the aorta, and d-transposition of the great arteries *Am. J. Med. Genet. A* **124**(3), 225–230

132. Rajamannan, N. M., Gersh, B., and Bonow, R. O. (2003) Calcific aortic stenosis: From bench to the bedside--emerging clinical and cellular concepts *Heart* **89**(7), 801–805
133. Kruglyak, L., Daly, M. J., Reeve-Daly, M. P., and Lander, E. S. (1996) Parametric and nonparametric linkage analysis: a unified multipoint approach *Am. J. Hum. Genet.* **58**(6), 1347–1363
134. Cohen, J., Pertsemlidis, A., Kotowski, I. K., Graham, R., Garcia, C. K., and Hobbs, H. H. (2005) Low LDL cholesterol in individuals of African descent resulting from frequent nonsense mutations in PCSK9 *Nature genetics* **37**(2), 161-165
135. Nakagawa, O., McFadden, D. G., Nakagawa, M., Yanagisawa, H., Hu, T., Srivastava, D., and Olson, E. N. (2000) Members of the HRT family of basic helix-loop-helix proteins act as transcriptional repressors downstream of Notch signaling *Proc. Natl. Acad. Sci. USA* **97**(25), 13655–13660
136. Ducy, P., Zhang, R., Geoffroy, V., Ridall, A. L., and Karsenty, G. (1997) Osf2/Cbfa1: A transcriptional activator of osteoblast differentiation *Cell* **89**(5), 747–754
137. Kathiriya, I. S., King, I. N., Murakami, M., Nakagawa, M., Astle, J. M., Gardner, K. A., Gerard, R. D., Olson, E. N., Srivastava, D., and Nakagawa, O. (2004) Hairy-related transcription factors inhibit GATA-dependent cardiac gene expression through a signal-responsive mechanism *J. Biol. Chem.* **279**(52), 54937–54943
138. Artavanis-Tsakonas, S., Rand, M. D., and Lake, R. J. (1999) Notch signaling: Cell fate control and signal integration in development *Science* **284**(5415), 770–776
139. Frischmeyer, P. A., van Hoof, A., O'Donnell, K., Guerrerio, A. L., Parker, R., and Dietz, H. C. (2002) An mRNA surveillance mechanism that eliminates transcripts lacking termination codons *Science* **295**(5563), 2258–2261
140. Krebs, L. T., Xue, Y., Norton, C. R., Shutter, J. R., Maguire, M., Sundberg, J. P., Gallahan, D., Closson, V., Kitajewski, J., Callahan, R., et al. (2000) Notch signaling is essential for vascular morphogenesis in mice *Genes Dev.* **14**(11), 1343–1352
141. Timmerman, L. A., Grego-Bessa, J., Raya, A., Bertran, E., Perez-Pomares, J. M., Diez, J., Aranda, S., Palomo, S., McCormick, F., Izpisua-Belmonte, J. C., et al. (2004) Notch promotes epithelial-mesenchymal transition during cardiac development and oncogenic transformation *Genes Dev.* **18**(1), 99–115
142. Wen, C., Metzstein, M. M., and Greenwald, I. (1997) SUP-17, a Caenorhabditis elegans ADAM protein related to Drosophila KUZBANIAN, and its role in LIN-12/NOTCH signalling *Development (Cambridge, England)* **124**(23), 4759-4767
143. Sotillos, S., Roch, F., and Campuzano, S. (1997) The metalloprotease-disintegrin Kuzbanian participates in Notch activation during growth and patterning of Drosophila imaginal discs *Development (Cambridge, England)* **124**(23), 4769-4779
144. Struhl, G., and Adachi, A. (1998) Nuclear access and action of notch in vivo *Cell* **93**(4), 649-660
145. Struhl, G., and Greenwald, I. (1999) Presenilin is required for activity and nuclear access of Notch in Drosophila *Nature* **398**(6727), 522-525

146. Brown, M. S., and Goldstein, J. L. (1997) The SREBP pathway: regulation of cholesterol metabolism by proteolysis of a membrane-bound transcription factor *Cell* **89**(3), 331-340
147. Haines, N., and Irvine, K. D. (2003) Glycosylation regulates Notch signalling *Nature reviews* **4**(10), 786-797
148. O'Brien, K. D., Kuusisto, J., Reichenbach, D. D., Ferguson, M., Giachelli, C., Alpers, C. E., and Otto, C. M. (1995) Osteopontin is expressed in human aortic valvular lesions *Circulation* **92**(8), 2163–2168
149. Steitz, S. A., Speer, M. Y., Curinga, G., Yang, H. Y., Haynes, P., Aebersold, R., Schinke, T., Karsenty, G., and Giachelli, C. M. (2001) Smooth muscle cell phenotypic transition associated with calcification: upregulation of Cbfa1 and downregulation of smooth muscle lineage markers *Circ. Res.* **89**(12), 1147–1154
150. Rajamannan, N. M., Subramaniam, M., Springett, M., Sebo, T. C., Niekrasz, M., McConnell, J. P., Singh, R. J., Stone, N. J., Bonow, R. O., and Spelsberg, T. C. (2002) Atorvastatin inhibits hypercholesterolemia-induced cellular proliferation and bone matrix production in the rabbit aortic valve *Circulation* **105**(22), 2660–2665
151. Vega, R. B., Matsuda, K., Oh, J., Barbosa, A. C., Yang, X., Meadows, E., McAnally, J., Pomajzl, C., Shelton, J. M., Richardson, J. A., et al. (2004) Histone deacetylase 4 controls chondrocyte hypertrophy during skeletogenesis *Cell* **119**(4), 555–566
152. Nakagawa, O., Nakagawa, M., Richardson, J. A., Olson, E. N., and Srivastava, D. (1999) HRT1, HRT2, and HRT3: A new subclass of bHLH transcription factors marking specific cardiac, somitic, and pharyngeal arch segments *Dev. Biol.* **216**(1), 72–84
153. McLarren, K. W., Lo, R., Grbavec, D., Thirunavukkarasu, K., Karsenty, G., and Stifani, S. (2000) The mammalian basic helix loop helix protein HES-1 binds to and modulates the transactivating function of the runt-related factor Cbfa1 *J. Biol. Chem.* **275**(1), 530–538
154. Iso, T., Sartorelli, V., Poizat, C., Iezzi, S., Wu, H. Y., Chung, G., Kedes, L., and Hamamori, Y. (2001) HERP, a novel heterodimer partner of HES/E(spl) in Notch signaling *Mol. Cell Biol.* **21**(17), 6080–6089
155. McDaniell, R., Warthen, D. M., Sanchez-Lara, P. A., Pai, A., Krantz, I. D., Piccoli, D. A., and Spinner, N. B. (2006) NOTCH2 mutations cause Alagille syndrome, a heterogeneous disorder of the Notch signaling pathway *Am. J. Hum. Genet.* **79**(1), 169–173
156. Tanaka, T., Sato, H., Doi, H., Yoshida, C. A., Shimizu, T., Matsui, H., Yamazaki, M., Akiyama, H., Kawai-Kowase, K., Iso, T., et al. (2008) Runx2 represses myocardin-mediated differentiation and facilitates osteogenic conversion of vascular smooth muscle cells *Mol Cell Biol* **28**(3), 1147-1160
157. Doi, H., Iso, T., Sato, H., Yamazaki, M., Matsui, H., Tanaka, T., Manabe, I., Arai, M., Nagai, R., and Kurabayashi, M. (2006) Jagged1-selective notch signaling induces smooth muscle differentiation via a RBP-Jkappa-dependent pathway *J Biol Chem* **281**(39), 28555-28564
158. Nakagawa, O., Nakagawa, M., Richardson, J. A., Olson, E. N., and Srivastava, D. (1999) HRT1, HRT2, and HRT3: a new subclass of bHLH transcription factors

marking specific cardiac, somitic, and pharyngeal arch segments *Dev Biol* **216**(1), 72-84
159. Xin, M., Small, E. M., van Rooij, E., Qi, X., Richardson, J. A., Srivastava, D., Nakagawa, O., and Olson, E. N. (2007) Essential roles of the bHLH transcription factor Hrt2 in repression of atrial gene expression and maintenance of postnatal cardiac function *Proc Natl Acad Sci U S A* **104**(19), 7975-7980
160. Weng, A. P., Ferrando, A. A., Lee, W., Morris, J. P. t., Silverman, L. B., Sanchez-Irizarry, C., Blacklow, S. C., Look, A. T., and Aster, J. C. (2004) Activating mutations of NOTCH1 in human T cell acute lymphoblastic leukemia *Science (New York, N.Y* **306**(5694), 269-271
161. Buckingham, M., Meilhac, S., and Zaffran, S. (2005) Building the mammalian heart from two sources of myocardial cells *Nat. Rev. Genet.* **6**(11), 826–835
162. Srivastava, D. (2006) Making or breaking the heart: From lineage determination to morphogenesis *Cell* **126**, 1037–1048
163. Olson, E. N. (2006) Gene regulatory networks in the evolution and development of the heart *Science* **313**(5795), 1922–1927
164. Thom, T., Haase, N., Rosamond, W., Howard, V. J., Rumsfeld, J., Manolio, T., Zheng, Z. J., Flegal, K., O'Donnell, C., Kittner, S., et al. (2006) Heart disease and stroke statistics--2006 update: A report from the American Heart Association Statistics Committee and Stroke Statistics Subcommittee *Circulation* **113**(6), e85–e151
165. Soonpaa, M. H., and Field, L. J. (1998) Survey of studies examining mammalian cardiomyocyte DNA synthesis *Circ. Res.* **83**(1), 15–26
166. Oh, H., Bradfute, S. B., Gallardo, T. D., Nakamura, T., Gaussin, V., Mishina, Y., Pocius, J., Michael, L. H., Behringer, R. R., Garry, D. J., et al. (2003) Cardiac progenitor cells from adult myocardium: Homing, differentiation, and fusion after infarction *Proc. Natl. Acad. Sci. USA* **100**(21), 12313–12318
167. Beltrami, A. P., Barlucchi, L., Torella, D., Baker, M., Limana, F., Chimenti, S., Kasahara, H., Rota, M., Musso, E., Urbanek, K., et al. (2003) Adult cardiac stem cells are multipotent and support myocardial regeneration *Cell* **114**(6), 763–776
168. Martin, C. M., Meeson, A. P., Robertson, S. M., Hawke, T. J., Richardson, J. A., Bates, S., Goetsch, S. C., Gallardo, T. D., and Garry, D. J. (2004) Persistent expression of the ATP-binding cassette transporter, Abcg2, identifies cardiac SP cells in the developing and adult heart *Dev. Biol.* **265**(1), 262–275
169. Laugwitz, K. L., Moretti, A., Lam, J., Gruber, P., Chen, Y., Woodard, S., Lin, L. Z., Cai, C. L., Lu, M. M., Reth, M., et al. (2005) Postnatal isl1+ cardioblasts enter fully differentiated cardiomyocyte lineages *Nature* **433**(7026), 647–653
170. Zhao, Y., and Srivastava, D. (2007) A developmental view of microRNA function *Trends Biochem. Sci.* **32**, 189–197
171. Ambros, V. (2004) The functions of animal microRNAs *Nature* **431**(7006), 350–355
172. Meister, G., and Tuschl, T. (2004) Mechanisms of gene silencing by double-stranded RNA *Nature* **431**(7006), 343–349
173. He, L., and Hannon, G. J. (2004) MicroRNAs: Small RNAs with a big role in gene regulation *Nat. Rev. Genet.* **5**(7), 522–531

174. Kloosterman, W. P., and Plasterk, R. H. (2006) The diverse functions of microRNAs in animal development and disease *Dev. Cell* **11**(4), 441–450
175. Berezikov, E., Thuemmler, F., van Laake, L. W., Kondova, I., Bontrop, R., Cuppen, E., and Plasterk, R. H. (2006) Diversity of microRNAs in human and chimpanzee brain *Nat. Genet.* **38**(12), 1375–1377
176. Sokol, N. S., and Ambros, V. (2005) Mesodermally expressed *Drosophila* microRNA-1 is regulated by Twist and is required in muscles during larval growth *Genes Dev.* **19**(19), 2343–2354
177. Moss, E. G., Lee, R. C., and Ambros, V. (1997) The cold shock domain protein LIN-28 controls developmental timing in *C. elegans* and is regulated by the lin-4 RNA *Cell* **88**(5), 637–646
178. Kwon, C., Han, Z., Olson, E. N., and Srivastava, D. (2005) MicroRNA1 influences cardiac differentiation in Drosophila and regulates Notch signaling *Proc. Natl. Acad. Sci. USA* **102**(52), 18986–18991
179. Pasquinelli, A. E., Reinhart, B. J., Slack, F., Martindale, M. Q., Kuroda, M. I., Maller, B., Hayward, D. C., Ball, E. E., Degnan, B., Muller, P., et al. (2000) Conservation of the sequence and temporal expression of let-7 heterochronic regulatory RNA *Nature* **408**(6808), 86–89
180. Reinhart, B. J., Slack, F. J., Basson, M., Pasquinelli, A. E., Bettinger, J. C., Rougvie, A. E., Horvitz, H. R., and Ruvkun, G. (2000) The 21-nucleotide let-7 RNA regulates developmental timing in *Caenorhabditis elegans Nature* **403**(6772), 901–906
181. Wightman, B., Ha, I., and Ruvkun, G. (1993) Posttranscriptional regulation of the heterochronic gene lin-14 by lin-4 mediates temporal pattern formation in *C. elegans Cell* **75**(5), 855–862
182. Johnston, R. J., and Hobert, O. (2003) A microRNA controlling left/right neuronal asymmetry in Caenorhabditis elegans *Nature* **426**(6968), 845–849
183. Lee, R. C., Feinbaum, R. L., and Ambros, V. (1993) The *C. elegans* heterochronic gene lin-4 encodes small RNAs with antisense complementarity to lin-14 *Cell* **75**(5), 843–854
184. Brennecke, J., Hipfner, D. R., Stark, A., Russell, R. B., and Cohen, S. M. (2003) bantam encodes a developmentally regulated microRNA that controls cell proliferation and regulates the proapoptotic gene hid in Drosophila *Cell* **113**(1), 25–36
185. Cohen, S. M., Brennecke, J., and Stark, A. (2006) Denoising feedback loops by thresholding--a new role for microRNAs *Genes Dev.* **20**(20), 2769–2772
186. Hornstein, E., Mansfield, J. H., Yekta, S., Hu, J. K., Harfe, B. D., McManus, M. T., Baskerville, S., Bartel, D. P., and Tabin, C. J. (2005) The microRNA miR-196 acts upstream of Hoxb8 and Shh in limb development *Nature* **438**(7068), 671–674
187. Harfe, B. D., McManus, M. T., Mansfield, J. H., Hornstein, E., and Tabin, C. J. (2005) The RNaseIII enzyme Dicer is required for morphogenesis but not patterning of the vertebrate limb *Proc. Natl. Acad. Sci. USA* **102**(31), 10898–10903
188. Yi, R., O'Carroll, D., Pasolli, H. A., Zhang, Z., Dietrich, F. S., Tarakhovsky, A., and Fuchs, E. (2006) Morphogenesis in skin is governed by discrete sets of differentially expressed microRNAs *Nat. Genet.* **38**(3), 356–362

189. Zhao, Y., Samal, E., and Srivastava, D. (2005) Serum response factor regulates a muscle-specific mircroRNA that targets *Hand2* during cardiogenesis *Nature* **436**, 214–220
190. Rao, P. K., Kumar, R. M., Farkhondeh, M., Baskerville, S., and Lodish, H. F. (2006) Myogenic factors that regulate expression of muscle-specific microRNAs *Proc. Natl. Acad. Sci. USA*, (in press)
191. Chen, J. F., Mandel, E. M., Thomson, J. M., Wu, Q., Callis, T. E., Hammond, S. M., Conlon, F. L., and Wang, D. Z. (2006) The role of microRNA-1 and microRNA-133 in skeletal muscle proliferation and differentiation *Nat. Genet.* **38**(2), 228–233
192. Lagos-Quintana, M., Rauhut, R., Lendeckel, W., and Tuschl, T. (2001) Identification of novel genes coding for small expressed RNAs *Science* **294**(5543), 853–858
193. Kim, H. K., Lee, Y. S., Sivaprasad, U., Malhotra, A., and Dutta, A. (2006) Muscle-specific microRNA miR-206 promotes muscle differentiation *J. Cell. Biol.* **174**(5), 677–687
194. van Rooij, E., Sutherland, L. B., Liu, N., Williams, A. H., McAnally, J., Gerard, R. D., Richardson, J. A., and Olson, E. N. (2006) A signature pattern of stress-responsive microRNAs that can evoke cardiac hypertrophy and heart failure *Proc. Natl. Acad. Sci. USA* **103**(48), 18255–18260
195. Sayed, D., Hong, C., Chen, I. Y., Lypowy, J., and Abdellatif, M. (2007) MicroRNAs play an essential role in the development of cardiac hypertrophy *Circ. Res.* **100**(3), 416–424
196. Bentwich, I. (2005) Prediction and validation of microRNAs and their targets *FEBS Lett.* **579**(26), 5904–5410
197. Lewis, B. P., Burge, C. B., and Bartel, D. P. (2005) Conserved seed pairing, often flanked by adenosines, indicates that thousands of human genes are microRNA targets *Cell* **120**(1), 15–20
198. Rajewsky, N. (2006) microRNA target predictions in animals *Nat. Genet.* **38 Suppl**, S8–S13
199. Brennecke, J., Stark, A., Russell, R. B., and Cohen, S. M. (2005) Principles of microRNA-target recognition *PLoS Biol.* **3**(3), e85
200. Bartel, D. P. (2004) MicroRNAs: Genomics, biogenesis, mechanism, and function *Cell* **116**(2), 281–297
201. Lewis, B. P., Shih, I. H., Jones-Rhoades, M. W., Bartel, D. P., and Burge, C. B. (2003) Prediction of mammalian microRNA targets *Cell* **115**(7), 787–798
202. Didiano, D., and Hobert, O. (2006) Perfect seed pairing is not a generally reliable predictor for miRNA-target interactions *Nat. Struct. Mol. Biol.* **13**(9), 849–851
203. Moses, K. A., DeMayo, F., Braun, R. M., Reecy, J. L., and Schwartz, R. J. (2001) Embryonic expression of an Nkx2-5/Cre gene using ROSA26 reporter mice *Genesis* **31**(4), 176–180
204. Tamura, T., Onodera, T., Said, S., and Gerdes, A. M. (1998) Correlation of myocyte lengthening to chamber dilation in the spontaneously hypertensive heart failure (SHHF) rat *J. Mol. Cell. Cardiol.* **30**(11), 2175–2181
205. Shin, C. H., Liu, Z. P., Passier, R., Zhang, C. L., Wang, D. Z., Harris, T. M., Yamagishi, H., Richardson, J. A., Childs, G., and Olson, E. N. (2002) Modulation

of cardiac growth and development by HOP, an unusual homeodomain protein *Cell* **110**(6), 725–735
206. Bernstein, E., Caudy, A. A., Hammond, S. M., and Hannon, G. J. (2001) Role for a bidentate ribonuclease in the initiation step of RNA interference *Nature* **409**(6818), 363–366
207. Wienholds, E., Kloosterman, W. P., Miska, E., Alvarez-Saavedra, E., Berezikov, E., de Bruijn, E., Horvitz, H. R., Kauppinen, S., and Plasterk, R. H. (2005) MicroRNA expression in zebrafish embryonic development *Science* **309**(5732), 310–311
208. Srivastava, D., Cserjesi, P., and Olson, E. N. (1995) A subclass of bHLH proteins required for cardiac morphogenesis *Science* **270**(5244), 1995–1999
209. Srivastava, D., Thomas, T., Lin, Q., Kirby, M. L., Brown, D., and Olson, E. N. (1997) Regulation of cardiac mesodermal and neural crest development by the bHLH transcription factor, dHAND *Nat. Genet.* **16**(2), 154–160
210. Yamagishi, H., Yamagishi, C., Nakagawa, O., Harvey, R. P., Olson, E. N., and Srivastava, D. (2001) The combinatorial activities of Nkx2.5 and dHAND are essential for cardiac ventricle formation *Dev. Biol.* **239**(2), 190–203
211. McFadden, D. G., Barbosa, A. C., Richardson, J. A., Schneider, M. D., Srivastava, D., and Olson, E. N. (2005) The Hand1 and Hand2 transcription factors regulate expansion of the embryonic cardiac ventricles in a gene dosage-dependent manner *Development* **132**(1), 189–201
212. Aiyer, A. R., Honarpour, N., Herz, J., and Srivastava, D. (2005) Loss of Apaf-1 leads to partial rescue of the HAND2-null phenotype *Dev. Biol.* **278**(1), 155–162
213. Yelon, D., Ticho, B., Halpern, M. E., Ruvinsky, I., Ho, R. K., Silver, L. M., and Stainier, D. Y. (2000) The bHLH transcription factor hand2 plays parallel roles in zebrafish heart and pectoral fin development *Development* **127**(12), 2573–2582
214. Gonzalez, E., Kulkarni, H., Bolivar, H., Mangano, A., Sanchez, R., Catano, G., Nibbs, R. J., Freedman, B. I., Quinones, M. P., Bamshad, M. J., et al. (2005) The influence of CCL3L1 gene-containing segmental duplications on HIV-1/AIDS susceptibility *Science* **307**(5714), 1434–1440
215. Desai, A. D., Yaw, T. S., Yamazaki, T., Kaykha, A., Chun, S., and Froelicher, V. F. (2006) Prognostic Significance of Quantitative QRS Duration *Am. J. Med.* **119**(7), 600–606
216. Costantini, D. L., Arruda, E. P., Agarwal, P., Kim, K.-H., Zhu, Y., Lebel, M., Cheng, C. W., Park, C. Y., Pierce, S., Guerchicoff, A., et al. (2005) The homeodomain transcription factor Irx5 establishes the mouse cardiac ventricular repolarization gradient *Cell* **123**, 347–358
217. Wei, Y., Mizzen, C. A., Cook, R. G., Gorovsky, M. A., and Allis, C. D. (1998) Phosphorylation of histone H3 at serine 10 is correlated with chromosome condensation during mitosis and meiosis in Tetrahymena *Proc. Natl. Acad. Sci. USA* **95**(13), 7480–7484
218. Clubb, F. J., Jr., and Bishop, S. P. (1984) Formation of binucleated myocardial cells in the neonatal rat. An index for growth hypertrophy *Lab. Invest.* **50**(5), 571–577

219. Li, F., Wang, X., Capasso, J. M., and Gerdes, A. M. (1996) Rapid transition of cardiac myocytes from hyperplasia to hypertrophy during postnatal development *J. Mol. Cell. Cardiol.* **28**(8), 1737–1746
220. Valencia-Sanchez, M. A., Liu, J., Hannon, G. J., and Parker, R. (2006) Control of translation and mRNA degradation by miRNAs and siRNAs *Genes Dev.* **20**(5), 515–524
221. Lim, L. P., Lau, N. C., Garrett-Engele, P., Grimson, A., Schelter, J. M., Castle, J., Bartel, D. P., Linsley, P. S., and Johnson, J. M. (2005) Microarray analysis shows that some microRNAs downregulate large numbers of target mRNAs *Nature* **433**(7027), 769–773
222. Stark, A., Brennecke, J., Russell, R. B., and Cohen, S. M. (2003) Identification of *Drosophila* MicroRNA targets *PLoS Biol.* **1**(3), E60
223. Lai, E. C. (2002) Micro RNAs are complementary to 3' UTR sequence motifs that mediate negative post-transcriptional regulation *Nat. Genet.* **30**(4), 363–364
224. Du, T., and Zamore, P. D. (2005) microPrimer: The biogenesis and function of microRNA *Development* **132**(21), 4645–4652
225. Vella, M. C., Choi, E. Y., Lin, S. Y., Reinert, K., and Slack, F. J. (2004) The C. elegans microRNA let-7 binds to imperfect let-7 complementary sites from the lin-41 3'UTR *Genes Dev.* **18**(2), 132–137
226. Vella, M. C., Reinert, K., and Slack, F. J. (2004) Architecture of a validated microRNA::target interaction *Chem. Biol.* **11**(12), 1619–1623
227. Liao, J., Kochilas, L., Nowotschin, S., Arnold, J. S., Aggarwal, V. S., Epstein, J. A., Brown, M. C., Adams, J., and Morrow, B. E. (2004) Full spectrum of malformations in velo-cardio-facial syndrome/DiGeorge syndrome mouse models by altering Tbx1 dosage *Hum. Mol. Genet.* **13**(15), 1577–1585
228. Tartaglia, M., Mehler, E. L., Goldberg, R., Zampino, G., Brunner, H. G., Kremer, H., van der Burgt, I., Crosby, A. H., Ion, A., Jeffery, S., et al. (2001) Mutations in PTPN11, encoding the protein tyrosine phosphatase SHP-2, cause Noonan syndrome *Nat. Genet.* **29**(4), 465–468
229. Redon, R., Ishikawa, S., Fitch, K. R., Feuk, L., Perry, G. H., Andrews, T. D., Fiegler, H., Shapero, M. H., Carson, A. R., Chen, W., et al. (2006) Global variation in copy number in the human genome *Nature* **444**(7118), 444–454
230. Hoffman, J. I., Kaplan, S., and Liberthson, R. R. (2004) Prevalence of congenital heart disease *Am. Heart J.* **147**(3), 425–439
231. Fischer, A., and Gessler, M. (2003) Hey genes in cardiovascular development *Trends Cardiovasc. Med.* **13**(6), 221–226
232. Srivastava, D. (1999) HAND proteins: Molecular mediators of cardiac development and congenital heart disease *Trends Cardiovasc. Med.* **9**(1-2), 11–18
233. Xin, M., Davis, C. A., Molkentin, J. D., Lien, C. L., Duncan, S. A., Richardson, J. A., and Olson, E. N. (2006) A threshold of GATA4 and GATA6 expression is required for cardiovascular development *Proc. Natl. Acad. Sci. USA* **103**(30), 11189–11194
234. Zipes, D. P., and Wellens, H. J. (1998) Sudden cardiac death *Circulation* **98**(21), 2334–2351

235. Gourdie, R. G., Kubalak, S., and Mikawa, T. (1999) Conducting the embryonic heart: Orchestrating development of specialized cardiac tissues *Trends Cardiovasc. Med.* **9**(1-2), 18–26
236. Gottlieb, P. D., Pierce, S. A., Sims, R. J., Yamagishi, H., Weihe, E. K., Harriss, J. V., Maika, S. D., Kuziel, W. A., King, H. L., Olson, E. N., et al. (2002) Bop encodes a muscle-restricted protein containing MYND and SET domains and is essential for cardiac differentiation and morphogenesis *Nat. Genet.* **31**(1), 25–32
237. Nerbonne, J. M., and Guo, W. (2002) Heterogeneous expression of voltage-gated potassium channels in the heart: roles in normal excitation and arrhythmias *J. Cardiovasc. Electrophysiol.* **13**(4), 406–409
238. MacLellan, W. R., and Schneider, M. D. (2000) Genetic dissection of cardiac growth control pathways *Annu. Rev. Physiol.* **62**, 289–319
239. Xie, X., Lu, J., Kulbokas, E. J., Golub, T. R., Mootha, V., Lindblad-Toh, K., Lander, E. S., and Kellis, M. (2005) Systematic discovery of regulatory motifs in human promoters and 3' UTRs by comparison of several mammals *Nature* **434**(7031), 338–345
240. Jackson, A. L., Burchard, J., Schelter, J., Chau, B. N., Cleary, M., Lim, L., and Linsley, P. S. (2006) Widespread siRNA "off-target" transcript silencing mediated by seed region sequence complementarity *Rna* **12**(7), 1179–1187
241. Birmingham, A., Anderson, E. M., Reynolds, A., Ilsley-Tyree, D., Leake, D., Fedorov, Y., Baskerville, S., Maksimova, E., Robinson, K., Karpilow, J., et al. (2006) 3' UTR seed matches, but not overall identity, are associated with RNAi off-targets *Nat. Methods* **3**(3), 199–204
242. Chen, J., Kitchen, C. M., Streb, J. W., and Miano, J. M. (2002) Myocardin: A component of a molecular switch for smooth muscle differentiation *J. Mol. Cell Cardiol.* **34**(10), 1345–1356
243. Han, J., Jiang, Y., Li, Z., Kravchenko, V. V., and Ulevitch, R. J. (1997) Activation of the transcription factor MEF2C by the MAP kinase p38 in inflammation *Nature* **386**(6622), 296-299
244. Harada, N., Tamai, Y., Ishikawa, T., Sauer, B., Takaku, K., Oshima, M., and Taketo, M. M. (1999) Intestinal polyposis in mice with a dominant stable mutation of the beta-catenin gene *EMBO J.* **18**(21), 5931–5942
245. Heery, D. M., and Fischer, P. M. (2007) Pharmacological targeting of lysine acetyltransferases in human disease: a progress report *Drug Discov Today* **12**(1-2), 88-99
246. Chen, Y., Shu, W., Chen, W., Wu, Q., Liu, H., and Cui, G. (2007) Curcumin, both histone deacetylase and p300/CBP-specific inhibitor, represses the activity of nuclear factor kappa B and Notch 1 in Raji cells *Basic Clin Pharmacol Toxicol* **101**(6), 427-433
247. Qiu, P., Ritchie, R. P., Fu, Z., Cao, D., Cumming, J., Miano, J. M., Wang, D. Z., Li, H. J., and Li, L. (2005) Myocardin enhances Smad3-mediated transforming growth factor-beta1 signaling in a CArG box-independent manner: Smad-binding element is an important cis element for SM22alpha transcription in vivo *Circ Res* **97**(10), 983-991

248. Callis, T. E., Cao, D., and Wang, D. Z. (2005) Bone morphogenetic protein signaling modulates myocardin transactivation of cardiac genes *Circ Res* **97**(10), 992-1000
249. Liu, N., Williams, A. H., Kim, Y., McAnally, J., Bezprozvannaya, S., Sutherland, L. B., Richardson, J. A., Bassel-Duby, R., and Olson, E. N. (2007) An intragenic MEF2-dependent enhancer directs muscle-specific expression of microRNAs 1 and 133 *Proc Natl Acad Sci U S A* **104**(52), 20844-20849
250. Tang, Y., Urs, S., and Liaw, L. (2008) Hairy-related transcription factors inhibit Notch-induced smooth muscle alpha-actin expression by interfering with Notch intracellular domain/CBF-1 complex interaction with the CBF-1-binding site *Circ Res* **102**(6), 661-668
251. Yang, B., Lin, H., Xiao, J., Lu, Y., Luo, X., Li, B., Zhang, Y., Xu, C., Bai, Y., Wang, H., et al. (2007) The muscle-specific microRNA miR-1 regulates cardiac arrhythmogenic potential by targeting GJA1 and KCNJ2 *Nat. Med.* **13**(4), 486–491
252. Christoffels, V. M., Habets, P. E., Franco, D., Campione, M., de Jong, F., Lamers, W. H., Bao, Z. Z., Palmer, S., Biben, C., Harvey, R. P., et al. (2000) Chamber formation and morphogenesis in the developing mammalian heart *Dev. Biol.* **223**(2), 266–278
253. Krutzfeldt, J., Rajewsky, N., Braich, R., Rajeev, K. G., Tuschl, T., Manoharan, M., and Stoffel, M. (2005) Silencing of microRNAs in vivo with 'antagomirs' *Nature* **438**(7068), 685-689
254. Kawahara, Y., Zinshteyn, B., Sethupathy, P., Iizasa, H., Hatzigeorgiou, A. G., and Nishikura, K. (2007) Redirection of silencing targets by adenosine-to-inosine editing of miRNAs *Science* **315**(5815), 1137-1140
255. Huang, J., Liang, Z., Yang, B., Tian, H., Ma, J., and Zhang, H. (2007) Derepression of microRNA-mediated protein translation inhibition by apolipoprotein B mRNA-editing enzyme catalytic polypeptide-like 3G (APOBEC3G) and its family members *J Biol Chem* **282**(46), 33632-33640
256. Kwak, J. E., and Wickens, M. (2007) A family of poly(U) polymerases *Rna* **13**(6), 860-867
257. Liu, Z. P., and Olson, E. N. (2002) Suppression of proliferation and cardiomyocyte hypertrophy by CHAMP, a cardiac-specific RNA helicase *Proc Natl Acad Sci U S A* **99**(4), 2043-2048
258. Care, A., Catalucci, D., Felicetti, F., Bonci, D., Addario, A., Gallo, P., Bang, M. L., Segnalini, P., Gu, Y., Dalton, N. D., et al. (2007) MicroRNA-133 controls cardiac hypertrophy *Nat Med* **13**(5), 613-618